UNIVERSITY OF CALIFORNIA

Santa Barbara

Novel disinfection system with recyclable magnetic nanoparticles and metal ions: evaluation with bacteria, algae and virus

A dissertation submitted in partial satisfaction of the

requirements for the degree Doctor of Philosophy

in Environmental Science and Management

by

Qian Gao

Committee in charge:

Professor Arturo Keller, Chair

Professor Patricia Holden

Professor Helene Gardner

March 2022

The dissertation of Qian Gao is approved.

_____

Patricia Holden

_____

Helene Gardner

_____

Arturo Keller, Committee Chair

February 2022

Novel disinfection system with recyclable magnetic nanoparticles and metal ions: evaluation with bacteria, algae and virus

by

Qian Gao

ACKNOWLEDGEMENTS

I feel very fortunate to spend five years for my PhD program at Santa Barbara, a place that gives me enough joy, love, support, and precious memories. It's hard for me to imagine how to overcome all the difficulties during this journey without the help from everyone I have met here. Firstly, I would like to express my appreciation to my faculty advisor, Prof. Arturo Keller, for the consistent support and guidance throughout this program. Working with Prof. Keller is always pleasant and inspiring, and this experience will encourage me in the future as well. I would like to thank Prof. Patricia Holden for providing constructive feedback on my projects with her profound knowledge and deep expertise. My gratitude also goes to the other faculties and staffs at Bren School, who make me feel like home ever since the first day I was here.

I am grateful to my lab mates at the Keller Lab, Weiwei Li, Xiangning Huang, Nicol Parker and Violaine Desgens-Martin for their suggestions and encouragements to me in my research projects. I thank Jiajia Zheng, Yang Qiu, and Haozhe Yang for the enjoyable time we spent together. My gratitude also extends to my best friends, Wei Lei, Shuran Zhang, Yinnan Zheng and Yu Qiao, for our solid friendship during the past over 10 years. They make me feel that they are always there for me, although we cannot meet in person frequently.

Lastly, I would like to thank my parents, Chunrong Zhao and Guolong Gao, for their unconditional support and love all these years. They give me enough freedom to do whatever I want ever since I was a child. This dissertation is also dedicated to my grandfather, Baoyu Zhao. He passed away three years ago, but I know that he is proud of me forever.

VITA OF QIAN GAO

February 2022

EDUCATION

- Ph.D., Environmental Science & Management — Feb 2022
  University of California, Santa Barbara *(GPA: 3.92/4.0)*
- M.S., Environmental Sciences — Jun 2017
  Peking University, China
- B.S., Environmental Sciences & B.A. in Laws (Intellectual Property) — Jun 2014
  Peking University, China

RESEARCH EXPERIENCE

Graduate Student Researcher — Oct 2017 - Current
Bren School of Environmental Science & Management — ***UC Santa Barbara***

Graduate Student Researcher — Sep 2014 - Jun 2017
College of Urban and Environmental Sciences — ***Peking University***

PUBLICATIONS

- **Gao, Q.**; Chen, W.; Chen, Y.; Werner, D.; Cornelissen, G.; Xing, B.; Tao, S.; Wang, X. "Surfactant removal with multiwalled carbon nanotubes" Water Research, 2016.
- **Gao, Q.**; Wu, F.; Hu, J.; Chen, W.; Zhang, X.; Guo, X.; Wang, B.; Wang, X. "Chemical composition-dependent removal of cationic surfactants by carbon nanotubes" Science of the Total Environment, 2020.
- **Gao, Q.**; Keller, A. A. "Redesigning Water Disinfection Using Recyclable Nanomaterials and Metal Ions: Evaluation with *Escherichia coli*" ACS ES&T Water, 2021.
- **Gao, Q.**; Keller, A. A. "Novel disinfection method with metal ions on *Oscillatoria tenuis* and simultaneous removal of cyanotoxins aided by recyclable magnetic nanoparticles" Journal of Environmental Chemical Engineering, 2021.
- Wang, X.; Liu, Y.; Zhang, H.; Shen, X.; Cai, F.; Zhang, M.; **Gao, Q.**; Chen, W.; Wang, B.; Tao, S. "The impact of carbon nanotubes on bioaccumulation and translocation of phenanthrene, 3-CH3-phenanthrene and 9-NO2-phenanthrene in maize (Zea mays) seedlings" Environmental Science: Nano, 2016.
- Zhang, M.; Shen, X.; Zhang, H.; Cai, F.; Chen, W.; **Gao, Q.**; Ortega-Calvo, J. J.; Tao, S.; Wang, X. "Bioavailability of phenanthrene and nitrobenzene sorbed on carbonaceous materials" Carbon, 2016.
- Cai, F.; Wu, X.; Zhang, H.; Shen, X.; Zhang, M.; Chen, W.; **Gao, Q.**; White, J. C., Tao, S.; Wang, X. "Impact of TiO2 nanoparticles on lead uptake and bioaccumulation in rice (*Oryza sativa L.*)" NanoImpact, 2017.
- Chen, W.; Wang, H.; **Gao, Q.**; Chen, Y.; Li, S.; Yang, Y.; Werner, D.; Tao, S.; Wang, X. "Association of 16 priority polycyclic aromatic hydrocarbons with humic acid and

humic fractions in a peat soil and implications for their long-term retention" Environmental Pollution, 2017.

- Chen, Y.; **Gao, Q.**; Chen, W.; Wu, F.; Yang, Y.; Werner, D.; Tao, S.; Wang, X. "A mechanistic study of stable dispersion of titanium oxide nanoparticles by humic acid" Water Research, 2018.

FIELDS OF STUDY

Environmental Microbiology, Water Treatment, Nanotechnology

Faculty Advisor: Prof. Arturo A. Keller

HONORS & AWARDS

- Bren School Graduate Fellowship, UCSB 2019-2021
- Mellichamp Sustainability Fellowship, UCSB Jun 2019
- 8th Annual SNO Conference Student Award, Sustainable Nanotechnology Organization Nov 2019

TALKS & SEMINARS

- Poster Presentation, American Chemistry Society Fall 2019 National Meeting, San Diego, USA, 08/27/2019
- Poster Presentation, 8th Annual Sustainable Nanotechnology Organization Conference, San Diego, USA, 11/08/2019

ABSTRACT

Novel disinfection system with recyclable magnetic nanoparticles and metal ions: evaluation with bacteria, algae and virus

by

Qian Gao

Water pollution with pathogenic microorganisms is a serious threat to human health, particularly in developing countries. Although traditional disinfection technologies, such as the use of chlorine-containing substances, ozone and UV radiation, are effective to control microorganism contamination in water sources, they present some disadvantages such as the generation of disinfection byproducts or high energy consumption, which are major concerns when considering their sustainable use. Thus, this dissertation proposes a novel disinfection system employing metal ions as disinfectants, which can be recovered using magnetic nanoparticles to reuse the disinfecting agents. Various microorganisms, including bacteria, toxic cyanobacteria and waterborne virus are used for case studies to evaluate the efficacy of this novel method, and the reusability of disinfectants and magnetic nanoparticles are explored for long term application.

Chapter II presents a sustainable disinfection method with recyclable metal ions and magnetic nanoparticles applied to *E. coli* K12. The disinfection ability of Ag^{+}, Cu^{2+} and Zn^{2+} were evaluated. Ag^{+} performed best to inactivate *E. coli* K12, compared to Cu^{2+} and Zn^{2+},

with minimal effect of the general water characteristics except Cl^-. The concentration of residual metal ions was maintained under a safe level, according to EPA guidelines, via sorption by magnetic nanoparticles. Both the magnetic nanoparticles and metal ions can be regenerated and reused with simple operating conditions and high recovery efficiency after 5 continuous cycles, indicating that this method is very promising for practical application.

Chapter III optimizes the disinfection method to address toxic cyanobacteria contamination. A combination of metal ions, namely Ag^+ and Cu^{2+}, was applied to the disinfection of cyanobacteria. The disinfection effectiveness of the combination was more effective compared to individual Ag^+ or Cu^{2+}, especially at low concentration of disinfectants and short contact time. In addition, the results in Chapter III demonstrate that the cyanotoxins produced during disinfection and the residual metal ions can be removed effectively via simultaneous sorption by recyclable magnetic nanoparticles.

Chapter IV explores the disinfection of waterborne viruses with magnetic nanoparticles coated by various metal ions, including Ag^+, Cu^{2+} and Fe^{3+}. All three magnetic nanoparticles with metal ions can inactivate above 99% of the target viruses within 0.5 hours, and the magnetic nanoparticles with Cu^{2+} and Fe^{3+} are more suitable for large-scale application than with Ag^+, considering the price of metal ions. The recovery of the nanoparticles can be easily achieved with external magnetic field, for their regeneration and recycling. The disinfection efficiency remains above 99% after 5 continuous disinfection cycles.

This dissertation contributes to overcome some of the disadvantages of traditional disinfection methods in a drinking water treatment plant, providing a novel approach that recovers a large fraction of the disinfectants for reuse. It serves as a scientific reference for

environmental engineers in drinking water treatment, by providing an innovative approach for disinfection of water sources contaminated with a range of pathogens.

TABLE OF CONTENTS

I. Introduction

A. Background

The global water crisis is a growing issue in the 21st century due to several reasons, one of which is the increasing pollution of freshwater resources. As a main source of contamination, various microorganisms, including pathogenic bacteria, harmful algal blooms and waterborne viruses, can reduce water quality and spread disease through water, which is a major concern for public health [1, 2]. According to the data from the Centers for Disease Control and Prevention (CDC), 119 outbreaks of waterborne pathogens in untreated recreational water were reported from 31 states voluntarily during 2009-2019, with 22% related to Shiga toxin-producing *Escherichia coli* and 19% due to norovirus [3], both of which are associated with severe bloody diarrhea [4, 5]. Different from the outbreak of waterborne pathogens, harmful algal blooms reduce water quality by depleting the oxygen level in natural water [6] and releasing toxins and secondary metabolites [7]. Specifically, the cyanotoxins produced by some cyanobacteria will lead to vomiting, acute liver failure, respiratory irritation or even death when humans are exposed to them, even at very low concentrations in water [8]. Thus, disinfection, the process that reduces the levels of harmful microorganisms through physical or chemical inactivation, is an important component of a drinking water treatment plant.

Disinfection methods have been explored, studied, and developed ever since ancient times. Traditional disinfection methods of water include the use of chlorine-containing substances, ozone and ultraviolet radiation (UV) radiation, which have wide applications for different purposes in water treatment. Chlorine-containing substances are common

disinfectants due to the strong oxidative power of chlorine. Common forms used as disinfectants include gaseous chlorine (Cl_2), hypochlorite (ClO^-) and chlorine dioxide (ClO_2). The main mechanism of disinfection with chlorine is to depolymerize cell walls, penetrate cell membrane [9], destroy enzyme systems through oxidation or to interrupt the synthesis of metabolism related proteins [10], thus inhibiting their development and reproduction. Chlorine-containing substances are widely used disinfectants in drinking water treatment plants, due to their simple production and storage, easily achieved disinfecting conditions and residual effect [11]. However, several factors need to be considered for operation, one of which is the natural organic content in water. Many common natural organic compounds, such as humic acids, can react with chlorine in water to form harmful byproducts including trihalomethanes (THMs), haloacetic acids (HAAs), chlorophenols, chloral hydrate and haloacetonitriles (HANs) [12], and the effects of these byproducts on human health have been studied [13]. For example, recent epidemiological studies have shown that long-term exposure to THMs via oral ingestion, dermal contact and inhalation is associated with development of bladder and colon cancers [14]. Toxicological evidence has also revealed that chloroform and bromodichloromethane are possibly carcinogenic to humans [15]. In addition, the control of pH in a disinfection system is very important, since pH determines the speciation of chlorine-containing disinfectants and an inappropriate pH can greatly reduce the effectiveness of disinfection [16]. Some chlorine-containing disinfectants such as ClO_2 are quite unstable and must be produced on-site for direct use. Thus, correct design and operation of a chlorine-containing disinfection system is important, and the production of disinfection by-products must be monitored constantly [13].

The use of ozone as disinfectant is another conventional disinfection method. As a strong oxidant, ozone can react with various components of cell walls and cause damage to cell surfaces [17]. Thus, ozone has a great potential to be used as disinfectant. Advantages of ozone as disinfectant include short contact time (approximately 10 to 30 minutes) and elevation of dissolved oxygen (DO) concentration in the effluent [18]. However, there are several disadvantages that prevent ozonation from being a prevalent disinfection approach. Firstly, ozone is quite reactive, corrosive and unstable. Thus, it requires corrosion-resistant materials such as stainless steel for storage [18], and needs to be generated *in-situ* during disinfection. An ozone generator consists of feed gas preparation, electrical power supply, high voltage and ground electrodes with dielectric material forming the discharge gap, and cooling system to remove heat generated [11]. The high energy use of an ozone generator is a major concern. Secondly, the ozonation system, which consists of an ozone generator, contactor, destruction unit, instrumentation and controls [11], is complex and requires significant operator training and safety considerations [19]. Thirdly, both organic and inorganic disinfection by-products may be produced during ozonation [20]. By-products resulting from ozonation of wastewater include aldehydes (e.g. formaldehyde, acetaldehyde, glyoxal, methyl glyoxal), acids (e.g. acetic acids, formic acid, oxalic acid and succinic acid), aldo- and ketoacids (such as pyruvic acid), brominated byproducts (e.g. bromate ion, bromoform, brominated acetic acids, brominated acetonitriles, cyanogen bromide) and other byproducts (such as hydrogen peroxide) [21]. These by-products may lead to additional contamination to the environment and present health risks. For example, bromoform may be produced when the bromide ions in water are oxidized by ozone, and it is related to cancer, liver, kidney and reproductive effects to humans [22].

UV is a physical disinfection process. Since no chemicals are added during disinfection, UV has the advantage of no toxic residuals that may threaten human health and the environment. UV can destroy nucleic acid in microorganisms to achieve disinfection [23]. As UV radiation needs to pass through the cell wall of microorganism to damage the nucleic acid, the composition and thickness of cell well are two factors that determine the effectiveness of disinfection [23]. Other factors, such as lamp intensity, time of exposure and characteristics of water (color and turbidity) will influence the effectiveness as well [11]. Although UV disinfection has the advantages of short contact time, wide range of target microorganisms, and simpler controls than ozonation, some limitations of this disinfection approach cannot be ignored [24-25]. The main considerations focus on high energy demand, and operation and maintenance of the disinfection system. To solve these problems, some advanced disinfection methods tend to combine UV radiation with other chemicals, to improve the efficiency, and reduce the energy demand at the same time. For example, in many cases, UV is combined with ozone or hydrogen peroxide to increase the effectiveness [26], or with peracetic acid (PAA) [27], albeit at a higher operating requirement. Precise operating conditions (for example, dosage of chemicals and radiation, and current density of electricity) are required during disinfection, and these conditions need to be adjusted carefully for each water source, considering seasonal variance in source water composition.

Membrane filtration, including microfiltration, ultrafiltration, nanofiltration and reverse osmosis (RO), is another typical treatment for water purification, which allows the separation of ions, molecules, and particles from drinking water through a physical barrier [11]. The main differences between microfiltration, ultrafiltration, nanofiltration and reverse osmosis are the pore sizes of the membranes and the pressure gradient across the membrane. Generally, a

membrane with smaller pores (e.g., reverse osmosis) requires higher pressure for separation than one with larger pores (e.g., microfiltration). Since both the suspended solids and biological species can be removed efficiently from water with less sludge generated and minimized disinfectants demanded compared to other conventional disinfection methods [11], this process can achieve a higher level of disinfection albeit it doesn't serve as the main disinfection step. However, the efficiency of the membranes depends on the water quality, the load of solids and membrane fouling during treatment [11]. Membrane biofouling is a prominent problem for these systems, as it will not only deteriorate the permeate quality of the membrane, but also increase the operational energy and chemical additions to minimize this issue [28]. Thus, membrane filtration is usually combined with other disinfection treatment (e.g., final chlorination) to make sure the number of target microorganisms are maintained below a certain level, and to prevent them from regrowth during the distribution of the treated water.

To overcome the disadvantages of traditional disinfection methods, a number of studies on improving disinfection systems with nanoparticles have been conducted, including the use of titanium dioxide (TiO_2), magnesium oxide (MgO), zinc oxide (ZnO) and nanosilver (nAg). TiO_2 is the most widely used metal oxide nanoparticle for pathogen inactivation in water. The mechanism of disinfection with TiO_2 nanoparticles is based on the formation of reactive oxygen species (ROS) such as hydroxyl radical (OH・), superoxide radical (O2・), and hydrogen peroxide (H_2O_2), generated by TiO_2 photocatalytic reactions [29], which will not only puncture the cell wall, destroy cell membranes, damage or even breakdown DNA of microorganisms, but also interfere with metabolic activities, such as oxidizing important protein structures or hampering electron transfer [30]. Several studies using pristine and

functionalized TiO_2 nanoparticles (TiO_2 NPs) for inactivating bacteria (such as *E. coli*, *S. Aureus*, *P. Aeuroginosa* and *L.monocytogens*) have shown that the disinfection process can be achieved with high efficiency in a short contact time [31-34]. Apart from metal oxide nanoparticles, silver nanoparticles (Ag NPs) have generated considerable interest as disinfectants during recent years [35-37], mainly due to the antimicrobial properties of silver. Recent studies on the application of Ag NPs in disinfection focus on the combination of Ag NPs and polymers to fully develop the disinfection potential of Ag NPs. Ag NPs have been applied in a gravity-driven membrane for disinfection [38], and have also been deposited on polypropylene filters that completely remove pathogens from drinking water [39-40]. Other novel Ag NP-based membranes have been developed, such as silver nanowire-polyacrylonitrile/thermoplastic polyurethane (AgNW-PAN/TPU) composite membrane [41] and silver/reduced graphene oxide hydrogel [42] for point-of-use drinking water disinfection. Despite the great potential of nanoparticles as novel disinfectants, several concerns need to be addressed before practical application. Firstly, the separation of nanoparticles from water after disinfection is needed, to reduce the environmental impact on the ecosystem. However, due to their small (nanoscale) size and high surface area over volume ratio, nanoparticles cannot be efficiently separated from water by classic water treatment such as filtration [43]. Thus, additional technologies may be needed to deal with the nanoparticles after disinfection, which may require extra energy and cost. Secondly, free metal ions may be released from the nanoparticles during disinfection. The loss of dissolved metal ions will weaken the disinfection ability of nanoparticles and make them not suitable for sustainable use. Besides, the released metal ions may threaten ecological health if the concentration is not kept at a low enough level before the treated water eventually reaches the natural environment.

Considering the issues related to microbial contamination of water sources, as well as the disadvantages of current disinfection processes, this dissertation proposes a more sustainable disinfection method with recyclable metal ions and magnetic nanoparticles, to achieve high disinfection efficiency with easier operating conditions and reduced environmental effects compared to other nanoparticle-based approaches. In this system, contaminated water containing the target microorganisms is mixed with various metal ions as disinfectants for sufficient time to achieve the required disinfection level. After disinfection, treated water is filtered to separate the dead cells, and the residual metal ions are captured and removed by magnetic nanoparticles via sorption. Magnetic nanoparticles with adsorbed metal ions can be easily removed from the water with an external magnet, which effectively reduces the environmental effect caused by the free metal ions in the water. Later, the magnetic nanoparticles and metal ions are regenerated under proper conditions, and the key materials are reused for several cycles.

Compared to traditional disinfection methods, this novel system has several advantages which make it suitable for practical application in drinking water treatment plants. Firstly, there is no need to generate the metal ions disinfectants on site for direct use during disinfection, thus no extra generator for disinfectants is needed and the disinfection system can be simplified compared to the use of unstable chlorine-containing disinfectants or ozone. Secondly, free metal ions remaining after disinfection can be maintained at a low level by recovering them with the magnetic nanoparticle, which will not only reduce their environmental effects, but also serve as residual disinfectants to prevent the regrowth of microorganisms during distribution [44]. Thus, the proposed approach may be a better choice than membrane filtration which requires further steps for residual disinfection. Lastly, the

key materials for the system can be easily regenerated for recyclable use, which is an important breakthrough compared to the use of other nanoparticles as disinfectants. However, a more in-depth life-cycle assessment should be conducted, following the proof-of-concept studies presented in this dissertation.

B. Objectives and significance

The main objective of this dissertation is to develop a novel and sustainable disinfection method, using metal ions and recyclable magnetic nanoparticles, which overcomes the disadvantages of traditional technologies such as the production of disinfection byproducts, environmental effects caused by residual disinfectants and high operation cost or energy consumption. To achieve this objective, the following chapters address these research questions: (1) What effective metal ions can be used as disinfectants for the target microorganisms, and what are the factors that determine disinfection effectiveness? (2) How to reduce the environmental effect caused by residual metal ions after disinfection? (3) How to recover and regenerate key materials, and what is the recovery efficiency after long term application?

Throughout the dissertation, the feasibility of this novel disinfection method was demonstrated, with case studies covering bacteria, toxic cyanobacteria, and waterborne viruses, and the method was optimized according to different target microorganisms with the disinfection effectiveness evaluated under a wide range of environmental conditions. The reusability of key materials in the disinfection method was explored as well, to achieve more sustainable use for practical application in the future.

This dissertation contributes to overcome the disadvantages of traditional disinfection methods by proposing a novel disinfection system that is easy to operate, capable to achieve

high disinfection efficiency and suitable for recyclable use. Specifically, Chapter II addresses the issue related to the residual metal ions after disinfection through the efficient adsorption with magnetic nanoparticles and achieves the sustainable use of key materials under proper regenerating conditions. Chapter III broadens the range of target microorganisms of this disinfection method and improves the method correspondingly, lowering the time and concentration of disinfectants needed for the system. The simultaneous removal of residual metal ions and cyanotoxins after disinfection makes this method suitable for a complicated environment including toxins released by microorganisms. Chapter IV further shortens the time needed to disinfection by adsorbing the metal ions onto magnetic nanoparticles, eliminating the use of free metal ions and the need for a metal ion recovery step. Compared to other nanoparticles that have been considered as disinfectants which release metal ions and lose their disinfection ability gradually, the adsorbed metal ions on magnetic nanoparticles will remain stable during the continuous disinfection process, making them suitable for long term application. The evaluation with waterborne viruses, as well as the studies with bacteria and cyanobacteria, support the finding that this novel disinfection system is suitable for various target microorganisms and may be suitable for practical application in drinking water treatment plants in the future.

II. Redesigning water disinfection using recyclable nanomaterials and metal ions: evaluation with *Escherichia coli*

Material from:

Gao, Q. and Keller, A.A.. Redesigning water disinfection using recyclable nanomaterials and metal ions: evaluation with *Escherichia coli*. *ACS ES&T Water* **1,** 185-194 (2021).

Abstract We present a novel disinfection method that redesigns the conventional approach, by recycling the disinfectant. This can lead to lower energy requirements and minimize environmental impacts. In this study, metal ions were mixed with target microorganisms in water for disinfection, followed by the sorption of metal ions with magnetic nanoparticles for reuse. As a proof of concept, the disinfection effectiveness of various metal ions (e.g. Ag^+, Cu^{2+} and Zn^{2+}) on a target microorganism, *E. coli* K12, were compared. Only Ag^+ exhibited a bactericidal effect on *E. coli* K12, while Cu^{2+} and Zn^{2+} just reduced the growth rate. Disinfection efficiency of Ag^+ remained stable within a range of environmental conditions (pH, temperature, water hardness, nutrient content and initial cell concentration) indicating that Ag^+ speciation and effectiveness is not modified. The initial ratio of Ag^+ per cell is a major factor that will determine disinfection effectiveness. Sorption of Ag^+ by one type of magnetic nanomaterial (Mag-Ligand) was studied to explore the removal of Ag^+ after disinfection. Mag-Ligand can effectively reduce the concentration of Ag^+ from 100 mg/L to nearly 100 μg/L in one cycle, and below 10 μg/L in three recovery cycles. Changes in environmental conditions (pH, concentration of Cl^-, water hardness and addition of *E. coli* K12) were studied to determine how these changes will affect the sorption process. Results

showed that sorption capacity will be influenced when the concentration of free Ag^+ is reduced (e.g. when Cl^- concentration is elevated), or when there are competitive metal ions in the aqueous environment (i.e. water hardness). Sorption efficiency remained stable when the speciation of Ag^+ was not influenced (e.g. pH and addition of *E. coli* K12). The regeneration of Ag^+ was studied to evaluate the reuse of disinfectant. We demonstrate that Ag^+ can be recovered after sorption in an acidic environment, and the recovery remains above 80% after 5 continuous cycles, indicating that this disinfection method may be sustainable for practical use.

A. Introduction

Waterborne pathogens are one of the major sources of microbial contamination in water. The US Environmental Protection Agency (EPA) has determined that over 500 waterborne pathogens can increase human health risk by spreading diseases in drinking water.[1] Among various waterborne pathogens, *Escherichia coli* (*E. coli*) is a ubiquitous and widely studied bacterium. *E. coli* is a rod-shaped, Gram-negative bacterium which is commonly found in the lower intestine of warm-blooded organisms [45]. As one of the most common microbial contaminants in natural waters, *E. coli* is usually used as an indicator organism to evaluate the effectiveness of water disinfection [46-47]. Although most strains of *E. coli* are harmless, there are some pathogenic strains that can cause severe diseases (such as diarrhea) and are a major concern in public health [48-50]. For example, an outbreak of diarrheagenic *E. coli* occurred on June 8, 2015, when a group of middle school students from Korea developed diarrhea and vomiting after attending a school camp. Further microbiological analysis of patient stools and environmental water samples indicated that the contamination of water bodies by enterohemorrhagic *E. coli*, enteropathogenic *E. coli* and enteroaggregative *E. coli*

were responsible for this outbreak [51]. Another outbreak of pathogenic *E. coli* happened in Japan in April and May 2011, when 181 patients suffered from serious food-poisoning because of the enterohemorrhagic *E. coli* strains *O111:H8* and *O157:H7* from raw beef dishes [52]. Since the outbreak of pathogenic *E. coli* may lead to severe bloody diarrhea and haemolytic uraemic syndrome (HUS) [4], it is essential to develop efficient disinfection approaches, to improve water quality and protect human health.

Disinfection methods have been explored, studied, and developed ever since ancient times. Several important factors need to be considered when choosing disinfection treatment, including water characteristics, final effluent quality, disinfectant agent toxicity, disinfection byproducts formation, local characteristics and energy and other costs [11]. Based on these needs, many disinfection technologies have been explored and developed for different environmental purposes. Traditional disinfection technologies include chlorination, ozonation and ultraviolet (UV) radiation. While traditional disinfection processes have demonstrated very good performance, the disadvantages of these conventional methods cannot be ignored. For example, chlorine may react with natural organic matter (NOM) in the source water and produce disinfection byproducts (DBPs) during the disinfection process [53], and some DBPs have proven to be toxic and will threaten human health [13]. To overcome the issues related to production of DBPs [20], high energy cost [54], frequent maintenance [18-19] and other aspects [24, 55], a number of novel disinfection methods have been explored in recent years, among which the application of nanotechnology in disinfection has generated considerable interest. In some studies, nanomaterials are embedded in water treatment membranes for disinfection and purification [38, 41-42]. However, since the technology relies on the release of metal ions, which are left in the treated water, these nanotechnologies have a

relatively short life and must be replaced frequently. The metal ion is completely lost, remains in the treated water, passes through the human body and eventually is discharged to the environment, with a single use. Dissolution and leakage of the nanomaterials does not only reduce the disinfection efficiency of the filters and membranes for future use, but also threatens ecological health when these waters eventually reach the environment [56]. Separation of nanoparticles from water after disinfection is another challenge, due to their nano-scale, and cannot be efficiently separated from water by classic water treatment [43]. In addition, the cost of synthesizing these nanocomposite filters and membranes is a major concern for practical applications [11].

Given the issues related to microbial contamination of water sources, the need to meet more stringent requirements, as well as the disadvantages of current disinfection processes, we propose a radically different and sustainable disinfection method, using metal ions as the disinfectant, to be recovered through sorption after disinfection by magnetic nanoparticles coated with chelating agents, and recovered under proper conditions for reuse. The objectives of this study were to: (1) investigate the disinfection effects with metal ions on target microorganisms, and evaluate the influence of different environmental conditions (e.g. pH, temperature, water hardness); (2) study the sorption of metal ions with magnetic nanoparticles, and the influence of different environmental conditions on this process; and (3) explore the conditions needed to recover the metal ions from the magnetic nanoparticles for reuse.

B. Materials and Methods

1. Materials

Escherichia coli K-12 Strain (*E. coli* K12) was purchased from Carolina Biological Supply (USA) and was used as a target microorganism in this study. Tryptic soy broth (TSB) and tryptic soy agar, silver nitrate, copper sulfate, zinc chloride, nitric acid, sulfuric acid, sodium hydroxide, sodium chloride, and calcium carbonate were purchased from Fisher Scientific (USA). The recipe of TSB is shown in Table S1 (Supporting Information). Sodium dihydrogen phosphate was purchased from Acros Organics (Geel, Belgium). Mag-Ligand was synthesized using the method developed in our previous study[57], and the maghemite (iron (III) oxide) nanoparticles (30 nm in diameter) used for synthesis were purchased from Alfa Aesar (USA). In brief, the maghemite nanoparticles were dispersed in toluene and coated with amino groups by mixing with (3-aminopropyl) triethoxysilane and refluxed in a water bath (90 °C) for 2 h. After cooling down to room temperature, ethylenediaminetetraacetic acid (EDTA) and pyridine were added to the solution to make the maghemite nanoparticles functionalized with EDTA. The pH of the solution was adjusted, and the synthesized magnetic nanoparticles were rinsed and dried under room temperature. All chemicals were used as received without further purification. All solutions were prepared with deionized water (18 MΩ-cm) from a Barnstead NANOpure Diamond Water Purification System (USA).

2. Disinfection of *E. coli* K12 with Ag^{+}, Cu^{2+} and Zn^{2+}

Stock culture of *E. coli* K12 was prepared by inoculating the *E. coli* K12 strains in 50 mL of TSB medium and growing them at room temperature (20 °C) with constant shaking (200

rpm) overnight. 2 mL of stock culture were transferred into 50 mL of fresh TSB medium and inoculated for 1 h before disinfection, to make sure the growth of *E. coli* K12 was within the exponential phase. After inoculating, the culture was centrifuged at 5000 rpm for 10 min, and the supernatant was disposed. The pellet was then washed with TSB medium for 2-3 times and then re-dispersed and diluted with fresh TSB medium until the optical density at 600 nm (OD_{600}) of the diluted sample reached 0.05. The OD_{600} of bacterial samples were determined by a UV-1800 UV-Vis Spectrophotometer (Shimadzu Scientific Instruments Inc).

The disinfection of *E. coli* K12 was performed in 24-well tissue culture plates. Silver nitrate, copper sulfate, and zinc chloride were utilized as disinfectants. An *E. coli* K12 solution with an OD_{600} of around 0.045 was exposed to Ag^{+}, Cu^{2+} and Zn^{2+} at different concentrations (5-100 mg/L for Ag^{+}, 5-500 mg/L for Cu^{2+} and Zn^{2+}) for different contact times (up to 10 h) in TSB medium. The OD_{600} of each sample was measured after exposure.

Different operating conditions for disinfection were tested to explore their influence on disinfection. Temperature, pH, water hardness and nutrient content are typical aqueous environmental conditions that need to be considered. Thus, each of the conditions was changed within a proper range. The pH of the TSB medium was adjusted from 6 to 8 using 0.1 M nitric acid and 0.1 M sodium hydroxide, and temperature was adjusted from 10 °C to 30 °C. $CaCO_3$ was used to adjust the water hardness within a range from 50 mg/L to 200 mg/L, to simulate conditions from soft to moderately hard, hard, and very hard. The disinfection process was done at different nutrient content levels by diluting the TSB medium with deionized water to different percentages (full strength = 100%, 60% and 10%) to determine how this factor will influence disinfection effectiveness. In addition, the initial

OD_{600} of *E. coli* K12 was adjusted to different levels (0.013, 0.065 and 0.13) as well, to explore the differences in disinfection effectiveness.

3. Batch sorption of Ag^+ with Mag-Ligand

Adsorption of Ag^+ with Mag-Ligand was evaluated under different conditions. Different amounts of Mag-Ligand particles (50.0-200.0 mg) were mixed with 20 mL of Ag^+ solution (100 mg/L) in 20 mL glass vials, and the vials were placed in an end-over-end shaker on a Dayton-6Z412A Parallel Shaft (USA) roller mixer with a speed of 70 rpm at room temperature (22-25 °C) for 24 h to ensure sufficient equilibration time. Adsorption kinetics studies were carried out with the mixture of 20.0 mg Mag-Ligand and 20 mL Ag^+ solution (100 mg/L) at the same conditions but for a set amount of time, varying from 30 min to 24 h. All the studies were done at pH = 7 and room temperature. After mixing well, the Mag-Ligand particles were separated from the aqueous phase with an Eclipse magnet. Samples were collected from the supernatant and diluted with 2% HNO_3. Then the concentration of Ag^+ in the samples was analyzed by an Agilent 7900 (Agilent Technologies) inductively coupled plasma mass spectrometer (ICP-MS).

Influence of different environmental conditions on the removal efficiency of Ag^+ by Mag-Ligand, including pH, concentration of Cl^-, water hardness and the presence of bacterial cells, were studied as well. pH was adjusted to the desired condition (range from 6 to 8) by using sodium dihydrogen phosphate buffer. Different concentrations of Cl^- (1-100 mg/L) were added into the mixture to explore the possible influence on sorption, as different combinations of Cl^- and Ag^+ may affect the sorption behavior of Mag-Ligand. $CaCO_3$ with the range of concentration from 50 mg/L to 200 mg/L was used to adjust water hardness. In other experiments, different concentrations of bacteria (10^2-10^6 colony forming units

(CFU)/mL of *E. coli* K12) were introduced to the sorption system, to determine if the presence of bacteria would influence the sorption process.

4. Regeneration and reuse of Ag^+

To investigate the regeneration and reuse of Ag^+ after sorption with Mag-Ligand, 100 mg/L Ag^+ were adsorbed onto the Mag-Ligand particles, followed by separation of Mag-Ligand from solution with the handheld magnet. The Mag-Ligand collected was then washed with 0.01 M H_2SO_4 (pH=1.70) for 30 min at room temperature, and the Ag^+ concentration in the supernatant solution was determined by ICP-MS. The acid-washed Mag-Ligand particles were then reused for subsequent Ag^+ sorption experiments and the sorption, extraction, and reuse processes were repeated for five times.

5. Data analysis

All tests in this study were performed in triplicate and analysis of variance (ANOVA) was used to test the significance of results. A $p<0.05$ was considered to be statistically significant. The p values of each test are listed in Table 4, 6 and 9.

C. Results and discussions

1. Disinfection of *E. coli* K12 with metal ions

1.1 Comparison of disinfection effect with various metal ions

Results of disinfection with Ag^+, Cu^{2+} and Zn^{2+} at different concentrations and contact times are shown in Figure 1. Generally, the effectiveness of a disinfectant on its target can be described as bacteriostatic or bactericidal. Bacteriostatic refers to the phenomenon that bacteria are inhibited partially or totally from reproducing by the addition of disinfectant, and

bactericidal means killing the bacteria [58]. In this study, the effectiveness of disinfection was determined by comparing the OD_{600} of samples exposed to disinfectants with that of the control at the same contact time. Measurement of OD_{600} is a common technique to estimate the concentration of bacteria in microbiology, as the OD_{600} is quantitatively related to the biomass in cell suspension within a certain range [59]. Although OD_{600} cannot provide quantitative information about the living cells in samples, it can serve to determine whether the growth of bacteria is influenced by the disinfectants. An increase in OD_{600} correlates linearly with an increase of living cells within the experimental range, while a decrease in OD_{600} indicates there are fewer cells, likely since cell death occurred. Results of disinfection of *E. coli* K12 showed that the effectiveness is related to both the type and concentration of metal ions. As shown in Figure 1, addition of Cu^{2+} and Zn^{2+} only slowed the growth rate of *E. coli* K12 compared to that in the control group. However, no bacteriostatic or bactericidal effect was found at any concentration (5-500 mg/L in this study), as the OD_{600} increased continuously at longer contact times. Compared to Cu^{2+} and Zn^{2+}, Ag^{+} had much better disinfection efficacy. Cu^{2+} has a stronger disinfection ability on *E. coli* K12 than Zn^{2+}, as the growth rate of *E. coli* K12 exposed to Zn^{2+} was closer to the control than that exposed to Cu^{2+}. As shown in Figure 1 (D), the bactericidal effect appeared when the concentration of Ag^{+} was above 20 mg/L, and the effect was more noticeable at a higher concentration of Ag^{+}. Thus, the disinfection efficacy for these metal ions follows the order: $Ag^{+}>>Cu^{2+}>Zn^{2+}$. The reason for the difference of disinfection ability between Ag^{+}, Cu^{2+} and Zn^{2+} is mainly due to the mechanisms of interaction with cells [60]. Ag^{+} has several ways to interfere with the metabolism of cells and destroy the cell structure by binding with membranes, enzymes, nucleic acid and other cellular components. Compared to Ag^{+}, Cu^{2+} is not so effective in

inactivating cells as the main mechanism is just increasing intracellular reactive oxygen species and impairing cell membranes. Zn^{2+} has the weakest ability to inactivate cells compared with Ag^{+} and Cu^{2+}, as Zn^{2+} can only deplete the total cellular thiols to achieve protein dysfunction.

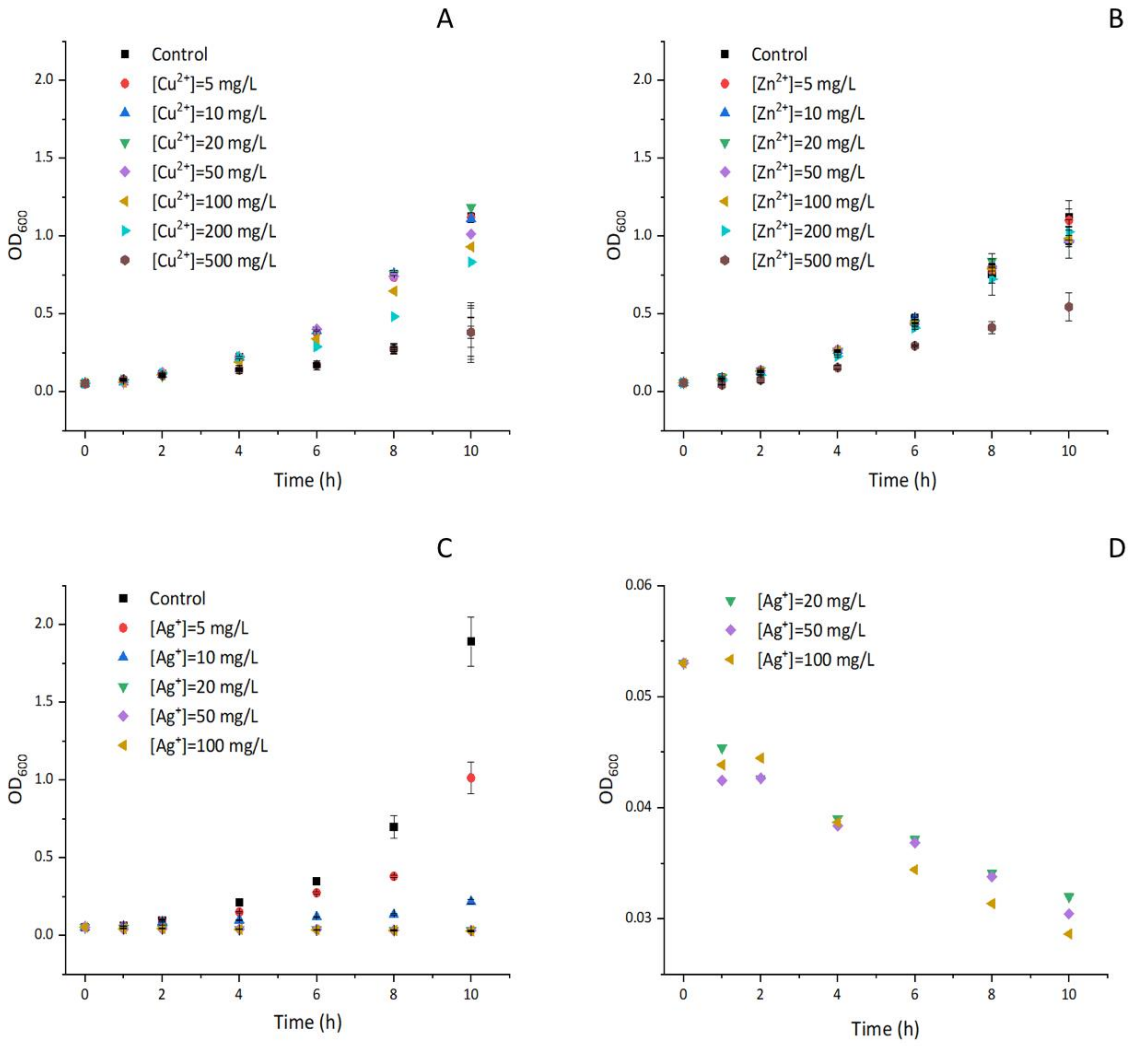

Figure 1. Disinfection effect on *E. coli* K12 (initial OD_{600}=0.053) with (A) Cu^{2+} (5-500 mg/L); (B) Zn^{2+} (5-500 mg/L); (C) Ag^{+} (5-100 mg/L); and (D) Ag^{+} (20-100 mg/L), to show more detail for this range of concentrations.

Table 1. Detailed results about the disinfection effect on *E. coli* K12 with Ag^{+}, Cu^{2+} and Zn^{2+} at different concentrations.

[Metal ions] (mg/L)		OD_{600}						
		t=0 h	t=1 h	t=2 h	t=4 h	t=6 h	t=8 h	t=10 h
Ag^{+}	0	0.053± 0.000	0.061± 0.002	0.096± 0.002	0.213± 0.004	0.348± 0.002	0.697± 0.072	1.890± 0.157
	5	0.053± 0.000	0.060± 0.000	0.094± 0.007	0.150± 0.004	0.274± 0.007	0.380± 0.007	1.013± 0.101
	10	0.053± 0.000	0.059± 0.001	0.087± 0.018	0.099± 0.004	0.119± 0.003	0.134± 0.006	0.217± 0.015
	20	0.053± 0.000	0.045± 0.000	0.043± 0.002	0.039± 0.000	0.037± 0.001	0.034± 0.001	0.032± 0.000
	50	0.053± 0.000	0.042± 0.002	0.043± 0.000	0.038± 0.002	0.037± 0.002	0.034± 0.004	0.030± 0.000
	100	0.053± 0.000	0.044± 0.000	0.044± 0.001	0.038± 0.001	0.037± 0.003	0.034± 0.000	0.030± 0.004
Cu^{2+}	0	0.054± 0.000	0.070± 0.001	0.115± 0.002	0.220± 0.009	0.393± 0.005	0.756± 0.008	1.117± 0.032
	5	0.054± 0.000	0.062± 0.002	0.114± 0.015	0.222± 0.008	0.380± 0.006	0.736± 0.018	1.120± 0.156
	10	0.054± 0.000	0.061± 0.005	0.110± 0.001	0.221± 0.004	0.392± 0.001	0.759± 0.013	1.110± 0.191
	20	0.054± 0.000	0.061± 0.002	0.102± 0.003	0.214± 0.006	0.384± 0.004	0.755± 0.034	1.184± 0.040
	50	0.054± 0.000	0.061± 0.000	0.123± 0.002	0.220± 0.010	0.401± 0.013	0.741± 0.006	1.013± 0.172
	100	0.054± 0.000	0.061± 0.002	0.108± 0.011	0.191± 0.001	0.340± 0.007	0.647± 0.034	0.930± 0.192
	200	0.054± 0.000	0.075± 0.006	0.118± 0.012	0.224± 0.026	0.289± 0.017	0.483± 0.021	0.833± 0.098
	500	0.054± 0.000	0.080± 0.009	0.106± 0.011	0.142± 0.012	0.171± 0.029	0.275± 0.030	0.382± 0.095

Zn^{2+}	0	0.058± 0.000	0.090± 0.009	0.129± 0.003	0.255± 0.005	0.472± 0.009	0.756± 0.060	1.117± 0.055
	5	0.058± 0.000	0.083± 0.004	0.136± 0.013	0.269± 0.000	0.454± 0.008	0.781± 0.040	1.100± 0.125
	10	0.058± 0.000	0.087± 0.001	0.132± 0.002	0.265± 0.007	0.472± 0.006	0.808± 0.004	0.977± 0.025
	20	0.058± 0.000	0.089± 0.004	0.136± 0.001	0.259± 0.002	0.439± 0.005	0.840± 0.046	0.956± 0.101
	50	0.058± 0.000	0.086± 0.003	0.136± 0.001	0.268± 0.003	0.433± 0.008	0.803± 0.049	0.966± 0.036
	100	0.058± 0.000	0.081± 0.000	0.132± 0.004	0.263± 0.002	0.419± 0.002	0.791± 0.013	0.983± 0.053
	200	0.058± 0.000	0.078± 0.013	0.107± 0.003	0.229± 0.008	0.411± 0.007	0.724± 0.102	1.027± 0.081
	500	0.058± 0.000	0.044± 0.003	0.076± 0.019	0.155± 0.012	0.296± 0.006	0.412± 0.039	0.545± 0.092

To further study the disinfection ability of Ag^{+}, we measured the survival kinetics of *E. coli* K12 exposed to a high concentration of Ag^{+} (100 mg/L) and long contact time (up to 32 h). Samples were collected and measured every 4 h (Figure 2). OD_{600} decreased until a contact time of 16 h, indicating that cells were killed by Ag^{+} during this time, and the death of *E. coli* K12 increased with longer contact time. However, after 16 h contact, the OD_{600} remained at a stable level (around 0.020) with a slight variance. To confirm if the cells were still alive after 16 h of contact time, an aliquot (0.1 mL) of the sample was transferred onto a tryptic soy agar plate for plate counting. The tryptic soy agar plate was then cultured on the incubator with a shaking speed of 200 rpm under 20 °C for more than 48 h, until colonies formed on the agar plate. Results of the plate counting test are shown in the Supplementary Information (Figure S1). Based on plate counting, the concentration of living cells after 16 h

of treatment with 100 mg/L Ag^+ decreased to 170 CFU/mL, slightly above the EPA standard (<126 CFU/100 mL) [61]. This may be due to precipitation of Ag^+ over time, which reduces the availability of disinfectant.

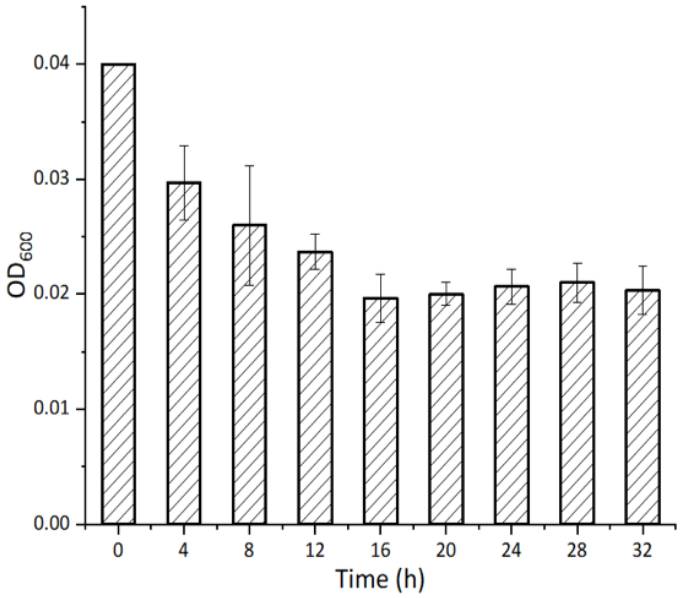

Figure 2. Disinfection kinetics with 100% nutrient and [Ag^+] = 100 mg/L (initial OD_{600}=0.04).

Table 2. Detailed results about the disinfection kinetics with 100% nutrient and [Ag^+] = 100 mg/L

Time (h)	OD_{600}
0	0.040±0.000
4	0.297±0.003
8	0.026±0.005
12	0.024±0.002
16	0.020±0.002
20	0.020±0.001

24	0.021±0.002
28	0.021±0.002
32	0.020±0.002

1.2 Influence of different environmental conditions on disinfection

1.2.1 Initial cell concentration

Different initial concentrations of *E. coli* K12 (initial OD_{600} = 0.013, 0.065 and 0.13) were studied, at [Ag^+] =100 mg/L and 4 h contact time, to explore their effect on disinfection effectiveness. As shown in Figure 3, the effectiveness of disinfection on *E. coli* K12 is influenced by the initial cell concentration. Under the same Ag^+ dosing, a lower initial OD_{600} (0.013) resulted in a larger decrease in final OD_{600} (around 34% of initial OD_{600}) compared to the higher initial OD_{600} (0.13) where the final OD_{600} was around 76% of initial OD_{600}. In all treatment cases, the final OD_{600} was less than the initial OD_{600}, which was not the case for the control. Note that even dead cells contribute to OD_{600}, but as shown above, the CFU can be quite low after treatment. This is supported by previous research stating that the disinfection effect is determined by the initial level of silver per cell [62], and a higher initial level of silver will lead to a more rapid disinfection process.

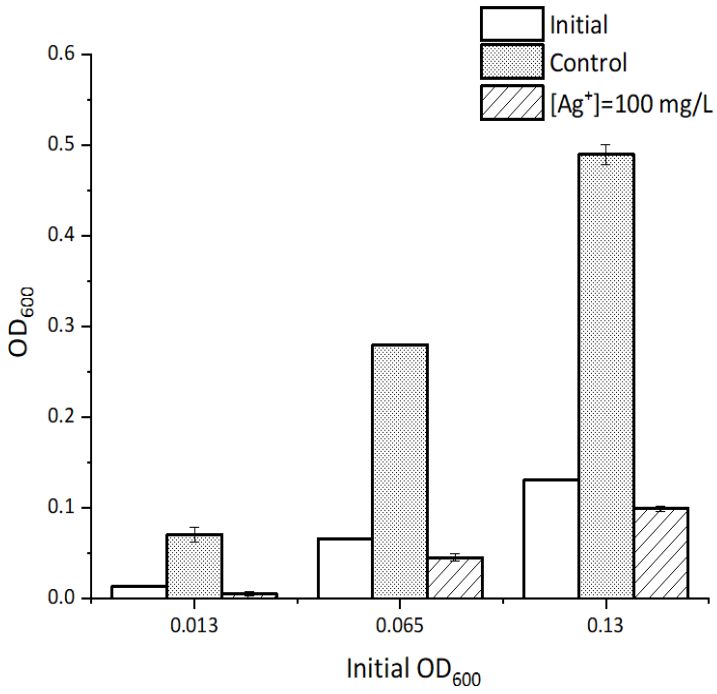

Figure 3. Comparison of disinfection effectiveness at [Ag^+] =100 mg/L, 4 h contact time and different initial OD_{600}.

Table 3. Detailed results about the comparison of disinfection effectiveness at [Ag^+] =100 mg/L, 4 h contact time and different initial OD_{600}.

Initial OD_{600}	End OD_{600}	
	Control	[Ag^+]=100 mg/L
0.013	0.070±0.008	0.004±0.003
0.065	0.280±0.000	0.045±0.004
0.130	0.489±0.011	0.099±0.003

1.2.2 pH

Effectiveness of disinfection at [Ag^+] =100 mg/L, 4 h contact time and initial OD_{600} = 0.043 under different pH (6, 7 and 8) was evaluated. As shown in Figure 4 (A), after 4 h the increase in OD_{600} in the control group was a function of initial pH. A more acidic

environment (pH = 6) decreased the growth rate of *E. coli* K12, compared to alkaline or neutral conditions. In the group exposed to Ag^+, there was a decrease of OD_{600} (from 0.043 to 0.029 at pH=6, from 0.043 to 0.028 at pH=7 and from 0.043 to 0.026 at pH=8) after the treatment. However, the differences in final OD_{600} between treatments were not significant ($p=0.057>0.05$). Ag^+ is a stable species in the environment at pH from 6 to 8 [63], leading to a stable disinfection effectiveness for *E. coli* K12.

1.2.3 Water hardness

Water hardness, usually expressed as the concentration of $CaCO_3$ in water, is one of the main environmental factors that determine the quality of freshwater. In this study, different concentrations of $CaCO_3$ (50, 100 and 200 mg/L) were added to simulate different degrees of water hardness. As shown in Figure 4 (B), the addition of $CaCO_3$ slightly influences the final OD_{600} in the control. However, no influence on the disinfection effectiveness was observed under different water hardness ($p=0.063>0.05$), as the addition of $CaCO_3$ did not change the speciation or concentration of Ag^+. This confirms a previous study on the disinfection effectiveness of Ag^+ even when the water is very hard [64]. Thus, water hardness will not influence the disinfection process.

1.2.4 Temperature

Different temperatures (10, 20 and 30 °C) were considered to explore their influence on disinfection effectiveness. As shown in Figure 4 (C), temperature is a factor that will affect the growth of *E. coli* K12. At a low temperature (10 °C), the final OD_{600} of the control is lower than the initial OD_{600}, indicating that a cold environment will inhibit the growth of *E. coli* K12. At higher temperatures (20 or 30°C), the final OD_{600} of *E. coli* K12 in control

increased, and growth was accelerated by an increase in temperature, while the temperature is below optimal (37 °C for *E. coli*) [65]. Based on the result that disinfection efficacy decreases with higher cell concentration (Figure 3), it is reasonable that the efficacy is lower at a higher temperature than that at a lower temperature (Figure 4 (D)).

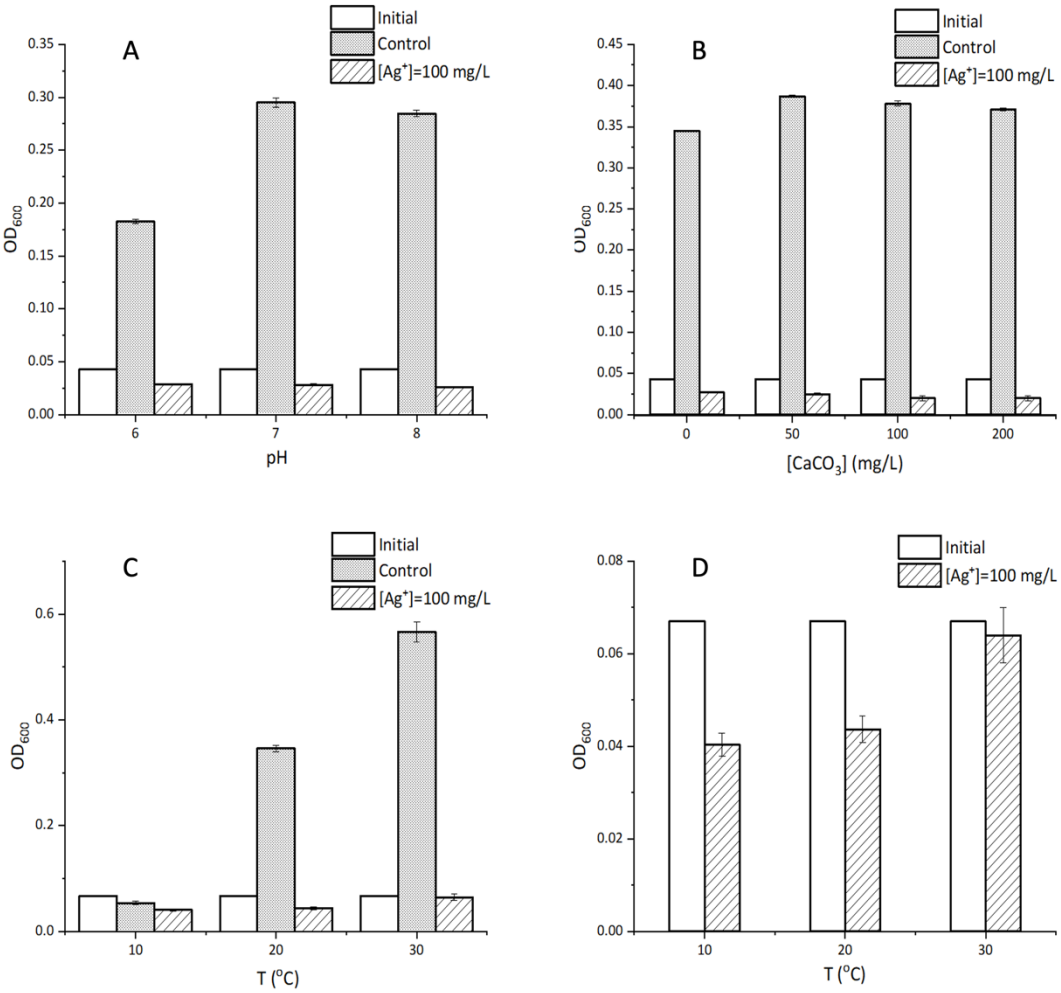

Figure 4. Disinfection effectiveness as a function of (A) pH; (B) water hardness; and (C) temperature with [Ag^+] =100 mg/L and 4 h contact time (initial OD_{600}=0.043, 0.043 and 0.067 respectively). (D) Detail on OD_{600} for the Ag^+ treatment condition at different temperatures.

Table 4. Detailed results and p value tests about the disinfection effectiveness as a function of pH, water hardness and temperature ($p < 0.05$ is considered to be statistically significant).

Environmental Conditions		OD_{600}		p value ($[Ag^+]$=100 mg/L)	Statistical Significance
		Control	$[Ag^+]$=100 mg/L		
pH	6	0.183±0.002	0.029±0.000	0.057	Statistically not significant
	7	0.295±0.005	0.028±0.001		
	8	0.285±0.003	0.026±0.000		
[CaCO3] (mg/L)	0	0.345±0.000	0.027±0.001	0.063	Statistically not significant
	50	0.387±0.001	0.025±0.001		
	100	0.378±0.003	0.022±0.003		
	200	0.371±0.000	0.022±0.003		
Temperature (C)	10	0.054±0.003	0.040±0.003	0.001	Statistically significant
	20	0.346±0.006	0.044±0.003		
	30	0.566±0.019	0.064±0.006		

1.2.5 Nutrient content

Nutrient content is another environmental factor that may affect the disinfection process, as it influences the degree to which bacteria grow in the aqueous environment. Some organic matter in water may be utilized by bacteria as nutrients and result in an outbreak. In this study, TSB medium with organic matter such as tryptone and glucose is used for the culture of *E. coli* K12, to provide an environment with abundant nutrients. However, the nutrient content in water samples from natural environments is usually not as rich as the laboratory conditions. Thus, a batch of experiments with different concentration of medium were done to explore the possible influence of organic matter as nutrients. The TSB medium (full strength = 100%) was diluted using deionized water to different degrees (60% and 10% of original) for the study, and the experiment was done with $[Ag^+]$ =100 mg/L, initial OD_{600}=0.062 and up to 32 h contact time. As shown in Figure 5 (A) which is the disinfection

effectiveness at 24 h contact time, the change in nutrient content did influence the growth rate of *E. coli* K12 in both unexposed and exposed cells, but in quite different ways. In the unexposed group (control), the final OD_{600} in different nutrient conditions follow the order: 100% nutrient>60% nutrient>10% nutrient, indicating that the nutrient conditions and growth of *E. coli* K12 have positive correlation; more nutrients, more growth. However, in the group exposed to 100 mg/L Ag^+ (Figure 5 (B)) the final OD_{600} and different nutrient conditions followed the order: 10% nutrient>60% nutrient>100% nutrient. A possible explanation may be that a low nutrient environment stimulates the metabolism of bacteria [66], making it more difficult to destroy the cell structure and thus reducing the effectiveness of disinfection.

The contact time was extended to determine if the OD_{600} would remain stable after enough contact time (up to 32 h) with 100 mg/L Ag^+ in 10%, 60% and 100% nutrient conditions (Figure 5 (C)). The time needed for OD_{600} to reach a stable level in various treatments was different. In the treatment with 10% nutrient, the OD_{600} decreased by 22.6% in 24 h and remained stable at the low level (OD_{600}=0.048, p=0.198>0.05). In the treatment with 60% nutrient, it took 24 h for the OD_{600} to reach a stable level of 0.047 (p=0.332>0.05) with a decrease of 24.2% compared to the initial OD_{600}. In the treatment with 100% nutrient, the decrease in OD_{600} at early stage (<16 h) was more significant (27.4%) than for nutrient-poor conditions, and the OD_{600} remained at 0.045 after 16 h (p=0.211>0.05). Thus, disinfection effectiveness reaches a stable level faster in a nutrient-rich environment than in nutrient-poor conditions.

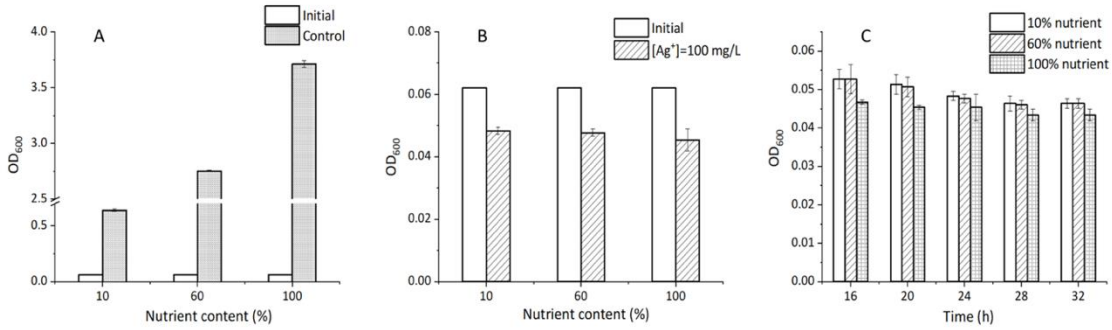

Figure 5. Disinfection tests under various nutrient contents with [Ag^+] =100 mg/L, initial OD_{600}=0.062 and 24 h contact time. (A) Influence of nutrient content on growth rate in control. (B) Influence of nutrient content on disinfection effectiveness. (C) Comparison of survival kinetics with different nutrient conditions (10%, 60% and 100%).

Table 5. Detailed results about the disinfection test under different nutrient conditions (10%, 60% and 100%).

Time (h)	OD_{600}		
	Nutrient content=10%	Nutrient content=60%	Nutrient content=100%
16	0.053±0.003	0.053±0.004	0.047±0.000
20	0.051±0.003	0.051±0.003	0.045±0.000
24	0.048±0.001	0.048±0.001	0.045±0.004
28	0.046±0.002	0.046±0.001	0.043±0.002
32	0.046±0.001	0.046±0.001	0.043±0.002

Table 6. P value tests about the disinfection test under different nutrient conditions (10%, 60% and 100%), $p<0.05$ is considered to be statistically significant.

Environmental Condition	p value test	Statistical Significance
Nutrient content (10%, >24 h)	0.198	Statistically not significant
Nutrient content (60%, >24 h)	0.332	Statistically not significant
Nutrient content (100%, >16 h)	0.210	Statistically not significant

2. Sorption of metal ions with Mag-Ligand

2.1 Sorption isotherm and kinetics

Sorption of Ag^+ (100 mg/L) at different concentrations of Mag-Ligand (2.5-10 g/L) at pH=7 and room temperature were studied. As shown in Figure 6 (A), removal efficiency of Ag^+ increased substantially with higher adsorbent dosage up to 5 g/L, reaching 96%. Above 5 g/L the removal efficiency increased asymptotically up to 98.3%, probably due to the challenge of keeping the Mag-Ligand particles suspended at concentrations above 5 g/L.

Kinetics of sorption of 100 mg/L Ag^+ with Mag-Ligand (2.5 g/L) were studied at pH=7 and room temperature (Figure 6 (B)). Rapid sorption occurred, with removal efficiency reaching a maximum of 55% at this dosage within 3 h. The results are consistent with our previous study on Mag-Ligand kinetics with other metal ions [57]. The kinetics is influenced by the amount of EDTA coated on Mag-Ligand, as well as the affinity between metal ions and EDTA [67].

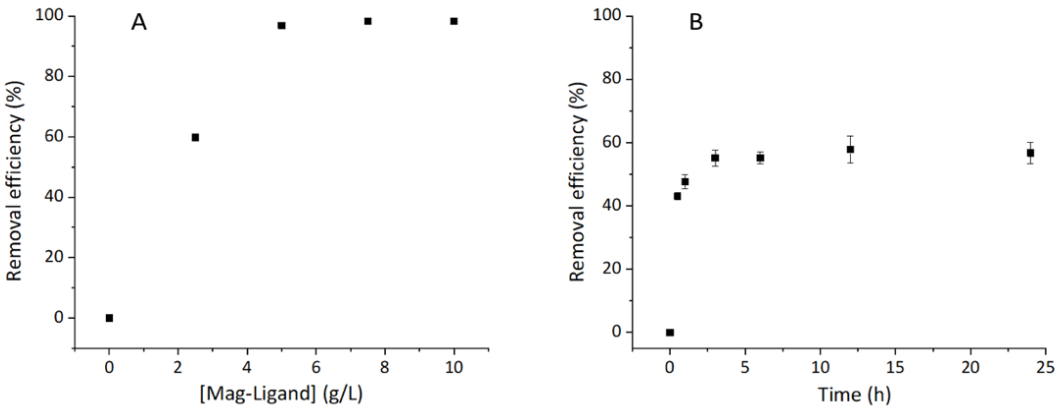

Figure 6. (A) Adsorption of Ag^+ onto Mag-Ligand as a function of adsorbent dose with [Ag^+] =100 mg/L. (B) Ag^+ sorption uptake versus time (with [Ag^+] =100 mg/L and [Mag-Ligand] =2.5 g/L).

Table 7. Detailed results about the adsorption of Ag^+ onto Mag-Ligand versus adsorbent dose or time.

Sorption Process		Removal Efficiency (%)
[Mag-Ligand] (g/L)	0	0.00±0.00
	2.5	59.76±0.10
	5	96.87±0.05
	7.5	98.32±0.04
	10	98.33±0.19
Time (h)	0	0.00±0.00
	0.5	43.05±0.81
	1	47.63±2.29
	3	55.16±2.53
	6	55.21±1.85
	12	57.80±4.34
	24	56.73±3.36

As discussed above, the removal efficiency reaches an asymptotic level of 98.3% even with increasing Mag-Ligand dose. However, the residual concentration of Ag^+ is above the USEPA secondary maximum contaminant standard (100 µg/L) [68]. To reduce the concentration of Ag^+ below 100 µg/L, another experiment was performed, with the same total dosage of Mag-Ligand but applied in separate sorption cycles. The total dosage of Mag-Ligand was 10 g/L, and the initial Ag^+ concentration = 100 mg/L. Three different sorption experiments were evaluated: (1) 10 g/L in 1 cycle; (2) 7.5 g/L in cycle 1 and 2.5 g/L in cycle 2; and (3) 5 g/L in cycle 1, 2.5 g/L in cycle 2 and 2.5 g/L in cycle 3. In experiments (2) and

(3), after allowing sorption to reach equilibrium (24 h) the Mag-Ligand were separated from the suspension using a magnet, and immediately after additional Mag-Ligand was dosed as indicated above. Samples were collected after each cycle, and the concentration of Ag^+ was measured. As indicated in Table 8, the concentration of Ag^+ decreases to 7 μg/L after 3 sorption cycles. Compared to the sorption with just 1 cycle, the removal effectiveness was substantially improved without increasing total Mag-Ligand dose. Further study showed that the concentration of Ag^+ can be reduced to below the secondary MCL after 3 sorption cycles with shorter time (2 h for each cycle, Table S2). Thus, increasing the number of sorption cycles can decrease [Ag^+] well below the secondary MCL; further optimization could be done to determine the minimum total Mag-Ligand dosage and sorption time, depending on conditions.

Table 8. Concentration of Ag^+ (mg/L) after different continuous sorption cycles.

Mag-Ligand dose	[Ag^+] after sorption (mg/L)		
	Cycle 1	Cycle 2	Cycle 3
10 g/L in one cycle	1.66		
7.5 g/L in cycle 1 + 2.5 g/L in cycle 2	1.67	0.11	
5 g/L in cycle 1 + 2.5 g/L in cycle 2 + 2.5 g/L in cycle 3	3.11	0.14	0.007

2.2 Influence of different environmental conditions on adsorption

2.2.1 pH

The influence of pH on the adsorption process of Ag^+ with Mag-Ligand was evaluated with 100 mg/L Ag^+ and 5 g/L Mag-Ligand (Figure 7). Removal efficiency remained stable at around 96%-97% when the pH varied from 6 to 8 ($p=0.179>0.05$) (Figure 7 (A)). This is mainly due to the sorption mechanism of Ag^+ and EDTA. The complex formation constant, $K_{Ag\text{-}EDTA}$, of Ag^+ and EDTA is very high with log ($K_{Ag\text{-}EDTA}$) = 7.20 [67], indicating that Ag^+ forms a stable complex with the EDTA coated on the surface of Mag-Ligand, resulting in high removal efficiency. Since the change in pH in the range of 6-8 does not affect the aqueous speciation of Ag^+ [69], the removal efficiency is not influenced.

2.2.2 Cl^-

Different concentrations of Cl^- (1, 10 and 100 mg/L) were considered to explore the influence on the adsorption process, as the presence of Cl^- could affect the speciation of Ag^+ by forming AgCl precipitates or an $AgCl_2^-$ complex in water, thus affecting the removal via Mag-Ligand. The addition of Cl^- reduced the removal of Ag^+ via adsorption (Figure 7 (B)). At a low Cl^- level (1 mg/L), a small percentage of Ag^+ (1.56% of initial Ag^+) will combine with Cl^- to form AgCl precipitates. This is calculated using the solubility product constant, K_{sp}, of AgCl, which is $1.77*10^{-10}$ at room temperature [70]. After sorption, 93.94% of the initial Ag^+ ions were captured by Mag-Ligand. When the concentration of Cl^- was increased to 10 mg/L, the percentage of Ag^+ in AgCl(s) increased to 27.63%, and the percentage adsorbed on Mag-Ligand decreased to 61.01%. Although AgCl(s) could be removed in the slurry in a commercial operation, the presence of Cl^- would result in a small loss of Ag^+ for reuse

directly. It may be possible to re-dissolve Ag^+ from the slurry for reuse; this was not evaluated here. At a concentration of Cl^- of 100 mg/L, soluble $AgCl_2^-$ ($logK_{AgCl2}$-=5.25) may form [71]. The Cl^- in water will compete with EDTA coated on nanoparticles to form a complex with Ag^+, resulting in a decrease of removal efficiency to 55.36%.

2.2.3 Water hardness

The addition of 50 mg/L $CaCO_3$ reduced the removal efficiency of Ag^+ by around 3.75%, compared to that with no $CaCO_3$ (Figure 7 (C)). When the concentration increased to 100 mg/L $CaCO_3$, the removal efficiency decreased to 89.1%. This is due to the increased concentration of dissolved Ca^{2+} in solution, which can combine with EDTA and form a complex, with a higher complex formation constant ($\log K_{Ca\text{-}EDTA} = 10.69$) than that of the Ag-EDTA complex [67]. However, due to the low solubility of $CaCO_3$, the dissolved Ca^{2+} is limited. At a concentration of 200 mg/L $CaCO_3$, the removal efficiency was almost the same as at 100 mg/L $CaCO_3$ ($p=0.123>0.05$).

2.2.4 *E. coli* concentration

Sorption experiments of Ag^+ on Mag-Ligand at different concentrations of E. coli K12 were performed to determine if the presence of bacteria interferes with the sorption process. No significant difference was found with addition of *E. coli* K12 at different concentrations ($p=0.873>0.05$) (Figure 7 (D)). Ag^+ likely does not adhere to *E. coli* K12 cell walls, and *E. coli* K12 does not appear to interact with the surface of Mag-Ligand. Given this result, the removal of Ag^+ with Mag-Ligand can take place immediately after the disinfection reaches the desired level without separating the bacteria first, thus reducing time and cost.

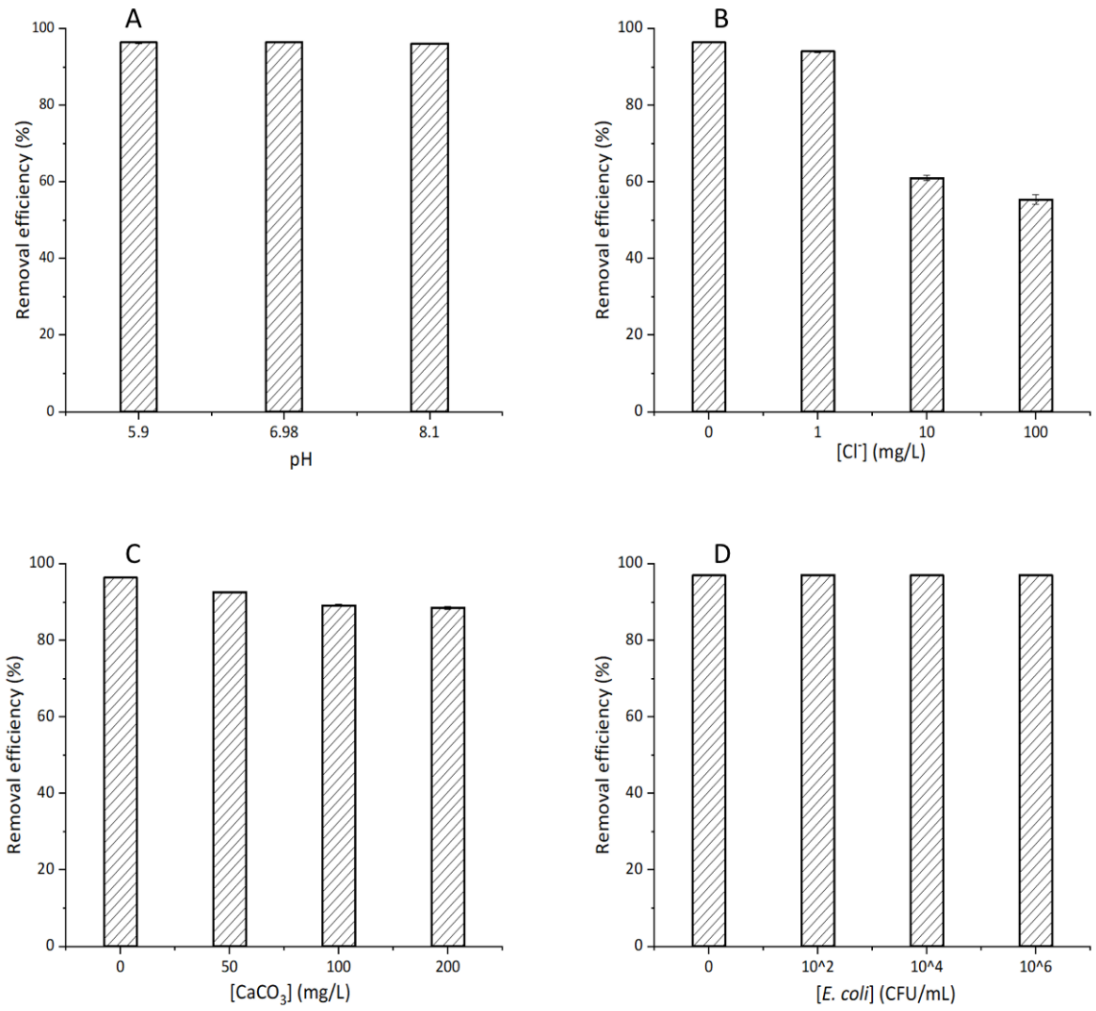

Figure 7. Influence on sorption for [Ag^+] =100 mg/L and [Mag-Ligand] =5 g/L of different (A) pH; (B) Cl^- concentration; (C) water hardness; and (D) *E. coli* concentration.

Table 9. Detailed results and p value tests about the influence of pH, Cl^- concentration, water hardness and *E. coli* concentration on the sorption of Ag^+ with Mag-Ligand ($p<0.05$ is considered to be statistically significant).

Environmental Conditions		Removal Efficiency (%)	p value test	Statistical Significance
pH	6	96.87±0.17	0.179	Statistically not significant
	7	96.92±0.10		
	8	96.71±0.09		

[Cl^-] (mg/L)	0	96.34±0.11	4.67 E-12	Statistically significant
	1	95.50±0.26		
	10	88.64±0.70		
	100	55.36±1.19		
[$CaCO_3$] (mg/L)	0	96.34±0.11	0.123 ([$CaCO_3$]>100 mg/L)	Statistically not significant
	50	92.59±0.20		
	100	89.07±0.29		
	200	88.51±0.40		
[*E. coli*] (CFU/mL)	0	96.92±0.11	0.873	Statistically not significant
	10^2	97.01±0.12		
	10^4	96.91±0.22		
	10^6	96.96±0.18		

3. Regeneration and reuse of metal ions and Mag-Ligand

Recovery of Ag^+ adsorbed onto Mag-Ligand was performed under acidic conditions (0.01 M H_2SO_4, pH = 1.7), using the initial Ag^+ and Mag-Ligand. The recovery efficiency of Ag^+ after five sequential cycles of Mag-Ligand regeneration remained above 80% (Figure 8), indicating that a large fraction of the initial Ag^+ can be reused for several cycles. Given the high price of $AgNO_3$ (e.g. $5.44 /g from Sigma-Aldrich, in small quantities), recycling Ag^+ as a disinfectant will reduce the cost of this disinfection method, making it a more sustainable practice than approaches using nanoAg where the Ag^+ is lost after just one cycle. Mag-Ligand can be captured and separated from the aqueous phase by an external magnet after use, thus reducing the potential environmental influence.

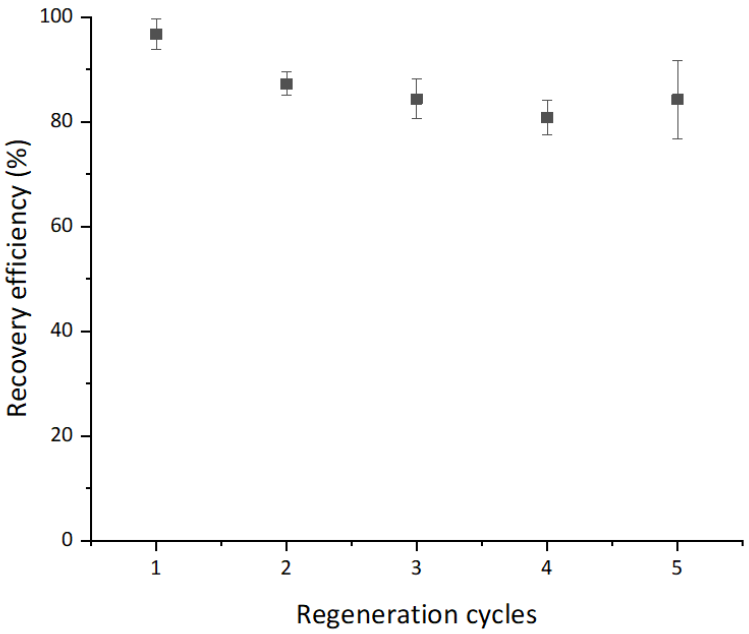

Figure 8. Recovery efficiency of Ag^{+} after five Mag-Ligand regeneration cycles.

Table 10. Detailed results about the recovery efficiency of Ag^{+} after five Mag-Ligand regeneration cycles.

Regeneration Cycle	Recovery Efficiency (%)
1	96.66±2.88
2	87.24±2.25
3	84.34±3.80
4	80.75±3.32
5	84.23±7.54

D. Conclusions

This study evaluated the disinfection effectiveness of various metal ions (Ag^{+}, Cu^{2+} and Zn^{2+}) on the target microorganism, *E. coli* K12, and explored the influence of different environmental conditions on the disinfection process. To make the disinfection process more

sustainable and economical, the metal ions were recovered using a magnetic nanomaterial (Mag-Ligand), which was then regenerated, recycling both the metal ion disinfectant and the nanomaterial. Ag^+ was shown to have a better disinfection efficiency than Cu^{2+} and Zn^{2+}, as the bactericidal effect occurred only with Ag^+. Factors that may determine the effectiveness of disinfection by Ag^+ include the initial level of Ag^+ per cell, as well as the speciation of Ag^+ in the environment. Different initial cell concentration and operating temperatures will influence the disinfection effectiveness, with higher cell to Ag^+ ratios and higher temperatures decreasing disinfection effectiveness. However, pH, water hardness and nutrient content have minimal influence on the disinfection process, since the speciation of Ag^+ remains stable under these conditions.

The adsorption of Ag^+ by Mag-Ligand can be used to reduce the concentration of Ag^+ to below 100 µg/L under proper conditions, but may require optimizing the dosage of Mag-Ligand and the number of sorption cycles, depending on conditions. The mechanism of sorption of Ag^+ by Mag-Ligand is the formation of a stable complex between Ag^+ and the EDTA coated on the surface of Mag-Ligand. The influence of several environmental conditions on sorption efficiency were evaluated as well. The addition of Cl^- will influence the concentration of free Ag^+ in solution thus reducing Ag^+ removal efficiency. Water hardness decreases Ag^+ sorption, since the dissolved Ca^{2+} will compete with Ag^+ for sorption site. The effect of hardness increases up to 100 mg/L $CaCO_3$; above that level there is no further effect of hardness on sorption. pH has no influence on the removal efficiency, as the speciation of Ag^+ remains stable within the range in this study. Addition of *E. coli* K12 also did not affect the removal efficiency, which means that removal of Ag^+ can proceed directly after disinfection. Mag-Ligand can be regenerated under an acidic environment after

sorption, and the recovery of Ag^+ remains above 80% after 5 sequential cycles. This novel approach allows for a recyclable disinfectant, aided by a regeneratable nanomaterial. Due to the simple method for synthesizing Mag-Ligand, as well as the recyclable use of both the metal ions and Mag-Ligand, this method is very promising for practical use in the future.

E. Acknowledgements

This work was supported by the National Science Foundation (NSF) and the U.S. Environmental Protection Agency (EPA) under cooperative agreement number NSF-EF0830117, as well as UCSB Mellichamp Sustainability Fellowship. Arturo A. Keller also appreciates Agilent Technologies for their Agilent Thought Leader Award. Any opinions, findings, conclusions, or recommendations expressed in this material are those of the authors do not necessarily reflect the views of the funding agencies.

The supporting information includes the evaluation of live cells after disinfection, recipe of tryptic soy broth, statistical analysis of results and determination of sorption time for Ag^+ removal using Mag-Ligand. The supporting information is available online. All photos in the manuscript (i.e. Figure S1 in Supporting Information) were taken by one of the authors, Qian Gao.

F. Appendix

1. Evaluation of live cells after disinfection

To further confirm if the living cells still exist after long-time disinfection, 0.1 mL of the sample after 16 h disinfection with 100 mg/L Ag^+ was transferred onto a tryptic soy agar plate for a plate counting test. The tryptic soy agar plate was then cultured on the incubator with a shaking speed of 200 rpm under 20 °C for more than 48 h, until the colony formed on

the agar plate. According to the plate counting test result shown in Figure S1, the number of colonies is 17. Thus, the concentration of living cells after 16 h disinfection is 170 CFU/mL.

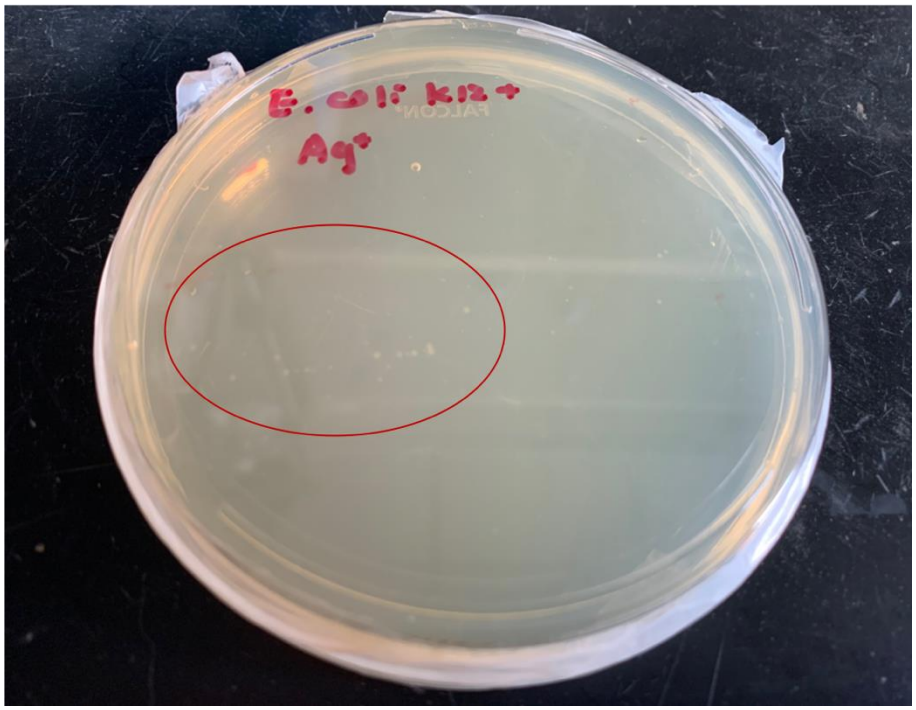

Figure S1. Plate counting test of sample after 16 h exposure to 100 mg/L Ag^+.

2. Recipe of tryptic soy broth

Table S1. Recipe of tryptic soy broth

Tryptone	17 g
Soy	3 g
NaCl	5 g
K_2HPO_4	2.5 g
Glucose	2.5 g
Distilled water	1 L

3. Determination of Sorption Time for Ag^+ Removal using Mag-Ligand

To determine the proper time for sorption in each continuous cycle, a batch of experiment was done with 3 continuous sorption cycles (with 5 g/L of Mag-Ligand for cycle 1, 2.5 g/L for cycle 2 and 2.5 g/L for cycle 3), and the contact time for each cycle are 1 h and 2 h respectively. The concentration of Ag^+ after each cycle was shown in Table S2. According to the results in Table S2, the concentration of Ag^+ reduced from 100 mg/L to 70 μg/L with 2 h contact time in each cycle, while that with 1 h contact time can only reduce the concentration of Ag^+ to 400 μg/L. Given the EPA standard that the concentration of Ag^+ should be under 100 μg/L in water, 2 h for each sorption is a proper contact time to reach an ideal removal effect.

Table S2. Concentration of Ag^+ after several continuous sorption cycles with different sorption time

Contact time for each cycle	Initial concentration (mg/L)	[Ag^+] after sorption cycle 1 (mg/L)	[Ag^+] after sorption cycle 2 (mg/L)	[Ag^+] after sorption cycle 3 (mg/L)
1h for each cycle	100	49.27	15.38	0.40
2h for each cycle	100	33.76	6.33	0.07

III. Novel disinfection method for toxic cyanobacteria *(Oscillatoria tenuis)* and simultaneous removal of cyanotoxins aided by recyclable magnetic nanoparticles

Material from:

Gao, Q. and Keller, A. A. Novel disinfection method for toxic cyanobacteria (*Oscillatoria tenuis*) and simultaneous removal of cyanotoxins aided by recyclable magnetic nanoparticles. *J. Environ. Chem. Eng.* 106589 (2021).

Abstract An optimized disinfection method with metal ions to address cyanobacteria contamination in freshwater is presented, based on recyclable magnetic nanoparticles. In this study, the disinfection ability of individual metal ions (Ag^+ and Cu^{2+}) and combined (Ag^+ + Cu^{2+}) were evaluated with a target cyanobacteria, *Oscillatoria tenuis*, under various environmental conditions. The usage of combined Ag^+ and Cu^{2+} reduces the time and concentration needed to achieve the same disinfection effectiveness compared to individual metal ions. However, the addition of Cu^{2+} and Ag^+ stimulated production of cyanotoxin during disinfection, with an increase of 24.8% for anatoxin-a. To reduce the potential health risk, we evaluated the recovery and reuse of metal ions, and removal of cyanotoxins after disinfection, using magnetic nanoparticles with permanently confined micelle arrays (Mag-PCMA) under various environmental conditions. Recovery efficiency of Ag^+, the most valuable ion, was excellent (99.8%), although it decreased to 74.5% with increasing Cl^- concentration (0-10 mg/L). The regeneration and reuse of Mag-PCMA was studied for 5 cycles. Removal efficiency of Cu^{2+}, anatoxin-a and cylindrospermopsin were minimally changed during the 5 sorption-desorption cycles, and that of Ag^+ remained above 93% by the

end of 5th cycle, indicating that this disinfection method may be sustainable for practical use with low energy requirements and minimized environmental impacts.

A. Introduction

Harmful algae blooms (HABs) refer to a rapid increase in toxic algae population in freshwater or marine systems, due to a nutrient overload. HABs threaten aqueous environment by decreasing water quality [2], depleting oxygen [6], accumulating biomass to alter food web dynamics [72], and releasing toxins and secondary metabolites [7]. In particular, some cyanobacteria species produce and release cyanotoxins when the cells rupture or die [8]. Humans and other organisms may be exposed to cyanotoxins either directly via inhalation, ingestion and dermal contact of contaminated water, and indirectly by contacting animals or plants exposed to cyanotoxins, resulting in threats to human and ecological health. People may suffer from acute intoxication and have the symptoms like visual disturbance, nausea, vomiting, acute liver failure, respiratory irritation or even death once exposed to water contaminated with even very low concentrations of cyanotoxins [8]. Apart from acute toxicity, cyanotoxins have a close relationship with various diseases through chronic exposure as well. For example, microcystins, a class of cyanotoxins, may cause gastroenteritis, allergic and irritation reactions, and liver diseases after chronic exposure [73]. Thus, seeking efficient ways to deal with HABs caused by cyanobacteria and providing safe drinking water sources is very important for public health.

Generally, particulate cyanobacteria cells can be removed through coagulation, sedimentation, filtration and chlorination in drinking water treatment plants according to the EPA guideline [74]. However, further disinfection is necessary to inactivate residual

cyanobacteria, as regrowth during distribution may increase health risks. The use of metal ions as algaecide has been well studied to solve this problem. For example, copper has been shown to be an effective algaecide for various cyanobacteria, including *Microcystis aeruginosa* [75] and *Lyngbya wollei* [76]. Ferrate (VI) can be used for the pre-treatment of two cyanobacteria, *Chlorella sp.* and *Pseudanabaena limnetica* in wastewater treatment plants due to its effective disinfection ability [77]. Compared to other disinfection methods which will produce disinfection by-products (e.g. the use of chlorine [78]) or require high cost of energy or maintenance (e.g. ozone or UV radiation [11]), the use of metal ions as algaecides is inexpensive and efficient, thus having great potential for wide application. However, some environmental issues related to metal ions need to be addressed before practical use. First, the residual metal ions in the water after treatment can cause potential environmental risks, as high concentrations of these metal ions are toxic to various aquatic organisms. For example, the 96-h lethal concentration 50% (LC50) of copper ion for 90-day old *Ctenopharyngodon idella* is 5.17 mg/L [79]. *Dentomuricea aff. meteor,* a cold-water gorgonian, is very sensitive to copper ions, with 96-h LC50 of 137 μg/L [80]. Thus, the concentration of residual metal ions needs to be decreased to a safe level after treatment.

Another concern is the release of cyanotoxins during disinfection with metal ions. Some studies have found that the addition of metal ions have a positive effect on the production of cyanotoxin, which will increase the release of cyanotoxin when the cells rupture or die. For example, the addition of Fe will increase the concentration of microcystins produced by *Microcystis aeruginosa* [81]. Traditional technologies such as the use of chemical oxidizing agents, UV radiation and activated carbon adsorption have been shown to be effective for only some types of cyanotoxins. For example, free chlorine is effective for

cylindrospermopsin and saxitoxin but not for anatoxin-a [74]. Thus, it is essential to seek an efficient way that can remove a broad range of cyanotoxins before further distribution of the treated water.

To address these issues (i.e, residual metal ions and released cyanotoxins after disinfection), we propose an innovative, more sustainable disinfection method, using magnetic nanoparticles with permanently confined micelle arrays (Mag-PCMA) to achieve simultaneous sorption of both metal ions and cyanotoxins, followed by the regeneration of Mag-PCMA under proper conditions for reuse. A schematic of the process is provided in the graphical abstract. Briefly, cyanobacteria are exposed to metal ions at concentrations needed for disinfection. After sufficient contact time, the treated water is filtered to separate dead algae cells, and Mag-PCMA are added to remove the residual metal ions as well as the cyanotoxins produced during disinfection. Previous studies have shown that Mag-PCMA can achieve simultaneous removal of both organic and inorganic chemicals (e.g. acenaphthene and Cd^{2+}) via hydrophobic interactions and electrostatic attraction [82]. Thus, we hypothesized that the metal ions and cyanotoxins could be effectively removed by Mag-PCMA after disinfection. In the final step, the metal ions adsorbed on Mag-PCMA can be regenerated under proper conditions and reused for several continuous cycles.

The objectives of this study were to: (1) explore the disinfection effectiveness of combined metal ions rather than individual ones to reduce the effective concentration and contact time, and evaluate the influence of different environmental conditions (e.g. pH, nutrient content, water hardness); (2) quantify the production and distribution of extracellular and intracellular cyanotoxins during disinfection; (3) study the simultaneous sorption of metal ions and cyanotoxins with magnetic nanoparticles, and the influence of different

environmental conditions on this process; and (4) explore the conditions needed to regenerate the magnetic nanoparticles, and release the metal ions for reuse in continuous cycles.

B. Materials and Methods

1. Materials

Oscillatoria tenuis (*O. tenuis*) was selected as target cyanobacteria in this study, as it can produce two types of cyanotoxins (i.e. anatoxin-a and cylindrospermopsin) which are of concern in water supply. Both *O. tenuis* and BG-11 medium (used for culturing *O. tenuis*) were purchased from UTEX Culture Collection of Algae at The University of Texas at Austin (USA). Silver nitrate, copper sulfate, nitric acid, sulfuric acid, sodium hydroxide, sodium chloride and calcium carbonate were purchased from Fisher Scientific (USA). Ag^{+} and Cu^{2+} are selected as the metal ions disinfectants as they are commonly used as algaecides in many studies [44, 75-76] and have demonstrated effectiveness. Our innovative approach allows the recovery of the metal ions for reuse, making it less expensive and more sustainable. The recipe of BG-11 is presented in Table S1 (Supporting Information). Mag-PCMA was synthesized using the method developed in our previous studies [82-88], and the maghemite (iron (III) oxide) nanoparticles (30 nm in diameter) used for synthesis were purchased from Alfa Aesar (USA). Detailed information about synthesizing Mag-PCMA is shown in Supporting Information. All chemicals were used as received without further purification. All solutions were prepared with deionized water (18 MΩ-cm) from a Barnstead NANOpure Diamond Water Purification System (USA).

2. Disinfection of *O. tenuis* with individual and combined metal ions

The disinfection of *O. tenuis* at exponential phase was performed in 125 mL baffled polycarbonate Erlenmeyer flasks purchased from Corning Inc. (USA), with silver nitrate and copper sulfate as disinfectants. *O. tenuis* culture was exposed to individual metal ions (i.e. Ag^{+}, Cu^{2+}) and combined metal ions (Ag^{+} + Cu^{2+}) at various concentrations (10-200 mg/L) for different contact times (up to 10 h) in BG-11 medium. The concentration of *O. tenuis* was determined by the Trilogy Laboratory Fluorometer (Turner Designs, Inc., USA) and was expressed as total chlorophyll fluorescence (raw fluorescence unit (RFU)/mL). All the chlorophyll fluorescence mentioned in this study refer to the total chlorophyll fluorescence. The chlorophyll fluorescence of *O. tenuis* was 75.91 RFU/mL ($1.8*10^5$ cells/mL in cell concentration). The disinfection process was evaluated under various environmental conditions (e.g. initial chlorophyll fluorescence, pH, water hardness, nutrient content, natural organic matter (NOM) and light conditions) within a broad range (Table 1), to simulate the natural environment with complex conditions. The chlorophyll fluorescence of *O. tenuis* for the study with different environmental conditions (except the study about initial chlorophyll fluorescence) was 89.89 RFU/mL ($2.1*10^5$ cells/mL in cell concentration).

Table 1. Range of environmental conditions for disinfection with Ag^{+} and Cu^{2+} and the methods for adjustment.

Environmental condition	Range	Method
Initial chlorophyll fluorescence	24.83-143.71 RFU/mL	Addition of different initial concentration of *O. tenuis*
pH	6-8	Adjusted by 0.1 M nitric acid and 0.1 M NaOH

Water hardness	[$CaCO_3$]=0-200 mg/L	Addition of $CaCO_3$ from 0 to 200 mg/L
Nutrient content	0% (with no nutrients)-100% (full strength)	Dilution of the BG-11 medium with deionized water to different percentage
NOM	[Humic acid]=0-10 mg/L	Addition of humic acid (HA) from 0 to 10 mg/L
Light condition	Light & dark	With/without light irradiation

3. Extracellular and intracellular cyanotoxin quantification

To explore how the concentration of extracellular and intracellular cyanotoxin may change over time, *O. tenuis* with initial chlorophyll fluorescence = 111.46 RFU/mL ($2.6*10^5$ cells/mL in cell concentration) were exposed to 50 mg/L Ag^+ and Cu^{2+}, and 5 mL culture samples were collected every 2.5 h. The culture samples were centrifuged at 1500 rpm for 20 min. After centrifugation, 800 µL of supernatant was taken for extracellular toxin quantification, and was transferred into a liquid chromatography glass vial followed by addition of 150 µL of methanol and 50 µL of 1000 ng/mL internal standard mix (^{13}C-labelled anatoxin-a and ^{15}N-labelled cylindrospermopsin). The pellets obtained from centrifugation were used for intracellular toxin extraction by suspending them in 5 mL of 5% aqueous acetic acid. The suspension was then vortexed for 30 minutes, sonicated for 30 min and centrifuged for 20 minutes at 4500 rpm. After centrifugation, 800 µL of supernatant was mixed with 150 µL of methanol and 50 µL of 1000 ng/mL internal standard mix. The toxin quantification was performed on an Agilent 6470 (Agilent Technologies) Triple Quad liquid chromatography/mass spectrometry (LC/MS).

4. Simultaneous sorption of metal ions and cyanotoxin with Mag-PCMA

Simultaneous adsorption of Ag^+, Cu^{2+} and two cyanotoxins produced by *O. tenuis* (i.e. anatoxin-a and cylindrospermopsin) with Mag-PCMA was evaluated under various conditions. Different amounts of Mag-PCMA particles (20.0-100.0 mg) were added to 20 mL of mixed solution (50 mg/L Ag^+, 50 mg/L Cu^{2+}, 20 μg/L anatoxin-a and 20 μg/L cylindrospermopsin) in 20 mL glass vials, and the vials were placed in an end-over-end shaker on a Dayton-6Z412A Parallel Shaft (USA) roller mixer with a speed of 70 rpm at room temperature (22-25 °C) for 24 h to ensure sufficient equilibration time. Adsorption kinetics studies were carried out with the mixture of 50.0 mg Mag-PCMA and 20 mL mixed solution at the same conditions but for a set amount of time, varying from 1 to 8 h. All the studies were done at pH = 7 and room temperature. After mixing well, the Mag-PCMA particles were separated from the aqueous phase with an Eclipse magnet. Samples were collected from the supernatant and diluted with 2% HNO_3 to measure metal ion concentration. The concentration of Ag^+ and Cu^{2+} was analyzed by an Agilent 7900 (Agilent Technologies) inductively coupled plasma mass spectrometer (ICP-MS). Supernatant samples were also analyzed for the concentrations of anatoxin-a and cylindrospermopsin by LC-MS.

The influence of different environmental conditions on the removal efficiency of Ag^+, Cu^{2+}, anatoxin-a and cylindrospermopsin by Mag-PCMA, including pH, concentration of Cl^-, water hardness, and NOM were evaluated as well. pH was adjusted to the desired condition (range from 6 to 8) by using 0.1 M NaOH. Different concentrations of Cl^- (0, 1 and 10 mg/L) were added into the mixture to explore the possible influence on sorption, as the combinations of Cl^- and Ag^+ may affect the sorption behavior of Mag-PCMA. $CaCO_3$ with a

range of concentrations from 50 mg/L to 200 mg/L was used to adjust water hardness. HA with concentration of 1-10 mg/L was introduced to the sorption system, to explore the influence of NOM.

5. Regeneration of Mag-PCMA and reuse of metal ions

Regeneration and reuse of Mag-PCMA was investigated in this study. 50 mg/L Ag^{+} and Cu^{2+} and 20 ug/L anatoxin-a and cylindrospermopsin were adsorbed onto the Mag-PCMA particles, followed by magnetic separation of Mag-PCMA from solution. Concentration of Ag^{+}, Cu^{2+}, anatoxin-a and cylindrospermopsin were determined after sorption. The Mag-PCMA collected was first rinsed with methanol to extract sorbed cyanotoxins, then washed with 0.01 M H_2SO_4 (pH=1.70) for 30 min at room temperature to remove sorbed metal ions. The acid-washed Mag-Ligand particles were reused for subsequent sorption experiments and the sorption, extraction, and reuse processes were repeated for five times.

6. Data analysis

All tests in this study were performed in triplicate and analysis of variance (ANOVA) was used to test the significance of results. A $p<0.05$ was considered to be statistically significant. The p values of each test are listed in Table 5, 6, 8, 10, 12 and 14.

C. Results and discussions

1. Disinfection of *O. tenuis* with metal ions

1.1 Comparison of disinfection effectiveness of various metal ions on *O. tenuis*

Cu^{2+} and Ag^{+} were selected as disinfectants, and disinfection effectiveness of both individual and combined metal ions at different concentrations were compared. The change

in total chlorophyll fluorescence as compared to the initial one was used to determine disinfection effectiveness, since monitoring the level of total chlorophyll is a direct way of tracking algae growth [77]. As shown in Figure 1 (A) and (B), chlorophyll fluorescence after treatment with low Cu^{2+} or Ag^{+} concentrations (10-20 mg/L) and short contact time (2.5 h for Ag^{+} and 5 h for Cu^{2+}) was higher than that in the control, indicating growth instead of cell death. This might be due to the stimulation of cyanobacteria metabolism at low metal ion concentrations and short exposure times, resulting in increased chlorophyll fluorescence. At longer contact times chlorophyll fluorescence decreased. When exposed to high Cu^{2+} or Ag^{+} concentrations (50-200 mg/L), chlorophyll fluorescence decreased even within a short contact time (2.5 h) and the reduction became more and more significant with longer contact times. Compared to the individual ions, the combination $Cu^{2+} + Ag^{+}$ has better disinfection effectiveness at the same concentration and contact time. As shown in Figure 1 (C), no abnormal increase in chlorophyll fluorescence was observed even at the lower dose and contact time, and the final chlorophyll fluorescence for the combined metal ion treatment was less than that with Cu^{2+} or Ag^{+} at all concentrations and contact times, indicating better disinfection effectiveness with the combined metal ions than the individual ions under same conditions. This is an important finding, since it reduces the use of Ag^{+}, a more expensive ion.

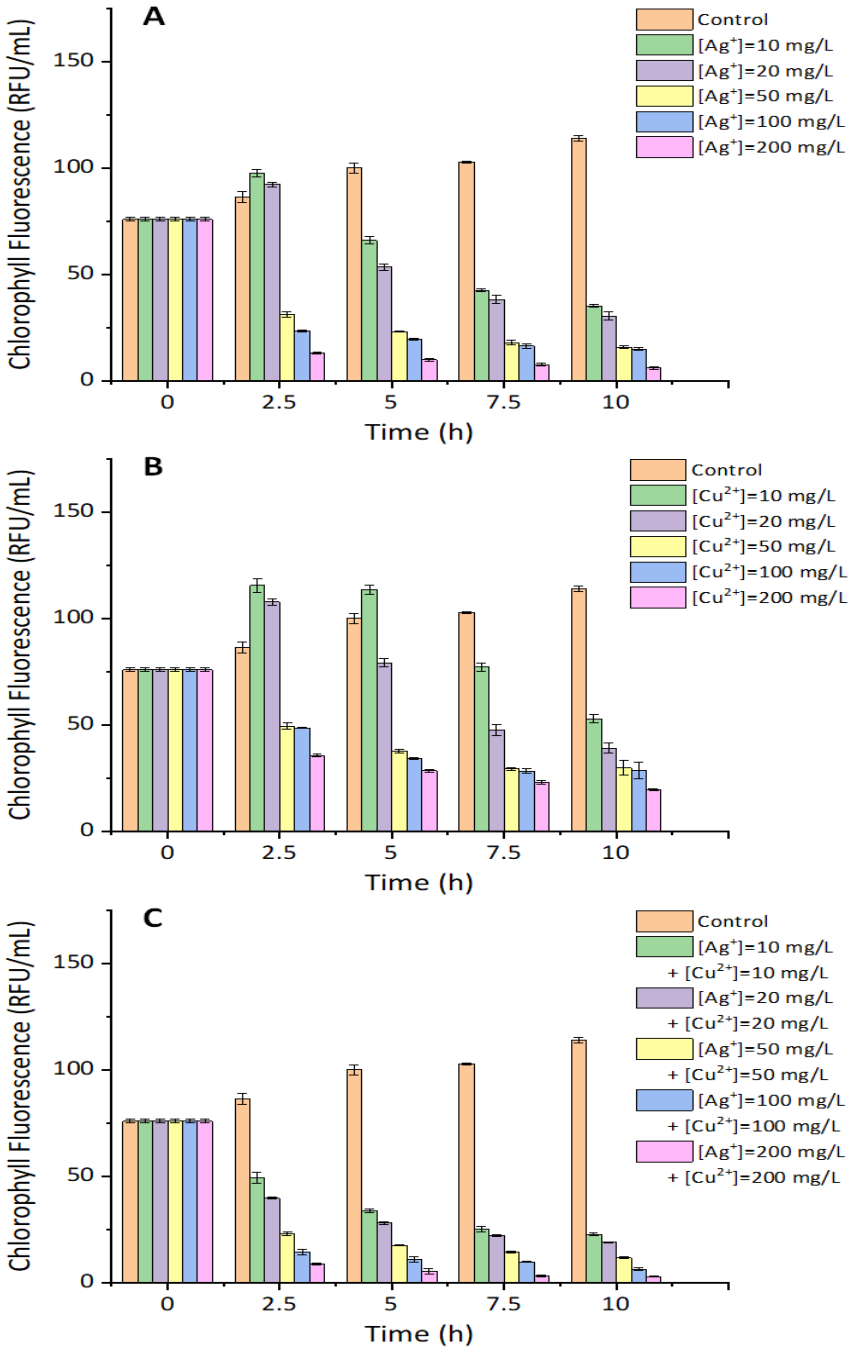

Figure 1. Disinfection kinetics of *O. tenuis* with different concentrations (10-200 mg/L) of (A) Ag^{+}; (B) Cu^{2+}; and (C) Cu^{2+}+Ag^{+}.

Table 2. Detailed results about the disinfection kinetics of *O. tenuis* with different concentrations of Ag^{+}, Cu^{2+} and Cu^{2+}+Ag^{+}.

[Disinfectants]		Chlorophyll fluorescence				
(mg/L)		t=0 h	t=2.5 h	t=5 h	t=7.5 h	t=10 h
Ag^{+}	0	75.91± 0.85	86.33± 2.56	100.04± 2.35	102.89± 0.44	114.07± 1.33
	10	75.91± 0.85	97.65± 1.75	66.03± 1.77	42.49± 0.70	35.31± 0.45
	20	75.91± 0.85	92.34± 1.02	53.44± 1.52	38.31± 1.89	30.48± 1.91
	50	75.91± 0.85	31.26± 1.34	23.22± 0.28	18.05± 1.23	15.91± 0.75
	100	75.91± 0.85	23.42± 0.57	19.64± 0.33	16.36± 1.23	15.02± 0.65
	200	75.91± 0.85	13.23± 0.50	10.00± 0.63	7.66± 0.59	6.02± 0.83
Cu^{2+}	0	75.91± 0.85	86.33± 2.56	100.04± 2.35	102.89± 0.44	114.07± 1.33
	10	75.91± 0.85	115.58± 3.33	113.68± 2.02	77.35± 1.96	52.97± 2.08
	20	75.91± 0.85	107.85± 1.43	79.28± 1.93	47.68± 2.51	39.21± 2.53
	50	75.91± 0.85	49.49± 1.38	37.65± 0.69	29.35± 0.55	29.82± 3.39
	100	75.91± 0.85	48.71± 0.23	34.36± 0.37	28.42± 1.16	28.57± 3.92
	200	75.91± 0.85	35.63± 0.62	28.50± 0.57	23.00± 0.72	19.50± 0.54
Ag^{+}+ Cu^{2+}	0	75.91± 0.85	86.33± 2.56	100.04± 2.35	102.89± 0.44	114.07± 1.33
	10	75.91±	49.37±	33.83±	25.17±	22.77±

		0.85	2.55	0.66	1.25	0.70
	20	75.91± 0.85	39.69± 0.43	28.03± 0.67	22.17± 0.30	18.98± 0.29
	50	75.91± 0.85	23.07± 0.97	17.63± 0.26	14.47± 0.56	11.84± 0.53
	100	75.91± 0.85	14.39± 1.40	10.94± 1.34	9.87± 0.32	6.38± 0.70
	200	75.91± 0.85	8.89± 0.43	5.40± 1.28	3.11± 0.53	2.89± 0.19

The concentration of disinfectants and contact time are the main factors that determine disinfection effectiveness. To further discuss these factors in a quantitative way, as well as to see if the disinfection effectiveness of combined metal ions is synergetic, the relationship between concentration of disinfectants, contact time and chlorophyll fluorescence can be described with two exponential equations. For a given disinfectant concentration, the relationship between chlorophyll fluorescence and contact time can be described by Equation (1):

$$\text{Chlorophyll fluorescence} = R_{mc} + R_{dc} e^{-Bc*t} \quad (1)$$

Here, R_{mc} is residual chlorophyll fluorescence after a long time of disinfection at a given disinfectant condition (i.e type of metal ion and concentration); R_{dc} is the decrease in chlorophyll fluorescence compared to the initial chlorophyll fluorescence at t = 0. B_c is the rate of disinfection, or the disinfectant ability, under a given condition. A larger value of B_c means it takes a shorter time for the system to reach the same disinfection effectiveness than other conditions. The values of R_{mc}, R_{dc}, and B_c for all systems in this study are shown in

Table 3. Due to the metabolic stimulation by individual Ag^{+} and Cu^{2+} treatments at 10 and 20 mg/L, the results of these systems cannot be described by Equation 1.

The value of B_c follows the order: $Cu^{2+}+Ag^{+} > Ag^{+} > Cu^{2+}$ for the same total concentration of disinfectant. Thus, the combined disinfectant has better disinfection effectiveness than the individual metal ions at the same concentration, and Ag^{+} is better than Cu^{2+} as an individual disinfectant. At low disinfectant concentrations (10 and 20 mg/L), there is clearly a synergistic effect by combining the two metal ions, since the metabolic stimulation is not observed and there is disinfection even at low contact times. To see if the disinfection effectiveness of combined metal ions is additional or synergetic, a comparison of B_c at the higher disinfectant concentration (50, 100 and 200 mg/L) is shown in Figure 2 (A). Here, the sum of B_c for the individual metal ions is compared to the combination. One can see that B_c ($Cu^{2+}+Ag^{+}$) is less than B_c (Ag^{+}) + B_c (Cu^{2+}) at higher levels of disinfectant concentrations (>50 mg/L). Thus, the disinfection effectiveness of combined disinfectant is not synergetic at high concentrations.

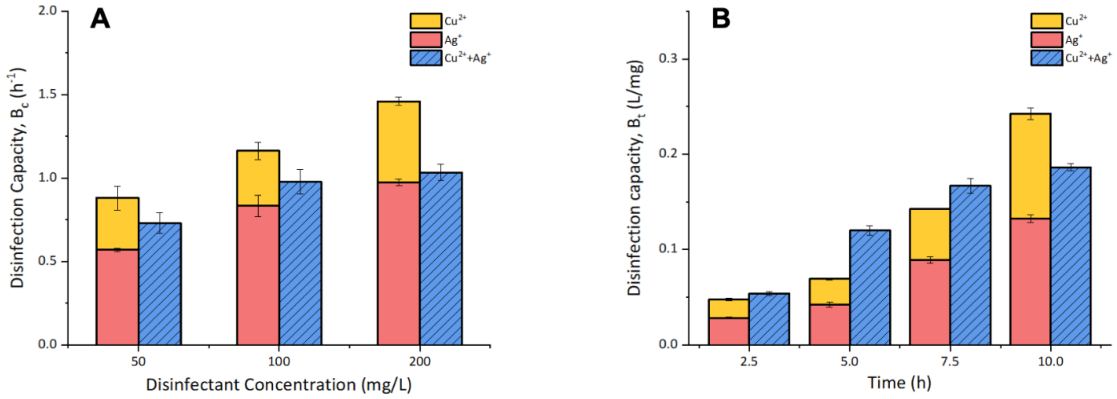

Figure 2. (A) Comparison of B_c with Ag^{+}, Cu^{2+} and $Ag^{+}+Cu^{2+}$ at different concentrations (p values given in Table S2). (B) Comparison of B_t with Ag^{+}, Cu^{2+} and $Ag^{+}+Cu^{2+}$ at different contact times (p values given in Table 5).

Table 3. Values of R_{mc}, R_{dc}, B_c and R^2 for Equation 1.

Disinfectant concentration	R_{mc} (RFU/mL)	R_{dc} (RFU/mL)	B_c (h^{-1})	R^2
$[Ag^+]$=50 mg/L	16.94±0.95	58.84±1.01	0.57±0.01	0.9965
$[Ag^+]$=100 mg/L	16.48±0.57	59.40±0.67	0.83±0.07	0.9969
$[Ag^+]$=200 mg/L	7.60±0.42	68.29±0.46	0.97±0.02	0.9981
$[Cu^{2+}]$=50 mg/L	25.78±4.33	50.10±3.84	0.31±0.07	0.9954
$[Cu^{2+}]$=100 mg/L	25.07±2.96	51.04±2.04	0.33±0.05	0.9926
$[Cu^{2+}]$=200 mg/L	21.03±0.90	54.66±1.60	0.49±0.03	0.9933
$[Ag^+]$=10 mg/L + $[Cu^{2+}]$=10 mg/L	18.80±0.50	57.14±1.36	0.27±0.00	0.9976
$[Ag^+]$=20 mg/L + $[Cu^{2+}]$=20 mg/L	18.53±0.61	57.23±0.57	0.38±0.02	0.9986
$[Ag^+]$=50 mg/L + $[Cu^{2+}]$=50 mg/L	13.77±0.47	62.08±0.41	0.73±0.06	0.9966
$[Ag^+]$=100 mg/L + $[Cu^{2+}]$=100 mg/L	8.77±0.67	67.23±1.52	0.98±0.07	0.9971
$[Ag^+]$=200 mg/L + $[Cu^{2+}]$=200 mg/L	3.58±0.57	72.32±1.04	1.03±0.05	0.9991

Table 4. Values of R_{mt}, R_{dt}, B_t and R^2 for Equation 2.

Disinfectant	Contact time	R_{mt} (RFU/mL)	R_{dt} (RFU/mL)	B_t (L/mg)	R^2
Ag^+	t=2.5 h	15.13±0.93	70.99±2.04	0.028±0.001	0.9932
	t=5 h	14.62±0.58	84.97±1.43	0.042±0.003	0.9892
	t=7.5 h	14.23±0.54	86.61±0.98	0.089±0.004	0.9662
	t=10 h	13.96±0.23	99.42±1.15	0.132±0.004	0.9764
Cu^{2+}	t=2.5 h	38.33±1.43	47.53±1.32	0.020±0.001	0.9610
	t=5 h	27.23±0.16	75.57±2.34	0.027±0.001	0.9599
	t=7.5 h	26.25±2.17	79.88±1.20	0.053±0.001	0.9850

	t=10 h	24.76±0.77	87.38±3.04	0.110±0.006	0.9853
Ag^{+}+Cu^{2+}	t=2.5 h	13.33±0.68	70.90±3.27	0.054±0.002	0.9790
	t=5 h	12.44±0.36	86.85±2.09	0.120±0.005	0.9731
	t=7.5 h	10.89±0.16	91.65±0.49	0.167±0.008	0.9781
	t=10 h	8.85±0.28	105.04±1.49	0.186±0.004	0.9871

Table 5. P value tests about the comparison of B_c and B_t with Ag^{+}, Cu^{2+} and Ag^{+}+Cu^{2+} at different concentrations or contact times.

Test	Conditions	p value	Statistical significance
Comparison of B_c with Ag^{+}, Cu^{2+} and Ag^{+}+Cu^{2+} at different concentrations	50 mg/L	0.044	Statistically significant
	100 mg/L	0.049	Statistically significant
	200 mg/L	$1.25*10^{-4}$	Statistically significant
Comparison of B_t with Ag^{+}, Cu^{2+} and Ag^{+}+Cu^{2+} at different contact times	2.5 h	0.016	Statistically significant
	5 h	$1.38*10^{-4}$	Statistically significant
	7.5 h	$9.36*10^{-3}$	Statistically significant
	10 h	$1.04*10^{-4}$	Statistically significant

The relationship between disinfectant concentration and chlorophyll fluorescence for a given contact time and type of disinfectant is exponential as well (Equation 2):

$$\text{Chlorophyll fluorescence}=R_{mt}+R_{dt}e^{-Bt*c} \quad (2)$$

Here, R_{mt} is the residual chlorophyll fluorescence when the concentration of disinfectant is theoretically close to infinity; R_{dt} is the corresponding decrease of chlorophyll fluorescence as compared to the chlorophyll fluorescence with concentration of disinfectants=0; and B_t indicates the disinfectant ability under specific conditions. A larger value of B_t means lower concentration of disinfectants is required for the system to reach the same disinfection

effectiveness. The values of R_{0t}, R_t, and B_t for all the systems in this study are shown in Table 4.

As shown in Table 4, B_t follows the order: $Cu^{2+}+Ag^{+} > Ag^{+} > Cu^{2+}$ with the same contact time. This means that combined disinfectant has better disinfection effectiveness than individual ions at the same contact time, and Ag^{+} is better than Cu^{2+}. The comparison of B_t ($Ag^{+}+Cu^{2+}$) and B_t (Ag^{+}) +B_t (Cu^{2+}) with different contact times (2.5, 5, 7.5 and 10 h) are shown in Figure 2 (B). The disinfection effectiveness of the combined metal ions is synergetic when contact time is less than 7.5 h. At t=10 h, B_t ($Ag^{+}+Cu^{2+}$) is less than B_t (Ag^{+}) +B_t (Cu^{2+}).

The better disinfection ability of the combined $Cu^{2+}+Ag^{+}$ relative to the individual Ag^{+} or Cu^{2+} is mainly due to the differences in disinfection mechanisms for Ag^{+} and Cu^{2+}. Ag^{+} inactivates the algae cells via extracellular binding and precipitating on the cell wall, and intracellular binding with enzymes, DNA or electron donor groups [60]. The disinfection mechanism of Cu^{2+} is mainly the increase in cell wall permeability and destruction of cell walls [89], but does not result in intracellular binding. Thus, the disinfection ability of Cu^{2+} is weaker than Ag^{+}. Both disinfectant concentration and contact time will influence the disinfection effectiveness. At low concentrations, the disinfectant will be attached onto the cell walls and once the concentration increases to a certain level, the cell walls will be damaged. If the concentration of disinfectant continues to increase beyond that level, the additional disinfectant will not accelerate the rate of disinfection, even though it will be attached onto the cell walls as well [89]. Contact time is another important factor in this process since the precipitation and uptake of disinfectant are time-dependent and it will take time for the attached disinfectant to destroy the cell structure [89]. Given enough contact time or

disinfectant concentration, the disinfection effectiveness will remain stable at a certain level under those conditions.

When a combination of metal ions (Cu^{2+}+Ag^{+}) is applied to the system, synergetic effects appear as it will be easier for Ag^{+} to enter the cell and interact with enzymes or DNA, since the cell wall is damaged by Cu^{2+}. The synergetic effect is significant at low concentrations and short contact times. When the concentration of individual disinfectant is high, or the contact time is long, the disinfection process may reach an equilibrium with individual disinfectants. Thus, no synergetic effect appears under those conditions, but the disinfection effectiveness of combined disinfectant is still better than that with individual metal ions.

In conclusion, disinfection effectiveness of combined metal ions is synergetic compared to the addition of individual ones at low concentration and short contact time. At high concentration and long contact time, the disinfection effectiveness of combined ones is weaker than the sum of individual ones but is still stronger than each of them. Thus, treatment with combined metal ions will reach expected disinfection effectiveness with lower concentration and shorter contact time than with individual metal ions. The cell concentration of *O. tenuis* in this study was very high ($1.8*10^5$ cells/mL) to be able to simulate an environment with cyanobacteria bloom, which required a high concentration of metal ions and longer contact times, for this proof-of-concept study. One can expect that lower dosages of combined metal ions will be needed to achieve desired disinfection effectiveness for the lower cell concentrations in normal environmental conditions. With further treatment of the residual metal ions in the water after disinfection (i.e. sorption with Mag-PCMA), the concentration of metal ions will be reduced to a safe level which minimizes the potential environmental risk.

1.2 Influence of various environmental conditions on the effectiveness of disinfection

Various environmental conditions, such as initial cell concentrations, pH, water hardness, NOM, nutrient content, and light condition, were considered and their influence on disinfection effectiveness were evaluated. All the experiments were done with exposure to 50 mg/L Cu^{2+} and 50 mg/L Ag^{+} and 2.5 h contact time. Results are shown in Figure 3 (A)-(F). The initial chlorophyll fluorescence was 89.89 RFU/mL ($2.1*10^5$ cells/mL in concentration) for experiments 3B to 3F. The pH of the BG-11 remained stable at 8 during the studies with different initial cell concentrations, water hardness, NOM, nutrient content, and lighting.

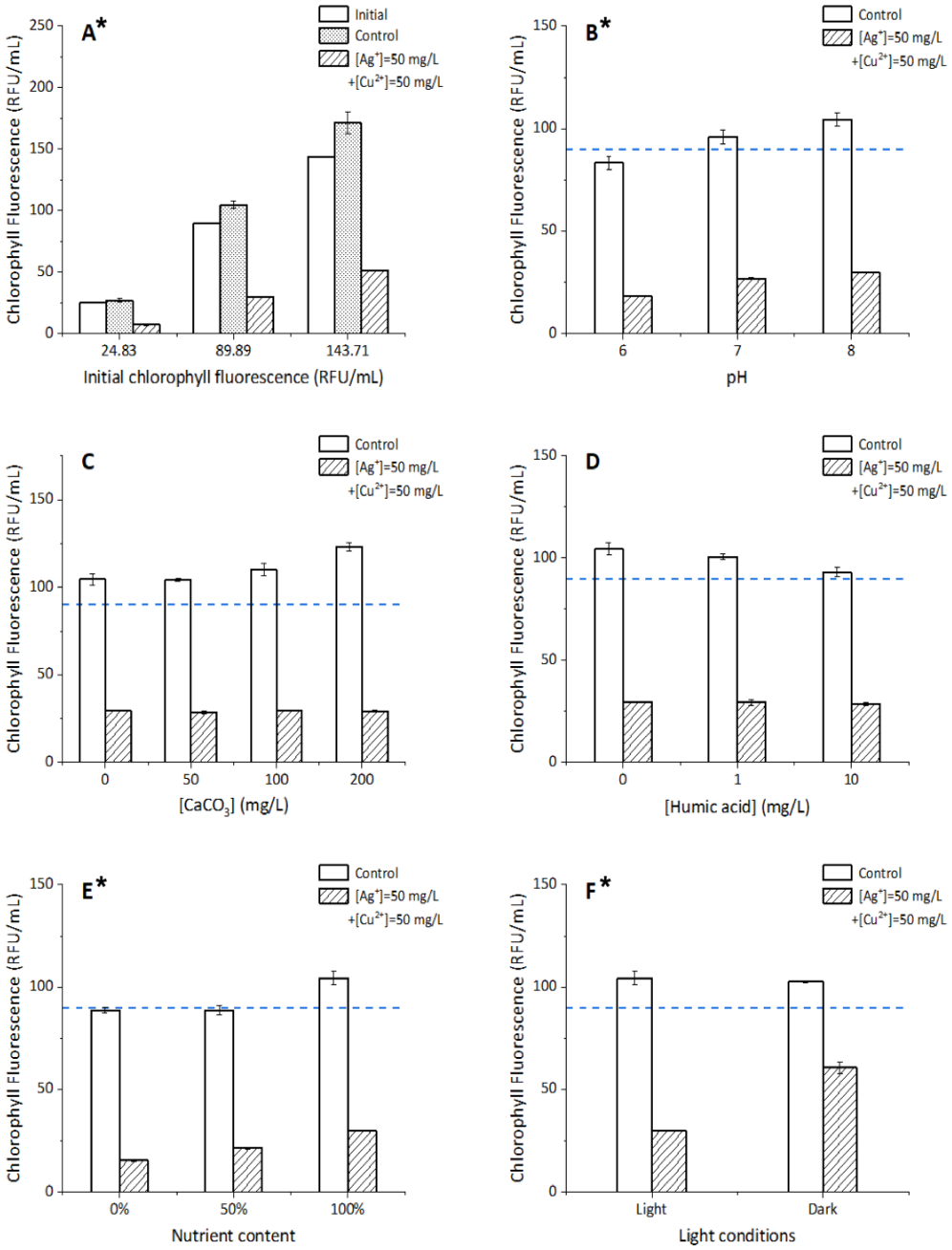

Figure 3. Disinfection effectiveness as a function of (A) initial chlorophyll fluorescence (24.83, 89.89 and 143.71 RFU/mL respectively); (B) pH; (C) water hardness; (D) NOM; (E) nutrient content; and (F) light condition with $[Cu^{2+}]$ = 50 mg/L, $[Ag^{+}]$ = 50 mg/L and 2.5 h contact time. The blue dash line refers to the initial chlorophyll fluorescence = 89.89 RFU/mL for (B) to (F), * means there is a statistically significant difference between treated groups under given conditions, p value given in Table 6.

Table 6. Detailed results and p value tests about the disinfection effectiveness as a function of initial chlorophyll fluorescence, pH, water hardness, NOM, nutrient content and light condition ($p<0.05$ is considered to be statistically significant).

Environmental Condition		Chlorophyll fluorescence (RFU/mL)		p value test ($[Ag^+]$=50 mg/L+$[Cu^{2+}]$ =50 mg/L)	Statistical Significance
		Control group	Metal ions treated group ($[Ag^+]$=50 mg/L+$[Cu^{2+}]$= 50 mg/L)		
Initial chlorophyll fluorescence (RFU/mL)	24.83	26.76±1.60	7.18±0.54	$5.04*10^{-11}$	Statistically significant
	89.89	104.48±3.09	29.71±0.13		
	143.71	171.50±8.69	51.53±0.49		
pH	6	83.31±3.24	18.23±0.15	$3.41*10^{-9}$	Statistically significant
	7	95.96±3.61	26.75±0.35		
	8	104.48±3.09	29.71±0.13		
$[CaCO_3]$ (mg/L)	0	104.48±3.09	29.71±0.13	0.165	Statistically not significant
	50	104.25±0.97	28.74±0.84		
	100	110.06±3.66	29.78±0.22		
	200	123.33±2.42	29.29±0.69		
[Humic acid] (mg/L)	0	104.48±3.09	29.71±0.13	0.423	Statistically not significant
	1	100.56±1.47	29.52±1.38		
	10	93.07±2.35	28.74±0.70		
Nutrient content (%)	0	88.68±1.25	15.31±0.31	$4.19*10^{-9}$	Statistically significant
	50	88.71±2.33	21.39±0.37		
	100	104.48±3.09	29.71±0.13		
Light conditions	Light	104.48±3.09	29.71±0.13	$4.24*10^{-5}$	Statistically significant
	Dark	102.77±0.52	60.72±2.78		

1.2.1 Effect of initial cyanobacteria concentration on disinfection

Initial cyanobacteria concentration (as determined from chlorophyll fluorescence) of the samples was adjusted to 24.83, 92.58 and 143.71 RFU/mL and then the cyanobacteria were exposed to 50 mg/L Ag^{+} and Cu^{2+} for 2.5 h, to explore the possible influence of cyanobacteria concentration on disinfection effectiveness. As shown in Figure 3 (A), initial chlorophyll fluorescence is a factor that determines disinfection effectiveness. When exposed to the same concentration of Cu^{2+} and Ag^{+}, the one with lowest initial chlorophyll fluorescence resulted in largest decrease of the final chlorophyll fluorescence (around 71.06% of initial RFU), followed by the medium RFU (66.94%) and the high RFU (64.14% of the initial one). This is supported by previous research stating that the disinfection effect is determined by the initial level of disinfectant per cell [90]. Thus, a higher initial level of disinfectant per cell will accelerate the disinfection process.

1.2.2 Effect of pH on disinfection

The pH of the BG-11 medium was adjusted to 6, 7 and 8 respectively with 0.1 M HNO_3 and 0.1 M NaOH to explore the possible influence of pH on disinfection effectiveness. As shown in Figure 3 (B), the growth and disinfection of *O. tenuis* are sensitive to the change of pH in the environment. Chlorophyll fluorescence decreased the most under an acidic environment (pH = 6), followed by neutral (pH = 7) and alkaline (pH = 8). The possible reason for this phenomenon is due to the speciation of Ag^{+} and Cu^{2+} in the medium under different pH conditions. Although the speciation and concentration of free Ag^{+} remains stable under the environment with pH=6 to 8, the change of pH will influence the speciation of Cu^{2+} in BG-11 medium, as the constituents include CO_3^{2-} which will combine with Cu^{2+} and form insoluble $CuCO_3$ [91]. Free Cu^{2+} is the dominant species in water under an acidic

environment, while $CuCO_3$ dominates at alkaline conditions [91]. Since the free Cu^{2+} ions are the predominant toxic species against microorganisms within short contact time [92], reduction of free Cu^{2+} ions in the medium will weaken the disinfection effectiveness. Thus, the difference of chlorophyll fluorescence in the disinfectant-treated group is due to the change of dominant species of Cu^{2+} at different pH.

1.2.3 Effect of water hardness on disinfection

Water hardness, usually expressed as the concentration of $CaCO_3$ in water, is one of the main environmental factors that determine the quality of freshwater. In this study, different concentrations of $CaCO_3$ (50, 100 and 200 mg/L) were added into the system to simulate soft, moderate hard and very hard water. As shown in Figure 3 (C), the chlorophyll fluorescence increased more with higher concentration of $CaCO_3$ in the control group. However, no significant change of the chlorophyll fluorescence was found in the group treated with Cu^{2+}+Ag^{+} and different concentrations of $CaCO_3$ ($p=0.165>0.05$). This is mainly because the speciation of Cu^{2+} and Ag^{+} was not changed substantially with the addition of $CaCO_3$ [64, 93]. Thus, water hardness is not a factor that will influence the disinfection process.

1.2.4 Effect of NOM on disinfection

NOM, which is derived from decaying plant and animal matter, is one of the main constituents in many environmental and drinking supply water sources, particularly those that harbor cyanobacteria. To evaluate the influence of NOM on the disinfection process, different concentrations of humic acid (HA) (0, 1 and 10 mg/L) were added into the system. As shown in Figure 3 (D), the growth of *O. tenuis* is influenced by the addition of HA, as the chlorophyll fluorescence decreased with the increasing concentration of HA in the control.

However, no significant difference of fluorescence was found between the groups treated with Cu^{2+}+Ag^{+} and different concentrations of HA ($p=0.423>0.05$). Although HA could form complexes with Cu^{2+} and Ag^{+}, and the Cu-HA and Ag-HA complex are not so toxic compared to free ions [94-95], the affinity is quite limited under the concentration range of HA considered in this study (0-10 mg/L). Thus, the concentration of effective free Cu^{2+} and Ag^{+} is not influenced noticeably, and no influence on disinfection effectiveness was observed.

1.2.5 Effect of nutrient content on disinfection

To explore the influence of different nutrient levels on the disinfection effectiveness, the BG-11 medium for *O. tenuis* was diluted to 0% (i.e. with no nutrient and only deionized water) and 50% of original concentration with deionized water. As shown in Figure 3 (E), the decrease of nutrients (0% and 50%) did not influence the fluorescence of the control group significantly. This is mainly because the poor nutrient environment will stimulate the metabolism of *O. tenuis* during the short contact time (2.5 h). In the group exposed to Cu^{2+}+Ag^{+}, the fluorescence decreased the most with 0% nutrient, followed by 50% and 100% nutrient. A possible reason for this phenomenon might be that the concentration of free Ag^{+} is affected to the nutrient concentration in the medium, as $CaCl_2$ is one of the ingredients of the medium (Table S1) and Cl^{-} will combine with Ag^{+} thus influencing the disinfection effectiveness. In a low nutrient environment, free Ag^{+} will be present in higher amounts and result in better disinfection effectiveness. Compared to Ag^{+}, the disinfection ability of Cu^{2+} is not influenced by the concentration of nutrients, as the ingredients of the medium do not change the speciation of Cu^{2+} in water.

1.2.6 Effect of lighting condition on disinfection

Illumination is essential for the growth of cyanobacteria, thus the influence of lighting conditions on disinfection effectiveness was considered as well. The disinfection process was done under both light and dark conditions for comparison., and the results are shown in Figure 3 (F). Change of lighting conditions within a short contact time (2.5 h) did not lead to noticeable difference of the chlorophyll fluorescence in the control group. However, the chlorophyll fluorescence decreased more under the lighting condition than that under a dark one in the group exposed to Cu^{2+}+Ag^{+}. As Cu^{2+} is not sensitive to the light, the main reason for this phenomenon is due to one of the disinfection mechanisms by Ag^{+} which is related to the lighting condition. Ag^{+} can combine with the thiol group of proteins and hinder their enzymatic function [60], but the behavior of Ag^{+}-protein complex may be affected by the light irradiation [96]. According to the results from a previous study about disinfection of *E. coli* by Ag^{+}, the inactivation of *E. coli* is enhanced by the photochemical reaction of Ag^{+}-protein complex under UV-A or visible light irradiation [96]. Thus, disinfection is more effective under the illuminated rather than dark conditions.

2. Cyanotoxin extraction and quantification

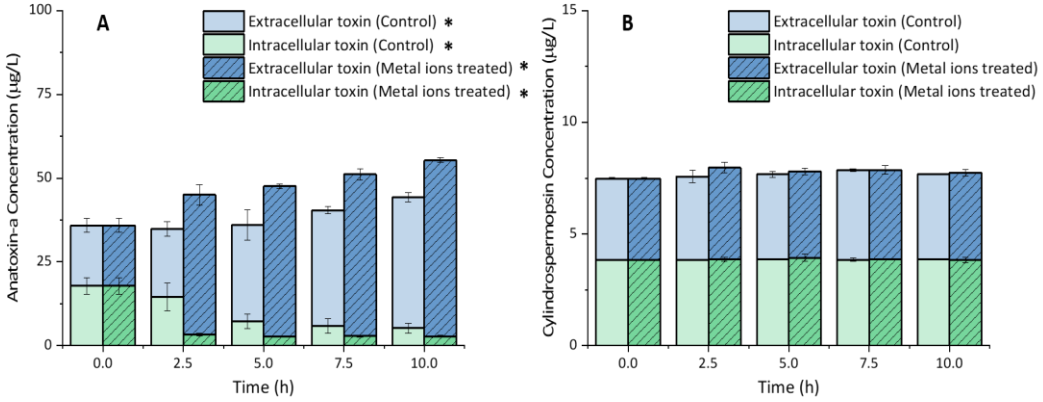

Figure 4. Concentration of extracellular and intracellular anatoxin-a (A) and cylindrospermopsin (B) versus time during disinfection with [Cu^{2+}] =50 mg/L and [Ag^{+}] =50 mg/L. * means there is a statistically significant difference between treated groups under given conditions, p value given in Table 8.

Table 7. Detailed results about the concentration of extracellular and intracellular anatoxin-a and cylindrospermopsin versus time during disinfection with combined Ag^{+} and Cu^{2+}.

Cyanotoxin		Time (h)	Extracellular concentration (ug/L)	Intracellular concentration (ug/L)
Anatoxin-a	Control group	0	18.04±2.07	17.82±2.38
		2.5	20.24±2.18	14.58±4.19
		5	28.66±4.22	7.35±2.15
		7.5	34.55±1.07	5.91±2.20
		10	39.10±1.41	5.22±1.55
	Metal ions treated group ([Ag^{+}]=50mg/L+[Cu^{2+}]=50 mg/L)	0	18.04±2.07	17.82±2.38
		2.5	41.78±3.03	3.27±0.41
		5	44.81±0.71	2.76±0.18
		7.5	48.21±1.70	2.90±0.32
		10	52.49±0.70	2.83±0.27
Cylindrospermopsin	Control group	0	3.65±0.04	3.83±0.03
		2.5	3.72±0.28	3.85±0.02
		5	3.79±0.14	3.87±0.02
		7.5	4.00±0.06	3.86±0.07
		10	3.79±0.01	3.88±0.02
	Metal ions treated group ([Ag^{+}]=50mg/L+[Cu^{2+}]=50 mg/L)	0	3.65±0.04	3.83±0.03
		2.5	4.10±0.23	3.86±0.09
		5	3.86±0.15	3.94±0.16
		7.5	3.99±0.19	3.88±0.02
		10	3.90±0.14	3.84±0.12

Table 8. P value tests about the concentration of extracellular and intracellular anatoxin-a and cylindrospermopsin versus time during disinfection with combined Ag^{+} and Cu^{2+} ($p<0.05$ is considered to be statistically significant).

Test		p value	Statistical Significance
Anatoxin-a	Extracellular (control)	$3.69*10^{-6}$	Statistically significant
	Extracellular (metal ions-treated)	$5.67*10^{-9}$	Statistically significant
	Intracellular (control)	$4.49*10^{-4}$	Statistically significant
	Intracellular (metal ions-treated)	$3.13*10^{-8}$	Statistically significant
Cylindrospermopsin	Extracellular (control)	0.097	Statistically not significant
	Extracellular (metal ions-treated)	0.056	Statistically not significant
	Intracellular (control)	0.616	Statistically not significant
	Intracellular (metal ions-treated)	0.714	Statistically not significant

In this study, 5 mL of *O. tenuis* culture was monitored at different times during disinfection to determine the levels of cyanotoxins. After centrifuging the culture, the extracellular toxin was collected from the supernatant, and the intracellular toxin was extracted from the pellet using 5 mL 5% aqueous acetic acid. Samples from both the control and the combined metal ions treatment (50 mg/L each of Cu^{2+} + Ag^{+}) groups were collected and quantified for comparison. Total and extracellular concentration of anatoxin-a increased (Figure 4 (A)), and the intracellular concentration decreased overtime in both the control and

metal ions treated groups. However, compared to the control group, in the combined metal ion treatment the total, extracellular and intracellular concentrations of anatoxin-a had pronounced changes. Both the increase of total and extracellular concentrations and the decrease of intracellular concentrations were amplified when the *O. tenuis* was treated with Cu^{2+} and Ag^{+}. This indicates that the addition of Cu^{2+} and Ag^{+} will stimulate not only the production of anatoxin-a, but also the release of anatoxin-a through the cell membrane.

In contrast, the addition of disinfectant (combined Cu^{2+} and Ag^{+}) did not lead to a significant change in the total, extracellular and intracellular concentrations of cylindrospermopsin in either the control or treatment groups over time (p values are given in Table 8). Since extracellular cylindrospermopsin concentration increases only in the late exponential or stationary phase [97], and the culture used for this study was at an early exponential phase, both the extracellular and intracellular concentrations of cylindrospermopsin remained stable within 10 h. Although cell lysis during disinfection may lead to the release of cylindrospermopsin, it has been studied that the main reason of increasing extracellular cylindrospermopsin concentration is not due to the release of cylindrospermopsin during cell lysis, but due to the active release or leakage from intact cells [98]. Since the addition of Cu^{2+} and Ag^{+} did not influence the release or leakage of cylindrospermopsin from intact cells, the intracellular and extracellular distribution of cylindrospermopsin remained stable over time.

3. Simultaneous sorption of Cu^{2+}, Ag^{+}, anatoxin-a and cylindrospermopsin by Mag-PCMA

3.1 Relationship between adsorbent dosage and removal efficiency

Simultaneous sorption of the disinfectants (Cu^{2+} and Ag^{+}, 50 mg/L each) and the cyanotoxins produced by *O. tenuis* (anatoxin-a and cylindrospermopsin, 20 ug/L) at different concentrations of Mag-PCMA (1-5 g/L) were studied at pH = 7 and room temperature. As shown in Figure 5 (A), Ag^{+} can be efficiently captured by Mag-PCMA, with a removal efficiency reaching 99.5% at 2 g/L of Mag-PCMA. Compared to Ag^{+}, Cu^{2+} cannot be adsorbed by Mag-PCMA with that level of removal efficiency. The removal efficiency of Cu^{2+} increased substantially with higher adsorbent dosage up to 3 g/L, reaching 38.89%. Above 3 g/L the removal efficiency increased asymptotically up to 40.34%, probably due to the challenge of keeping the Mag-PCMA particles suspended at concentrations above 3 g/L.

The main reason for the difference in removal efficiency of Cu^{2+} versus Ag^{+} by Mag-PCMA is due to the sorption mechanism and the core-shell structure of Mag-PCMA. Due to the negatively charged surface, Mag-PCMA can adsorb metal ions through electrostatic interactions. However, since the surface of the magnetite core is coated with cationic surfactant (3-trimethoxysilyl propyl octadecyl dimethyl ammonium chloride), there will be electrostatic repulsion between the coated cationic surfactant and the metal ions, which will cancel out part of the electrostatic interaction. The electrostatic repulsion is determined by the electronegativity of each metal ion (2.00 for Cu^{2+} and 1.93 for Ag^{+}, dimensionless [99]), resulting in the selectivity of sorption among various metal ions. Stronger repulsion will take place between the cationic surfactant and more positively charged metal ions. Thus, Ag^{+} can

be captured by Mag-PCMA with higher efficiency than Cu^{2+}. The concentration of metal ions can be further decreased by additional sorption cycles until reaching a safe level [90].

Simultaneous removal of anatoxin-a and cylindrospermopsin are shown in Figure 5 (A). Compared to cylindrospermopsin, anatoxin-a can be removed by Mag-PCMA with higher efficiency. 38.91% of anatoxin-a was removed by 3 g/L Mag-PCMA, and the removal efficiency increased slowly up to 42.80% with 5 g/L Mag-PCMA. As comparison, only 15.24% of cylindrospermopsin can be captured by 3 g/L Mag-PCMA, and the removal efficiency remains at this level even with additional dosing of Mag-PCMA up to 5 g/L. The differences in removal efficiency for anatoxin-a and cylindrospermopsin can be explained by considering the sorption mechanism and chemical structure of these two cyanotoxins (Figure S1). Mag-PCMA can attract anatoxin-a through electrostatic interaction due to its negatively charged surface [82], as anatoxin-a is positively charged in a neutral environment (pKa=9.4) [100]. Although the same mechanism is valid for sorption between cylindrospermopsin and Mag-PCMA, the anionic sulfur group in cylindrospermopsin (Figure S1) will weaken the attraction by Mag-PCMA [101]. Thus, the removal efficiency of cylindrospermopsin is lower than that of anatoxin-a at the same dosage of Mag-PCMA. Nevertheless, it is an added value to be able to partially remove these cyanotoxins with the same magnetic nanoparticles used to recover the metal ion disinfectants, thus reducing their concentrations in the treated water. Since in these studies we simulate a cyanobacteria bloom with very high cell concentrations, the concentration of metal ions and cyanotoxins are high. Even so, the simultaneous removal of metal ions and cyanotoxins is considered to be efficient. Less Mag-PCMA would be needed for practical use when the cyanotoxins and metal ions are at a lower level than under the tested conditions, and the removal efficiency of target chemicals will be improved with a

reduced initial concentration. Further optimization of the magnetic nanoparticle may result in tailored nanomaterials for this specific application. The high dosage of Mag-PCMA is due to the high concentration of cyanobacteria considered here, and would be optimized for lower concentrations.

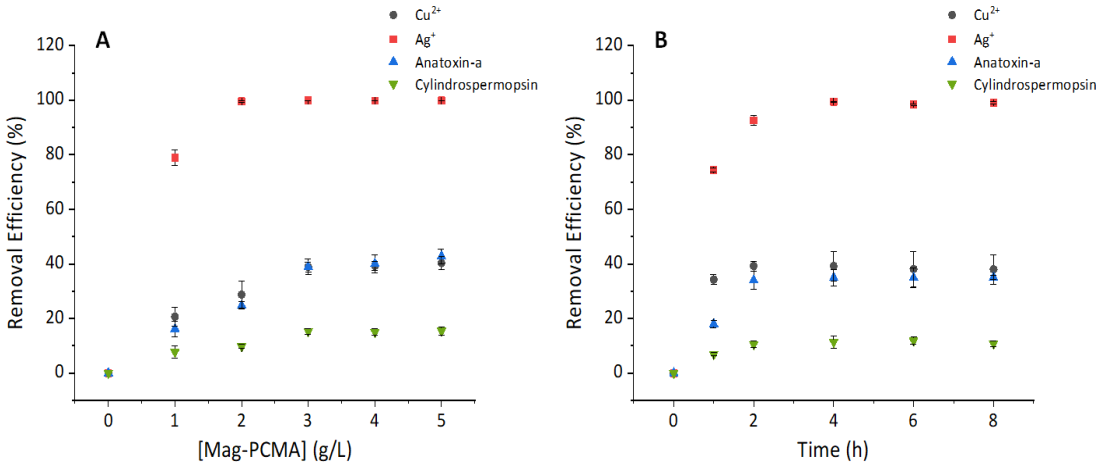

Figure 5. (A) Adsorption of Cu^{2+}, Ag^{+}, anatoxin-a and cylindrospermopsin onto Mag-PCMA as a function of adsorbent dose with [Ag^{+}] =50 mg/L, [Cu^{2+}] =50 mg/L, [anatoxin-a] =20 ug/L and [cylindrospermopsin] =20 ug/L. (B) Sorption uptake of Cu^{2+}, Ag^{+}, anatoxin-a and cylindrospermopsin versus time (with [Ag^{+}] =50 mg/L, [Cu^{2+}] =50 mg/L, [anatoxin-a] =20 ug/L, [cylindrospermopsin] =20 ug/L and [Mag-PCMA] =2.5 g/L).

Table 9. Detailed results about the simultaneous sorption of Cu^{2+}, Ag^{+}, anatoxin-a and cylindrospermopsin onto Mag-PCMA as a function of adsorbent dose or time.

Sorption process		Removal efficiency (%)			
		Ag^{+}	Cu^{2+}	Anatoxin-a	Cylindrospermopsin
[Mag-PCMA] (mg/L)	0	0.00±0.00	0.00±0.00	0.00±0.00	0.00±0.00
	20	78.91±2.83	20.70±3.37	16.19±2.80	7.75±2.23
	40	99.53±0.26	28.76±4.91	24.81±1.35	9.72±0.78

	60	99.86±0.02	38.90±1.77	38.92±2.91	15.25±1.02
	80	99.79±0.05	39.32±1.64	40.05±3.32	15.01±1.24
	100	99.85±0.03	40.34±2.34	42.80±2.66	15.42±1.58
Time (h)	0	0.00±0.00	0.00±0.00	0.00±0.00	0.00±0.00
	1	74.46±0.74	34.27±1.84	17.99±1.43	6.88±0.61
	2	92.61±1.91	39.25±1.76	34.03±3.20	10.55±1.26
	4	99.41±0.04	39.20±5.42	34.91±2.93	11.37±2.36
	6	98.39±0.26	38.12±6.38	34.95±3.57	11.87±1.27
	8	99.02±0.53	38.00±5.40	35.06±0.86	10.76±1.08

Table 10. P value tests about the simultaneous sorption of Cu^{2+}, Ag^{+}, anatoxin-a and cylindrospermopsin onto Mag-PCMA as a function of adsorbent dose or time ($p<0.05$ is considered to be statistically significant).

Test		p value	Statistical Significance
Cu^{2+}	[Mag-PCMA]>3 g/L	0.667	Statistically not significant
Ag^{+}	[Mag-PCMA]>2 g/L	0.053	Statistically not significant
Anatoxin-a	[Mag-PCMA]>3 g/L	0.327	Statistically not significant
Cylindrospermopsin	[Mag-PCMA]>3 g/L	0.928	Statistically not significant
Cu^{2+}	t>2 h	0.983	Statistically not significant
Ag^{+}	t>4 h	0.913	Statistically not significant
Anatoxin-a	t>2 h	0.967	Statistically not significant
Cylindrospermopsin	t>2 h	0.733	Statistically not significant

3.2 Sorption kinetics

Simultaneous sorption kinetics of 50 mg/L Ag^{+}, 50 mg/L Cu^{2+}, 20 ug/L anatoxin-a and 20 ug/L cylindrospermopsin with Mag-PCMA (2.5 g/L) were studied at pH = 7 and room temperature (Figure 5 (B)). As shown in Figure 5 (B), rapid sorption occurred within 1 h and the removal efficiency gradually increased until reaching a maximum (99% for Ag^{+} after 4 h, 38.5% for Cu^{2+} after 2 h, 35% for anatoxin-a after 2 h, and 10.5 % for cylindrospermopsin after 2 h). The kinetics is mainly influenced by the available sorption sites on the surface of Mag-PCMA. The rapid sorption within 1 h is due to the abundant sorption sites at first. With more and more adsorbates loaded onto the Mag-PCMAs, the available sorption sites decrease, and the sorption rate slows down. Thus, it will take longer time for a system with higher removal efficiency (e.g. Ag^{+}) to reach equilibrium.

3.3 Influence of different environmental conditions on adsorption

3.3.1 pH

The influence of pH on the adsorption process of the four target chemicals with Mag-PCMA was evaluated with 50 mg/L Ag^{+}, 50 mg/L Cu^{2+}, 20 ug/L anatoxin-a, 20 ug/L cylindrospermopsin and 2.5 g/L Mag-PCMA at room temperature. Removal efficiency of all these four chemicals remained stable when the pH was varied from 6 to 8 (around 99.5% for Ag^{+}, 28% for Cu^{2+}, 24.5% for anatoxin-a and 11.5% for cylindrospermopsin, Figure 6 (A)). The p-values for these experiments are given in Table 12. This is mainly due to the sorption mechanism of these four chemicals by Mag-PCMA, which is electrostatic interaction. Since the speciation of Ag^{+} and Cu^{2+} remains stable with the change of pH from 6 to 8 (K_{sp} $(AgOH)=2*10^{-8}$, K_{sp} $(Cu(OH)_2)=2.2*10^{-20}$ at room temperature [102-103]), the removal

efficiency was not influenced. Besides, there was no significant change in the surface charge of Mag-PCMA at different pH [82], resulting in stable removal of anatoxin-a and cylindrospermopsin.

3.3.2 Water hardness

Different concentrations of $CaCO_3$ were considered to evaluate the possible influence of hardness on the sorption process with Mag-PCMA. As shown in Figure 6 (B), no significant influence was observed on the removal efficiency (around 99.5% for Ag^+, 28% for Cu^{2+}, 24.5% for anatoxin-a and 11.5% for cylindrospermopsin, p values for these systems are given in Table 12). This is because the addition of $CaCO_3$ did not change the aqueous speciation of Ag^+ and Cu^{2+}, nor did it influence the surface charge of Mag-PCMA. Although a small fraction of Ca^{2+} may be dissolved from $CaCO_3$ and released into the water and be captured by Mag-PCMA, it does not compete significantly with the sorption of Ag^+ and Cu^{2+} (K_{sp} ($CaCO_3$) =2.8×10^{-9} at room temperature [104]). Thus, water hardness is not a major concern for the removal of the target chemicals.

3.3.3 Cl^-

The presence of Cl^- may be another factor that could influence the removal of the target chemicals in this study, as Cl^- is able to combine with Ag^+ to form precipitation thus reducing the concentration of free Ag^+ in water. Thus, different concentrations of Cl^- (0, 1 and 10 mg/L) were added. As shown in Figure 6 (C), no significant change in removal efficiency on Cu^{2+}, anatoxin-a and cylindrospermopsin was observed (around 28% for Cu^{2+}, 24.5% for anatoxin-a and 11.5% for cylindrospermopsin; p values for these systems are given in Table 12), since the presence of Cl^- did not influence the surface charge of Mag-

PCMA or the speciation of Cu^{2+} in water. However, the sorption process of Ag^{+} was influenced by Cl^{-}, as the concentration of Cl^{-} determines the percentage of free Ag^{+} in water. With the addition of 1 mg/L Cl^{-}, free Ag^{+} decreased from 100% to 96.74% (K_{sp} (AgCl)=$1.77*10^{-10}$ at room temperature [70]). After sorption, 90.97% of the free Ag^{+} was removed by Mag-PCMA, which is less than the removal efficiency without Cl^{-} (99.5%). When the concentration of Cl^{-} increased to 10 mg/L, the percentage of free Ag^{+} decreased to 41.96%, and the percentage of free Ag^{+} adsorbed by Mag-PCMA decreased to 75.64%. Thus, the presence of Cl^{-} is a factor that needs to be considered when evaluating the disinfection and sorption process with Ag^{+}. The AgCl complex is likely to precipitate, and Ag can be recovered in the sludges, but it would be a more expensive separation.

3.3.4 NOM

Similar to the addition of $CaCO_3$, the presence of humic acid with different concentrations did not influence the removal efficiency of the four chemicals significantly (around 99.5% for Ag^{+}, 28% for Cu^{2+}, 24.5% for anatoxin-a and 11.5% for cylindrospermopsin in Figure 6 (D); p values for these systems are given in Table 12). The added HA did not compete with the four target chemicals for sorption sites, as both HA and Mag-PCMA are negatively charged [82, 105]. Thus, the surface charge of Mag-PCMA remains stable with the addition of HA. Nor will HA change the speciation of Ag^{+} and Cu^{2+}, since the combination between Ag^{+} or Cu^{2+} and HA is quite limited at the range of concentrations considered for HA in this study (0-10 mg/L) and is not comparable to that between Ag^{+} or Cu^{2+} and Mag-PCMA. This is supported by a previous study of the simultaneous sorption of Cd^{2+}, acenaphthene and NOM. When a large amount of Mag-PCMA (>1 g/L) is added, the

difference of sorption capacity of Cd^{2+} and acenaphthene in the absence or presence of NOM is negligible [82].

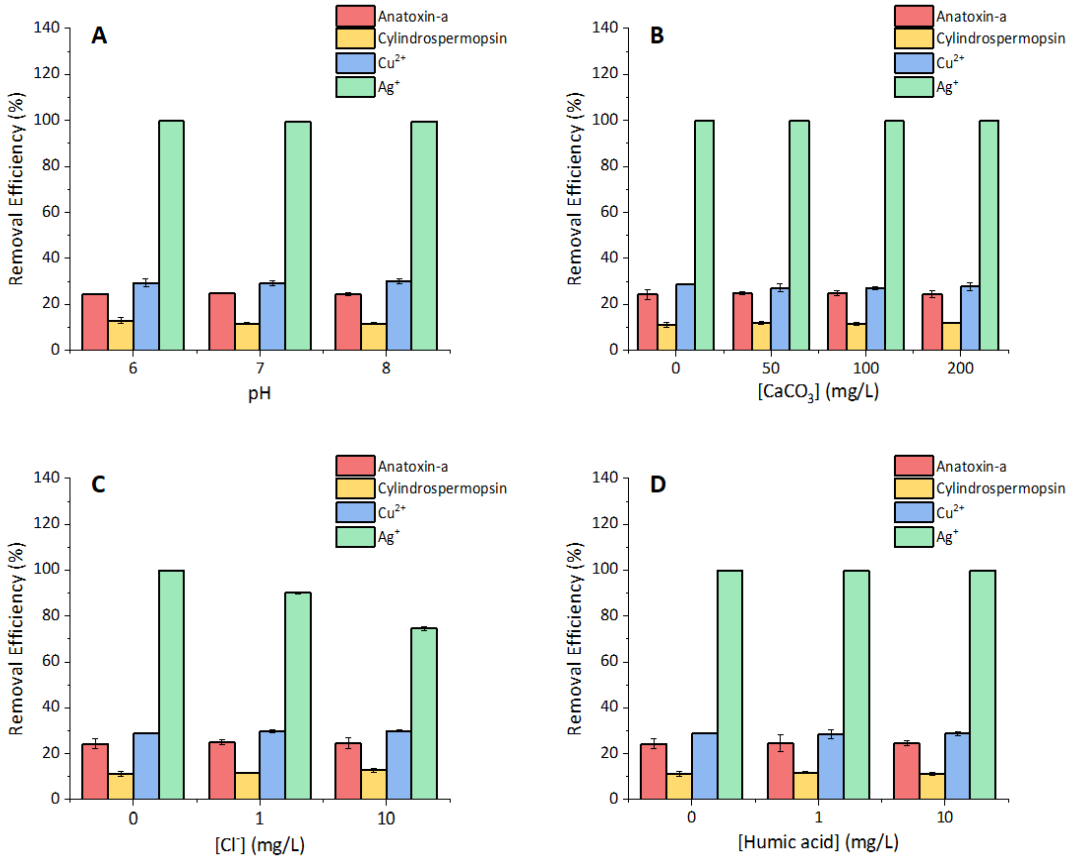

Figure 6. Influence on sorption for [Ag^+] =50 mg/L, [Cu^{2+}] =50 mg/L, [cylindrospermopsin] =20 ug/L, [anatoxin-a] =20 ug/L and [Mag-PCMA] =2.5 g/L of different (A) pH; (B) water hardness; (C) Cl^- concentration; and (D) NOM concentration.

Table 11. Detailed results about the influence on simultaneous sorption for Ag^+, Cu^{2+}, anatoxin-a and cylindrospermopsin with different pH, water hardness, Cl^- concentration and NOM concentration.

Environmental Conditions		Removal efficiency (%)			
		Ag^+	Cu^{2+}	Anatoxin-a	Cylindrospermopsin
pH	6	99.74±0.01	29.35±1.81	24.39±0.23	12.91±1.35
	7	99.39±0.05	29.32±1.05	24.78±0.20	11.64±0.53

	8	99.50±0.07	30.19±1.08	24.36±0.54	11.69±0.52
[$CaCO_3$] (mg/L)	0	99.81±0.06	28.65±0.15	24.32±2.11	11.03±1.03
	50	99.76±0.05	27.13±1.84	24.85±0.56	11.91±0.46
	100	99.84±0.05	27.12±0.68	24.86±1.19	11.48±0.52
	200	99.83±0.07	27.72±1.63	24.46±1.60	11.82±0.10
[Cl^-] (mg/L)	0	99.81±0.06	28.65±0.15	24.32±2.11	11.03±1.03
	1	90.13±0.42	29.04±0.89	25.01±1.21	11.52±0.19
	10	74.53±0.97	29.10±0.95	24.53±2.24	12.71±1.01
[Humic acid] (mg/L)	0	99.81±0.06	28.65±0.15	24.32±2.11	11.03±1.03
	1	99.80±0.08	28.33±2.03	24.61±3.56	11.81±0.55
	10	99.93±0.01	28.67±0.72	24.50±0.96	11.28±0.70

Table 12. P value tests about the influence on simultaneous sorption for Ag^+, Cu^{2+}, anatoxin-a and cylindrospermopsin with different pH, water hardness, Cl^- concentration and NOM concentration ($p<0.05$ is considered to be statistically significant).

Environmental Condition		p value	Statistical Significance
Cu^{2+}	pH	0.692	Statistically not significant
	Water hardness	0.460	Statistically not significant
	Cl^-	0.743	Statistically not significant
	NOM	0.934	Statistically not significant
Ag^+	pH	0.814	Statistically not significant
	Water hardness	0.473	Statistically not significant
	Cl^-	$1.22*10^{-8}$	Statistically significant

	NOM	0.060	Statistically not significant
Anatoxin-a	pH	0.345	Statistically not significant
	Water hardness	0.955	Statistically not significant
	Cl^-	0.903	Statistically not significant
	NOM	0.989	Statistically not significant
Cylindrospermopsin	pH	0.221	Statistically not significant
	Water hardness	0.365	Statistically significant
	Cl^-	0.115	Statistically significant
	NOM	0.509	Statistically not significant

4. Regeneration and reuse of Mag-PCMA

To evaluate the regeneration and reusability of Mag-PCMA, Cu^{2+}, Ag^+, anatoxin-a and cylindrospermopsin adsorbed onto Mag-PCMA were extracted with methanol (for anatoxin-a and cylindrospermopsin) and 0.01 M H_2SO_4 (for Cu^{2+} and Ag^+). After extraction, Mag-PCMA was mixed with 50 mg/L Ag^+, 50 mg/L Cu^{2+}, 20 ug/L anatoxin-a and 20 ug/L cylindrospermopsin immediately to evaluate the simultaneous removal performance of Mag-PCMA after regeneration. The sorption and regeneration processes were repeated for five continuous cycles, and the removal efficiency of Cu^{2+}, Ag^+, anatoxin-a and cylindrospermopsin are shown in Figure 7 (A) and (B). No significant change in removal

efficiencies of Cu^{2+}, anatoxin-a and cylindrospermopsin was observed for the regenerated Mag-PCMA up to 5 cycles (p values are given in Table 14). Although the removal efficiency of Ag^{+} decreased gradually during the sorption-desorption cycles, it still remained above 93%, indicating good reusability of Mag-PCMA.

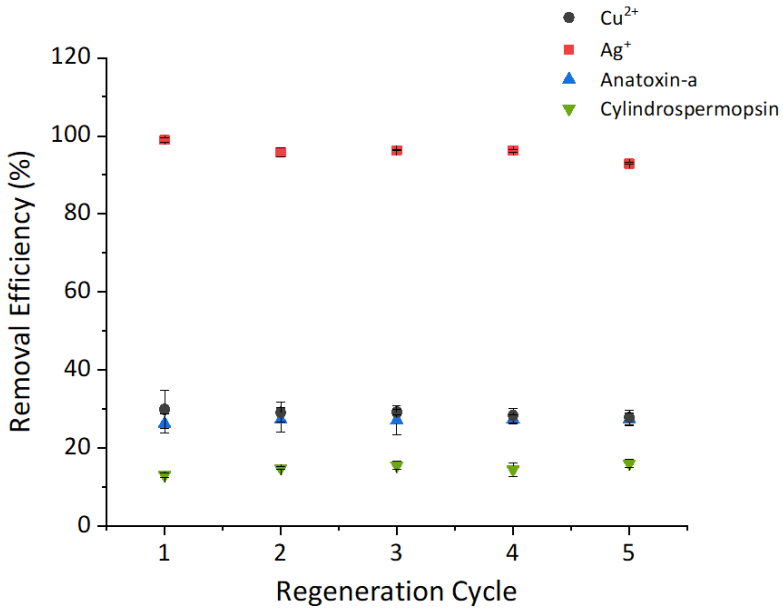

Figure 7. Sorption and recovery efficiency of Cu^{2+}, Ag^{+}, anatoxin-a and cylindrospermopsin after five Mag-PCMA regeneration cycles.

Table 13. Detailed results about the sorption and recovery efficiency of Cu^{2+}, Ag^{+}, anatoxin-a and cylindrospermopsin after five Mag-PCMA regeneration cycles.

Regeneration Cycle	Removal efficiency (%)			
	Ag^{+}	Cu^{2+}	Anatoxin-a	Cylindrospermopsin
1	98.97±0.55	29.88±4.95	26.25±2.52	13.04±0.56
2	95.75±1.19	29.16±2.49	27.24±3.12	14.85±0.43
3	96.31±0.10	29.21±0.65	27.13±3.70	15.50±1.01
4	96.19±0.28	28.32±1.89	27.35±1.26	14.43±1.67
5	92.91±0.21	27.82±1.94	27.41±1.64	16.00±0.97

Table 14. P value tests about Sorption and recovery efficiency of Cu^{2+}, Ag^{+}, anatoxin-a and cylindrospermopsin after five Mag-PCMA regeneration cycles ($p<0.05$ is considered to be statistically significant).

Continuous sorption after regeneration	p value	Statistical Significance
Cu^{2+}	0.900	Statistically not significant
Ag^{+}	$5.31*10^{-6}$	Statistically significant
Anatoxin-a	0.981	Statistically not significant
Cylindrospermopsin	0.523	Statistically not significant

D. Conclusions

In this study, a combination of metal ions (Ag^{+}+ Cu^{2+}) resulted in better disinfection of *O. tenuis* than the individual ions (Cu^{2+}, Ag^{+}), since the combination can achieve the same disinfection effectiveness with shorter time and lower concentration. Environmental conditions that will determine the dominant speciation of metal ions (i.e. pH and nutrient content) or will influence the ratio between cyanobacteria cells and free metal ions, will influence disinfection effectiveness, while those that do not influence the metal ions in water (i.e. water hardness and presence of humic acid) will not change the disinfection effectiveness. Although the addition of metal ions will stimulate the production of cyanotoxin during the disinfection process, both the metal ions and cyanotoxins can be effectively removed by Mag-PCMA through simultaneous adsorption later, and the sorption of metal ions and toxins remains stable under various environmental conditions. Thus, the potential environmental risk caused by the use of metal ions as disinfectant and the production of cyanotoxin during disinfection will be substantially reduced. The disinfection method in this study is sustainable, as metal ions and Mag-PCMA can be regenerated with high efficiency and reused for several continuous cycles (removal efficiency above 93% after

5 cycles). Thus, this novel disinfection method is very promising for practical application in the future.

E. Acknowledgements

This work was supported by the National Science Foundation (NSF) and the U.S. Environmental Protection Agency (EPA) under cooperative agreement number [NSF-EF0830117 and NSF 1901515]. Arturo A. Keller also appreciates Agilent Technologies for their Agilent Thought Leader Award. Any opinions, findings, conclusions, or recommendations expressed in this material are those of the authors and do not necessarily reflect the views of the funding agencies. All the figures in this manuscript are intended for color reproduction online.

F. Appendix

1. Recipe of BG-11 medium

Table S1. Recipe of BG-11 medium

$NaNO_3$	17.6 mM
K_2HPO_4	0.23 mM
$MgSO_4•7H_2O$	0.3 mM
$CaCl_2•2H_2O$	0.24 mM
Citric Acid•H_2O	0.031 mM
Ferric Ammonium Citrate	0.021 mM
$Na_2EDTA•2H_2O$	0.0027 mM
Na_2CO_3	0.19 mM
H_3BO_3	4.6*10-2 mM
$MnCl_2•4H_2O$	9*10-3 mM
$ZnSO_4•7H_2O$	7.7*10-4 mM

$Na_2MoO4•2H_2O$	1.6*10-3 mM
$CuSO_4•5H_2O$	3*10-4 mM
$Co(NO_3)_2•6H_2O$	1.7*10-4 mM

2. Method of synthesizing Mag-PCMA

The Mag-PCMA was prepared by a three-steps procedure [87]. First, maghemite iron (III) oxide nanoparticles were negatively activated by dispersing the magnetic nanoparticles in tetramethylammonium hydroxide solution under constant stirring overnight. Next, a cationic surfactant, 3-trimethoxysilyl propyl octadecyl dimethyl ammonium chloride, was deposited onto the activated magnetite surface with constant stirring of the suspension. In the end, tetraethyl orthosilicate was attached to the trimethoxysilyl groups of the surfactants through covalently bonds to cross-link the surfactant onto the magnetic iron core. All the steps were performed at room temperature.

3. Chemical structure of anatoxin-a and cylindrospermopsin

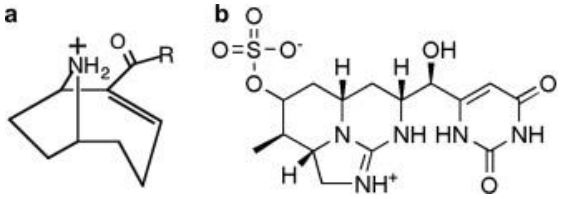

Figure S1. Chemical structure of (a) anatoxin-a and (b) cylindrospermopsin [101].

IV. Removal of MS-2 viruses with recyclable magnetic nanoparticles coated with metal ions

Abstract A novel disinfection method with recyclable magnetic nanoparticles is presented to optimize the traditional method with metal ions on virus contamination. In this study, magnetic nanoparticles with permanently confined micelle arrays (Mag-PCMA) were coated with Ag^{+}, Cu^{2+} and Fe^{3+} via sorption to increase the zeta potential from negative to positive. The increase of zeta potential was influenced by both the concentration of adsorbed metal ions, and the number of positive charges for each metal ion. Three types of Mag-PCMA coated with different metal ions (Mag-PCMA-MI) were mixed with a model virus, MS-2, to evaluate their disinfection ability. MS-2 removal by Mag-PCMA-MI was influenced by the concentration of Mag-PCMA-MI and contact time. MS-2 removal efficiency reached 99% with 0.5 g/L Mag-PCMA-Ag after 30 min. Removal with Mag-PCMA-MI remains stable under most environmental conditions (e.g., water hardness and presence of natural organic matter), except change in pH which decreases of removal efficiency (0.43% for Mag-PCMA-Ag, 0.35% for Mag-PCMA-Cu and 0.28% for Mag-PCMA-Fe) for an increase of pH from 6 to 8. As a common constituent in natural water bodies, the presence of Cl^{-} has no influence on removal with Mag-PCMA-Cu and Mag-PCMA-Fe, but it will weaken the disinfection ability of Mag-PCMA-Ag by combining with the adsorbed Ag^{+}, leading to a decrease in removal efficiency of 0.24% as the Cl^{-} concentration increases from 0 to 100 mg/L. The reuse of Mag-PCMA-MI can be achieved by simply rinsing the nanoparticles with deionized water to remove the inactivated virus after disinfection, and the removal efficiency remains above 99.8% for all three Mag-PCMA-MI after 5 continuous cycles, highlighting the recyclability of the process.

A. Introduction

The worldwide spread of COVID-19 has made the disinfection of viruses one of the hottest topics since 2020. As one of the major sources of microbial contamination in water, viruses have attracted much concern in wastewater treatment due to their potential for spreading diseases. The World Health Organization (WHO) has reported that several types of water-transmitted viruses, including DNA viruses (e.g. adenovirus and herpesviruses) and RNA viruses (e.g. astrovirus, rotavirus, norovirus and other caliciviruses), can spread disease through water, resulting in the increase of threat to human health [106]. For example, several enteric viruses including norovirus, rotavirus, sapovirus, astrovirus and adenovirus have been recognized to be the main causes of nonbacterial acute gastroenteritis, and they have been detected in tap water, especially in some developing countries [107-109]. During recent years, many outbreaks of water-transmitted viruses have been reported around the world due to fecal contamination, making it a major concern for public health, as hundreds of people were involved in each case. In April–May 2018, over 500 patients were infected by Hepatitis E virus due to an outbreak in Halisohor, Bangladesh caused by the fecal contamination of water [110]. Another large gastroenteritis outbreak that occurred in Northern Greece in 2019 was later identified as a waterborne norovirus outbreak [111]. Given the fact that many viruses can survive in the water for several weeks to months and are infectious even when highly diluted [112-113], seeking efficient methods to remove viruses from water is a high priority in water treatment.

Traditional microfiltration or ultrafiltration methods in drinking water treatment plants are not effective for the removal of viruses in the water due to their size (~0.01-0.1 μm) [113-114]. Other conventional disinfection methods, such as chlorination, ozonation or UV

radiation, may produce disinfection by-products [78, 115-116] or have a high maintenance requirement [11], which are major concerns during practical applications. In contrast, metal ions used as disinfectants have the advantages of good effectiveness without formation of byproduct(s) and low cost of operation. Metal ions can be attracted to the negatively charged surface of viruses through electrostatic interaction, and then destroy DNA, RNA or the enzymes to inactivate target microorganisms [117-118]. Some studies have shown that many metal ions, such as Ag^{+} and Cu^{2+}, are effective disinfectants for both DNA and RNA viruses [119]. However, the residual metal ions in the water after disinfection may be a major concern, as metal ions with concentration beyond a certain level are toxic to humans or ecological receptors. To address this issue, some improvements of the disinfection method with metal ions have been done, such as the combination with other disinfectants to reduce the concentration of metal ions [96], or the use of metal nanoparticles, such as silver nanoparticles [120], photocatalytic TiO_2 [121] and nano-sized ZnO [122], instead of dissolved metal ions. However, many issues need to be addressed before putting the improved methods into practical use. For example, some metal nanoparticles such as TiO_2 and ZnO cannot inactivate target microorganisms effectively without the help of visible light irradiation [121-122], which will increase the energy consumption and maintenance cost for the disinfection system. Besides, the removal of nanoparticles from the water after disinfection is another concern, as the nanoparticles will also generate environmental risk if they are discharged into the natural environment without efficient treatment. Thus, research on the optimization of disinfection with metal ions is still necessary to achieve both high efficiency, low environmental effect, as well as easy operating conditions.

To optimize the disinfection method of virus with metal ions, as well as to reduce the cost, energy consumption and environmental risk, novel magnetic nanoparticles with permanently confined micelle arrays (Mag-PCMA) were coated with metal ions through sorption, and were used to disinfect and remove the target virus under different environmental conditions. In contrast to previous disinfection methods where the waterborne viruses are exposed to the metal ions or to metallic nanoparticles, the proposed method adsorbs the metal ions on the surface of magnetic nanoparticles, and then the magnetic nanoparticles coated with metal ions (Mag-PCMA-MI) are used for disinfection. In this way, the novel magnetic nanoparticles can retain the disinfection ability of the metal ions, and can be easily removed from the water with the external magnetic field after treatment. After finishing one removal cycle, the magnetic nanoparticles can be regenerated and reused for several continuous cycles by simply rinsing with water, which makes this method suitable for sustainable use.

B. Materials and Methods

1. Materials

Escherichia bacteriophage MS-2 was selected as the target virus in this study, as it has been used as a surrogate for pathogenic RNA viruses in many studies to evaluate the efficacy of disinfection technology, since it is harmless to humans and is easy to propagate, store and quantified [123-124]. *E. coli* C-3000 was used as the host of MS-2. Both MS-2 and *E. coli* C-3000 were purchased from ATCC. Silver nitrate, copper sulfate, iron nitrate, nitric acid, sulfuric acid, sodium hydroxide, sodium chloride and calcium carbonate were purchased from Fisher Scientific (USA). The magnetic nanoparticle, Mag-PCMA, was synthesized

using the method developed in our previous studies [82-88], and the maghemite (iron (III) oxide) nanoparticles (30 nm in diameter) used for synthesis were purchased from Alfa Aesar (USA). In brief, the Mag-PCMA was prepared by a three-steps procedure. First, maghemite iron (III) oxide nanoparticles were negatively activated by dispersing the magnetic nanoparticles in tetramethylammonium hydroxide solution under constant stirring, overnight. Next, a cationic surfactant, 3-trimethoxysilyl propyl octadecyl dimethyl ammonium chloride, was deposited onto the activated magnetite surface with constant stirring of the suspension. In the end, tetraethyl orthosilicate was attached to the trimethoxysilyl groups of the surfactants through covalently bonds to cross-link the surfactant onto the magnetic iron core. All the steps were performed at room temperature. All chemicals were used as received without further purification. All solutions were prepared with deionized water (18 MΩ-cm) from a Barnstead NANOpure Diamond Water Purification System (USA).

2. Synthesis and characterization of Mag-PCMA coated with metal ions (Mag-PCMA-MI)

50 mg Mag-PCMA were exposed to different concentrations of metal ion solutions (Ag^{+}, Cu^{2+} and Fe^{3+}, 20-150 mg/L) in 20 mL vials for sorption under room temperature. After sorption reached equilibrium, the Mag-PCMA-MI were separated with a handheld magnet, and samples were collected from the supernatant to measure the concentration of metal ions via an Agilent 7900 (Agilent Technologies) inductively coupled plasma mass spectrometer (ICP-MS). Mag-PCMA-MI were then washed with deionized water for 2 times and dried in the oven at 75 ^{o}C for 24 h. Dried nanoparticles were dispersed in water again and the dispersion was used for zeta potential analysis by a Malvern Zetasizer.

3. Removal of MS-2 with Mag-PCMA-MI

MS-2 was mixed with different concentrations of the various Mag-PCMA-MI (0.5-2.5 g/L) in 20 mL glass vial for disinfection and removal. Samples were collected at various contact times (0.5, 1 and 2 h) and passed through a 0.22 μm Millipore filter for measurement. The removal process was done under a pH=6.0 environment adjusted via a phosphate buffer saline solution. The concentration of infectious MS-2 in each sample was determined by double layer agar plaque assay [125]. In brief, the sample was diluted properly, then 100 μl of the diluted sample was mixed with 100 μl *E. coli* host at exponential phase and 5 mL melted tryptic soy agar (with 0.75% agar) which was kept in a 45 ^{o}C water bath. The mixture was then poured onto the tryptic soy agar plate (with 1.5% agar) immediately, and the agar plate was incubated at 37 ^{o}C for 24 h. The number of plaques on the agar plate was then counted and the concentration of MS-2 was calculated and measured as plaque-forming units (PFU)/mL.

Different environmental conditions, including pH, water hardness, concentration of Cl^- and natural organic matter (NOM) were evaluated, to explore the possible influence on removal efficacy by Mag-PCMA-MI. The pH of the deionized water was adjusted from 6 to 8 using 0.1 M NaOH, and a phosphate buffer saline solution was added to maintain a stable pH. To adjust the water hardness from soft to hard, 50 and 100 mg/L $CaCO_3$ were used. Different concentrations of Cl^- (1-100 mg/L) were added into the mixture to explore the possible influence of Cl^- on removal. This could be especially important for Mag-PCMA-Ag, as the combination of free Cl^- and adsorbed Ag^+ on Mag-PCMA may affect the removal efficacy. In addition, humic acid (HA) with different concentrations (0, 1 and 10 mg/L respectively) was added into the system to explore the influence of NOM.

4. Regeneration and reuse of Mag-PCMA-MI

Regeneration and reuse of Mag-PCMA-MI were investigated in this study. A suspension of MS-2 (2.2 *10^6 PFU/mL) was exposed to 2.5 g/L Mag-PCMA-Ag, Mag-PCMA-Cu or Mag-PCMA-Fe for 1 h to achieve sufficient removal. After removal by an external handheld magnet, the Mag-PCMA-MI were then rinsed with deionized water for 2-3 times to remove the inactivated virus from the surface, and reused for another removal cycle immediately. The continuous removal and regeneration cycles were repeated for five times. Samples were collected in each cycle and the concentration of MS-2 was measured with a double layer agar plaque assay.

5. Data analysis

All tests in this study were performed in triplicate and analysis of variance (ANOVA) was used to test the significance of results. A $p<0.05$ was considered to be statistically significant. The p values of each test are listed in Table 4 and 6.

C. Results and discussions

1. Sorption-based characterization of Mag-PCMA by metal ions

Zeta potential is an important indicator that reflects the stability of nanoparticle dispersions. Previous studies have shown that the zeta potential of Fe_2O_3 nanoparticles with a size ~30 nm is negative when the pH is above 4 [126]. To attract negatively charged MS-2 in neutral environments, the surface of Mag-PCMA was modified to be positively charged using different concentrations of Ag^+, Cu^{2+} and Fe^{3+}. The metal ion solutions were individually mixed with Mag-PCMA to adsorb the metal ions. After sorption reached equilibrium, the relationship between the zeta potential of Mag-PCMA-Ag, Mag-PCMA-Cu

and Mag-PCMA-Fe, and the amount of adsorbed positive charges were explored. The amount of adsorbed positive charges can be calculated with the concentration of adsorbed metal ions on Mag-PCMA and the charge number for each metal ion (Equation 1):

[adsorbed positive charges] = [adsorbed metal ions] * charge number (1)

The relationship between zeta potential and adsorbed positive charges with data from the three systems are shown in Figure 1, and the linear relationship in Figure 1 can be described by Equation 2:

Zeta potential = K_{MI} * [adsorbed positive charges] + b (2)

Here K_{MI} (V*L/equivalents) is the coefficient of the relationship, and b (mV) equals to the zeta potential of Mag-PCMA with no metal ions on the surface. According to the calculation results based on Figure 1, the K_{MI} is 37.895 (V*L/equivalents), and b is -30 mV (R^2=0.9862).

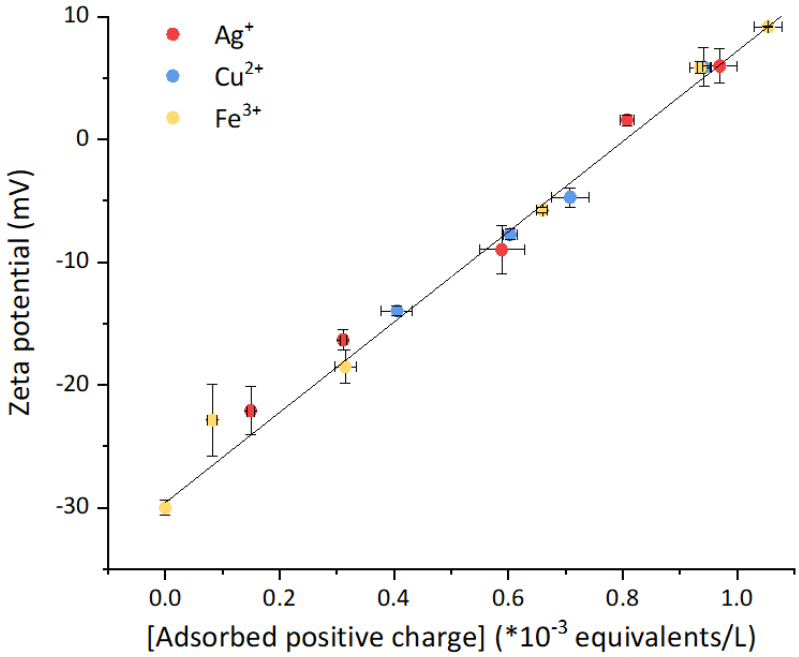

Figure 1. Relationship between concentration of adsorbed positive charge and zeta potential (red plots refer to the data from sorption of Ag^{+} by Mag-PCMA, blue ones refer to those from sorption of Cu^{2+} and yellow ones refer to those from sorption of Fe^{3+}).

Table 1. Detailed results about the concentration of adsorbed positive charge and zeta potential.

Metal ions	[Adsorbed positive charge] (*10-3 equivalents/L)	Zeta potential
Ag^{+}	0.00±0.00	-30.00±0.60
	0.15±0.01	-22.10±1.97
	0.31±0.01	-16.33±0.85
	0.59±0.04	-8.98±1.93
	0.81±0.01	1.57±0.44
	0.97±0.03	5.99±1.38
Cu^{2+}	0.00±0.00	-30.00±0.60
	0.41±0.03	-13.97±0.42

	0.60±0.01	-7.74±0.43
	0.71±0.03	-4.73±0.79
	0.94±0.01	5.90±1.58
	1.13±0.02	14.03±2.40
Fe^{3+}	0.00±0.00	-30.00±0.60
	0.08±0.01	-22.87±2.94
	0.31±0.02	-18.5±1.37
	0.66±0.01	-5.76±0.24
	0.94±0.02	5.86±0.46
	1.05±0.03	9.18±0.07

Based on the relationship in Figure 1 and the corresponding K_{MI} and b, as well as the relationship between the concentration of adsorbed metal ions and positive charges (Equation 1), the minimum concentration of adsorbed metal ions needed to convert the zeta potential of Mag-PCMA from negative to positive can be calculated. For Ag^{+}, the value is $7.9*10^{-4}$ equivalents/L, for Cu^{2+} it is $3.9 *10^{-4}$ equivalents/L and for Fe^{3+} it is $2.6*10^{-4}$ equivalents/L. Due to the limitation of available sorption sites on the surface of Mag-PCMA, there is a maximum sorption capacity which reflects the maximum adsorbed concentration of each metal ion under a specific condition. The maximum sorption capacity for Ag^{+}, Cu^{2+} and Fe^{3+} by Mag-PCMA was calculated based on the Langmuir isotherm equation, and the calculation results as well as the R^2 for each system are given in Table S1. Within the range between minimum and maximum adsorbed concentration mentioned above, one can control the zeta potential of Mag-PCMA-MI by adjusting the concentration of metal ions adsorbed to Mag-PCMA with Equation 1 and 2.

2. Disinfection effectiveness on MS-2 by three types of Mag-PCMA-MI

Three types of Mag-PCMA-MI with different adsorbed metal ions (i.e. Mag-PCMA-Ag, Mag-PCMA-Cu and Mag-PCMA-Fe) with similar zeta potential were used for the removal of MS-2, and the concentration of infectious virus after removal was measured. The removal efficiency is defined in terms of log removal value (removal efficiency=$-\log(N_t/N_0)$, where N_t is the number of MS-2 at t h and N_0 is the initial number of MS-2 ($1.6*10^6$ PFU/mL in this study). The concentration of MS-2 in the control remains stable during the removal process, as there is no disinfectant or *E. coli* host in the aqueous environment that may result in the decrease or increase of MS-2 concentration respectively. Figure 2 presents the relationship between removal efficiency and concentration of Mag-PCMA-MI while Figure 3 explores removal efficiency as a function of contact time. According to Figures 2 and 3, the removal ability of three Mag-PCMA-MI at the same concentration and contact time follow the order: Mag-PCMA-Ag>Mag-PCMA-Cu>Mag-PCMA-Fe. The main reasons are the mechanisms of the removal process including both electrostatic interaction between positively charged Mag-PCMA-MI and negatively charged MS-2 (at pH=6), and the destruction of the host-cell receptor or the nucleic acid of MS-2 by the adsorbed metal ions on the surface of Mag-PCMA [118]. Since the zeta potential of the three Mag-PCMA-MI are quite close (11.5 eV for Mag-PCMA-Ag, 11.9 eV for Mag-PCMA-Cu and 11.7 eV for Mag-PCMA-Fe), the difference in electrostatic interaction between three Mag-PCMA-MI and MS-2 is not significant. Thus, the slight difference in removal efficiency between the three Mag-PCMA-MI is mainly due to the disinfection ability of adsorbed metal ions on Mag-PCMA. Although the disinfection mechanism of metal ions on viruses have not been fully understood yet, it is believed that the inactivation of viruses by free metal ions is mainly due

to the combination with amino acids and prevention of RNA replication, and that disinfection capacity is proportional to the concentration of metal ions [127-128]. Based on the relationship between the concentration of adsorbed metal ions and zeta potential, to achieve the same zeta potential, more Ag^{+} needs to be adsorbed on Mag-PCMA than Cu^{2+} or Fe^{3+}. As a result, a higher concentration of adsorbed Ag^{+} will lead to more MS-2 being inactivated by Mag-PCMA-Ag than Mag-PCMA-Cu and Mag-PCMA-Fe during the removal process. In addition, previous studies have shown that free Ag^{+} is a better disinfectant than Cu^{2+} or Fe^{3+}, as less concentration of free Ag^{+} is needed to achieve the same disinfection effectiveness compared to other metal ions [124]. Thus, Mag-PCMA-Ag can disinfect MS-2 more effectively than Mag-PCMA-Cu or Mag-PCMA-Fe due to the difference in the disinfection ability of free metal ions.

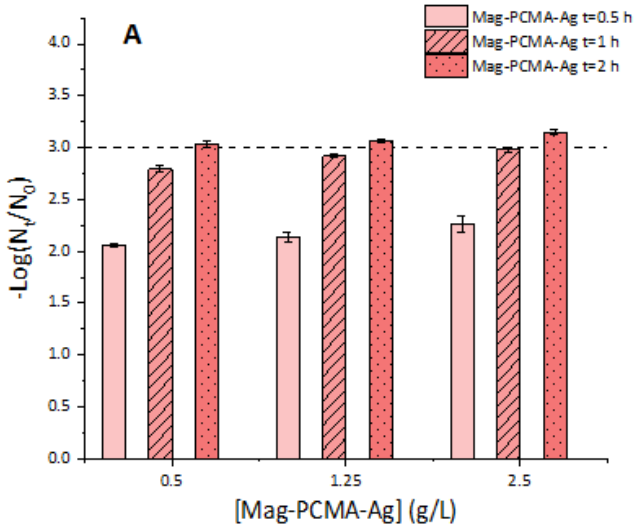
A
Mag-PCMA-Ag t=0.5 h
Mag-PCMA-Ag t=1 h
Mag-PCMA-Ag t=2 h
-Log(N_t/N_0)
0.0
0.5
1.0
1.5
2.0
2.5
3.0
3.5
4.0
0.5
1.25
2.5
[Mag-PCMA-Ag] (g/L)

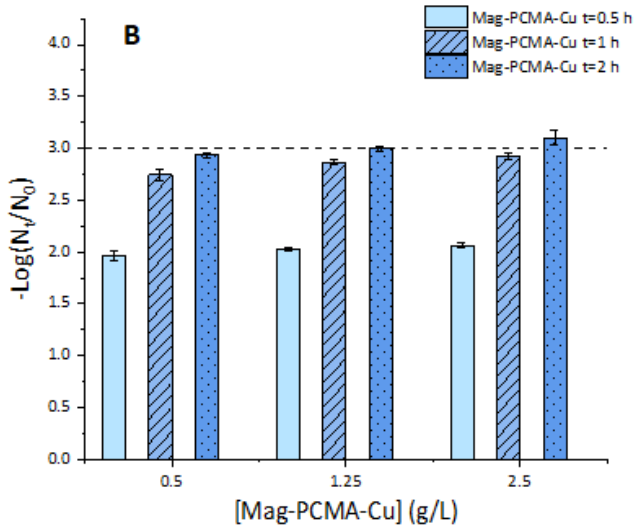
B
Mag-PCMA-Cu t=0.5 h
Mag-PCMA-Cu t=1 h
Mag-PCMA-Cu t=2 h
-Log(N_t/N_0)
0.0
0.5
1.0
1.5
2.0
2.5
3.0
3.5
4.0
0.5
1.25
2.5
[Mag-PCMA-Cu] (g/L)

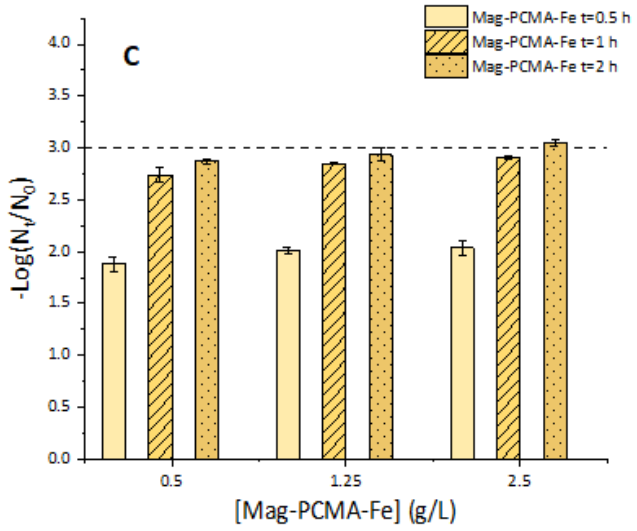
C
Mag-PCMA-Fe t=0.5 h
Mag-PCMA-Fe t=1 h
Mag-PCMA-Fe t=2 h
-Log(N_t/N_0)
0.0
0.5
1.0
1.5
2.0
2.5
3.0
3.5
4.0
0.5
1.25
2.5
[Mag-PCMA-Fe] (g/L)

Figure 2. Relationship between concentration of (A) Mag-PCMA-Ag, (B) Mag-PCMA-Cu and (C) Mag-PCMA-Fe and removal efficiency at different contact time. Dash line refers to -log(N_t/N_0)=3.0, a high removal efficiency of 99.9%.

Table 2. Detailed results about the removal efficiency with different concentration of Mag-PCMA-Ag, Mag-PCMA-Cu and Mag-PCMA-Fe, at different contact time.

[Magnetic nanoparticles] (g/L)		Removal efficiency (-Log(N_t/N_0))		
		t=0.5 h	t=1 h	t=2 h
Mag-PCMA-Ag	0.5	2.06±0.01	2.80±0.03	3.03±0.03
	1.25	2.13±0.05	2.92±0.02	3.06±0.01
	2.5	2.26±0.08	2.98±0.03	3.15±0.02
Mag-PCMA-Cu	0.5	1.97±0.05	2.75±0.06	2.93±0.02
	1.25	2.03±0.01	2.87±0.02	2.99±0.02
	2.5	2.07±0.02	2.92±0.03	3.10±0.07
Mag-PCMA-Fe	0.5	1.88±0.07	2.74±0.07	2.87±0.02
	1.25	2.01±0.04	2.85±0.01	2.93±0.06
	2.5	2.03±0.08	2.90±0.01	3.05±0.04

The concentration of magnetic nanoparticles and contact time are two major factors that determine the removal efficiency of MS-2. As shown in Figure 2, for all three types of Mag-PCMA-MI, the removal efficiency increased with an increasing concentration of Mag-PCMA-MI at any contact time. With more Mag-PCAM-MI added into the system, there will be more adsorbed metal ions in water which will both increase the positive surface exposed to MS-2 thus increasing the electrostatic interaction, and inactivate more MS-2 to reduce the concentration of viable virus. Contact time is another factor that determines the removal efficiency of MS-2. As shown in Figure 3, for all three types of Mag-PCMA-MI, the removal efficiency increased with longer contact time of Mag-PCMA-MI at any concentration, indicating that the disinfection processes are time-dependent. Although there will be a small

fraction of metal ions leached into the water after removal (0.8% of adsorbed Ag^{+}, 0.6% of adsorbed Cu^{2+} and 0.9% of adsorbed Fe^{3+}), the concentration of residual metal ions can be maintained below a safe level by adjusting the amount of metal ions coated onto Mag-PCMA during the sorption process [68]. The residual metal ions in the water can also serve as long term disinfectants during the distribution of treated water to prevent target viruses from regrowth [44]. Thus, the removal of MS-2 with Mag-PCMA-MI should not lead to additional environmental risk.

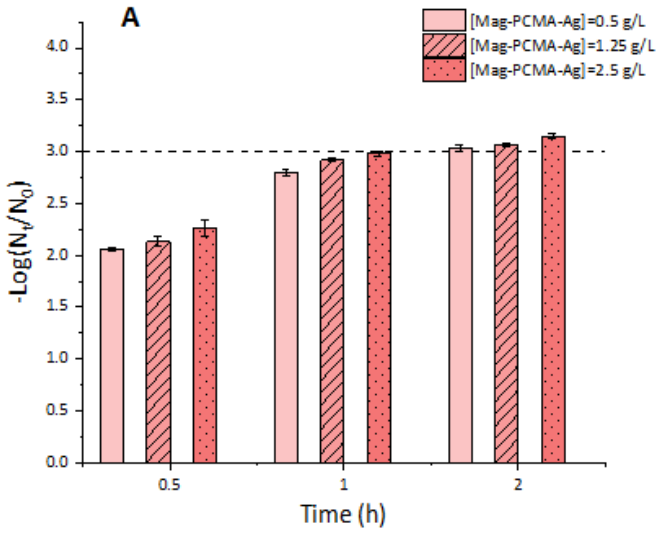
A
[Mag-PCMA-Ag]=0.5 g/L
[Mag-PCMA-Ag]=1.25 g/L
[Mag-PCMA-Ag]=2.5 g/L
-Log(N_t/N_0)
Time (h)

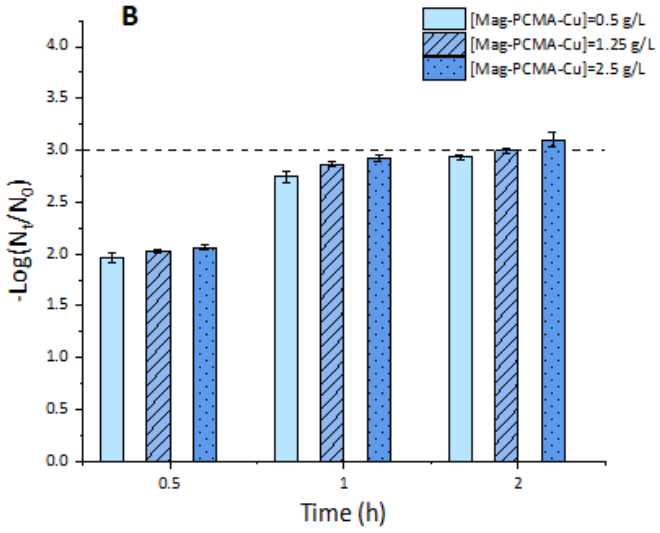
B
[Mag-PCMA-Cu]=0.5 g/L
[Mag-PCMA-Cu]=1.25 g/L
[Mag-PCMA-Cu]=2.5 g/L
-Log(N_t/N_0)
Time (h)

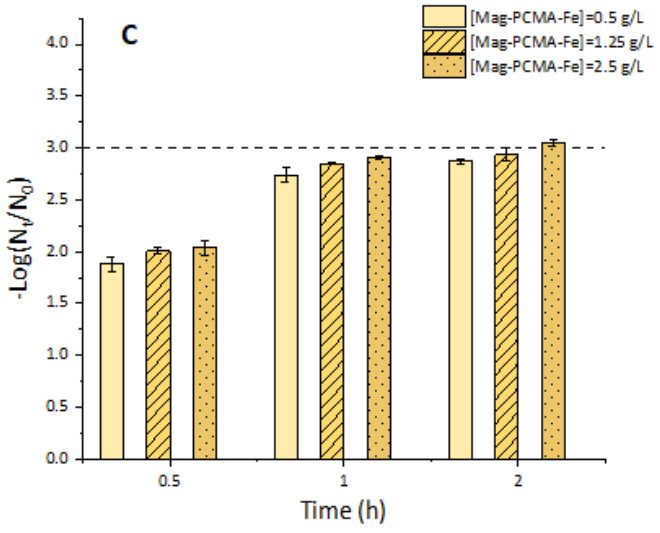
C
[Mag-PCMA-Fe]=0.5 g/L
[Mag-PCMA-Fe]=1.25 g/L
[Mag-PCMA-Fe]=2.5 g/L
-Log(N_t/N_0)
Time (h)

Figure 3. Relationship between contact time of (A) Mag-PCMA-Ag, (B) Mag-PCMA-Cu and (C) Mag-PCMA-Fe and removal efficiency at different concentrations. Dash line refers to -log(N_t/N_0)=3.0, a high removal efficiency of 99.9%.

3. Influence of environmental conditions on viral disinfection

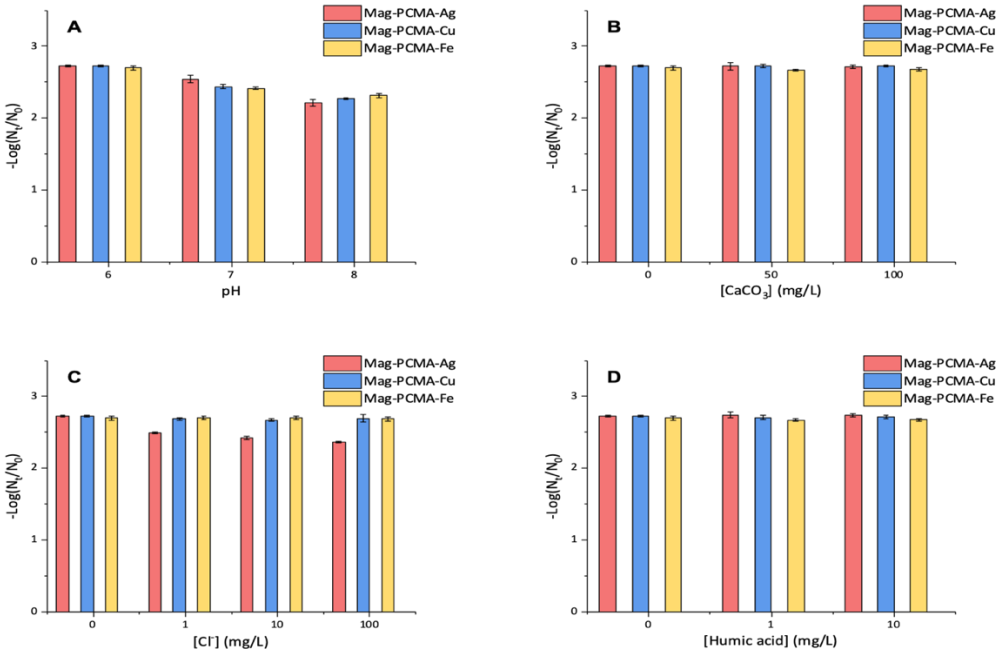

Figure 4. Influence of different (A) pH, (B) water hardness, (C) Cl^- concentration and (D) NOM concentration on the removal of MS-2 by three types of Mag-PCMA-MI.

Table 3. Detailed results about the influence of different pH, water hardness, Cl^- concentration and NOM concentration on the removal of MS-2 by three types of Mag-PCMA-MI.

Environmental Conditions		Removal efficiency (-Log(N_t/N_0))		
		Mag-PCMA-Ag	Mag-PCMA-Cu	Mag-PCMA-Fe
pH	6	2.73±0.01	2.73±0.01	2.70±0.03
	7	2.54±0.05	2.44±0.03	2.42±0.02
	8	2.21±0.04	2.27±0.02	2.31±0.03
[$CaCO_3$] (mg/L)	0	2.73±0.01	2.73±0.01	2.70±0.03

	50	2.72±0.05	2.73±0.03	2.67±0.01
	100	2.72±0.03	2.72±0.01	2.68±0.02
[Cl^-] (mg/L)	0	2.73±0.01	2.73±0.01	2.70±0.03
	1	2.49±0.01	2.68±0.01	2.70±0.02
	10	2.42±0.02	2.67±0.02	2.70±0.02
	100	2.37±0.01	2.69±0.06	2.69±0.03
[Humic acid] (mg/L)	0	2.73±0.01	2.73±0.01	2.70±0.03
	1	2.74±0.04	2.71±0.03	2.67±0.02
	10	2.74±0.02	2.71±0.03	2.67±0.02

Table 4. P value tests about the influence of different pH, water hardness, Cl^- concentration and NOM concentration on the removal of MS-2 by three types of Mag-PCMA-MI ($p<0.05$ is considered to be statistically significant).

Test		p value	Statistical significance
pH	Mag-PCMA-Ag	$1.16*10^{-5}$	Statistically significant
	Mag-PCMA-Cu	$3.80*10^{-7}$	Statistically significant
	Mag-PCMA-Fe	$4.08*10^{-6}$	Statistically significant
Water hardness	Mag-PCMA-Ag	0.893	Statistically not significant
	Mag-PCMA-Cu	0.888	Statistically not significant
	Mag-PCMA-Fe	0.315	Statistically not significant
Cl^- concentration	Mag-PCMA-Ag	$1.25*10^{-8}$	Statistically significant
	Mag-PCMA-Cu	0.216	Statistically not significant

	Mag-PCMA-Fe	0.898	Statistically not significant
NOM concentration	Mag-PCMA-Ag	0.839	Statistically not significant
	Mag-PCMA-Cu	0.503	Statistically not significant
	Mag-PCMA-Fe	0.355	Statistically not significant

3.1 pH

The influence of pH on the removal process with different Mag-PCMA-MI was evaluated by adjusting the pH from 6 to 8 with 0.1 M NaOH. As shown in Figure 4 (A), the removal efficiency of all three Mag-PCMA-MI decreased with increasing pH, and the decrease was more significant for Mag-PCMA-Ag than for Mag-PCMA-Cu or Mag-PCMA-Fe. The decrease in log10 reduction from pH=6 to pH=8 is 0.52 for Mag-PCMA-Ag, 0.46 for Mag-PCMA-Cu and 0.38 for Mag-PCMA-Fe. The most likely reasons are that the change of pH will not only influence the conformation of virus and its susceptibility to disinfection, but will also determine the speciation of adsorbed metal ions thus reducing the removal ability [119, 129-130]. Besides, the decrease of adsorbed free metal ions will lead to a decrease of zeta potential thus weakening the electrostatic interaction as well. The influence of increasing OH- is more significant for Mag-PCMA-Ag than Mag-PCMA-Cu or Mag-PCMA-Fe, indicating that Mag-PCMA-Fe is more stable in variable environmental conditions than Mag-PCMA-Ag or Mag-PCMA-Cu.

3.2 Water hardness

Different concentrations of $CaCO_3$ (0-100 mg/L) were added into the system to simulate a soft or hard water condition, and the influence of water hardness on the removal process was evaluated. As shown in Figure 4 (B), no significant influence on the removal efficiency of MS-2 was observed with all three Mag-PCMA-MI (p value test in Table 4). This is mainly because the speciation of adsorbed Ag^+, Cu^{2+} and Fe^{3+} did not change substantially with the addition of $CaCO_3$ [64, 93]. Thus, the removal ability of all three Mag-PCMA-MI remained stable with a change of water hardness in the water.

3.3 Cl^- concentration

The influence of Cl^- with different concentrations (0-100 mg/L) was evaluated as well to see if there would be a change in removal efficiency for the three Mag-PCMA-MI, as Cl^- is one of the common constituents in water. According to the results in Figure 4 (C), the presence of Cl^- had no influence on the removal process with Mag-PCMA-Cu and Mag-PCMA-Fe, as the adsorbed Cu^{2+} and Fe^{3+} are not influenced by Cl^-. However, Mag-PCMA-Ag will be affected by Cl^-, as Cl^- can combine with Ag^+ and form AgCl on the surface thus reducing the concentration of available Ag^+ and weakening the removal of MS-2. As the concentration of Cl^- increased from 0 to 100 mg/L. the log10 reduction with Mag-PCMA-Ag decreased from 2.73 to 2.37. However, the removal efficiency still remains above 99% (>2 in log10 reduction) even with high levels of Cl^- concentration, indicating that this method is quite stable with the change of natural environment.

3.4 NOM

NOM, which is derived from decaying plant and animal matter, is one of the main constituents in many environmental and drinking supply water sources, and is a major factor that needs to be considered in water treatment. In this study, humic acid was used as a representative of NOM and different concentrations of humic acid (0-10 mg/L) were added to the system for evaluation. As shown in Figure 4 (D), no significant influence on removal efficiency was observed for all three Mag-PCMA-MI (p value test in Table 4). Although HA could form complexes with Fe^{3+}, Cu^{2+} and Ag^{+}, and the metal ions-HA complex are not so toxic compared to free ions [94-95, 131], the affinity is quite limited under the concentration range of HA considered in this study (0-10 mg/L). Thus, the influence of humic acid to the removal process is negligible.

4. Regeneration and reuse of Mag-PCMA-MI

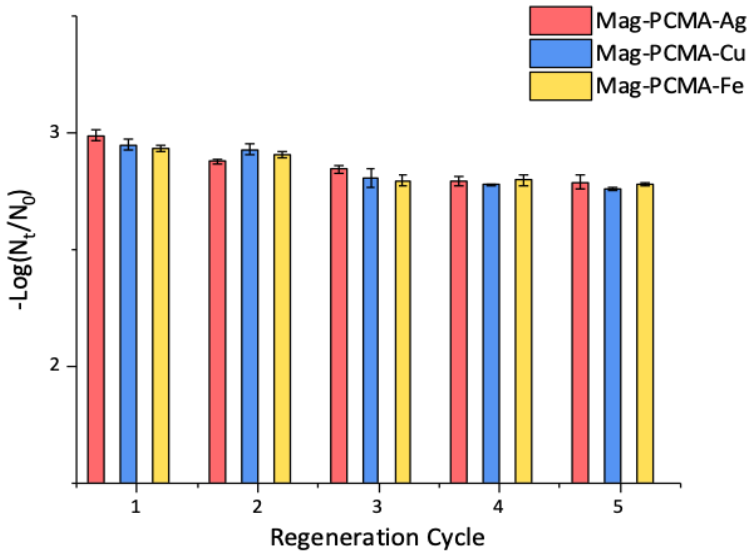

Figure 5. Removal efficiency of MS-2 by three types of Mag-PCMA-MI after 5 regeneration cycles.

Table 5. Detailed results about the removal efficiency of MS-2 by three types of Mag-PCMA-MI after 5 regeneration cycles.

Regeneration Cycle	Removal efficiency (%)		
	Mag-PCMA-Ag	Mag-PCMA-Cu	Mag-PCMA-Fe
1	2.99±0.03	2.95±0.02	2.93±0.01
2	2.88±0.01	2.93±0.02	2.90±0.01
3	2.84±0.02	2.80±0.04	2.79±0.02
4	2.79±0.02	2.78±0.00	2.80±0.02
5	2.79±0.03	2.76±0.01	2.78±0.01

Table 6. P value tests about the removal efficiency of MS-2 by three types of Mag-PCMA-MI after 5 regeneration cycles ($p<0.05$ is considered to be statistically significant).

Test		P value	Statistical significance
Continuous regeneration cycles	Mag-PCMA-Ag	$2.77*10^{-6}$	Statistically significant
	Mag-PCMA-Cu	$3.42*10^{-6}$	Statistically significant
	Mag-PCMA-Fe	$1.77*10^{-6}$	Statistically significant

The removal efficiency of three Mag-PCMA-MI in each regeneration cycle was measured and shown in Figure 5. The removal efficiency decreased slightly for all three types of Mag-PCMA-MI (a decrease of 0.20 in log10 for Mag-PCMA-Ag, 0.19 for Mag-PCMA-Cu and 0.15 for Mag-PCMA-Fe), mainly due to both the mass loss during the rinse and the loss of adsorbed metal ions after each cycle. However, the removal efficiency still remains at a high level even after 5 cycles (2.79 for Mag-PCMA-Ag, 2.76 for Mag-PCMA-Cu and 2.78 for Mag-PCMA-Fe), indicating that the reusability of all three Mag-PCMA is

very promising. The concentration of viable MS-2 in the rinsing water during each regeneration cycle is negligible, as previous studies have shown that MS-2 can be effectively inactivated by free metal ions within short contact time [119], thus most of the MS-2 attached onto Mag-PCMA-MI will be inactivated by the adsorbed metal ions during the removal process. Therefore, no additional environmental risk will arise during the regeneration cycles.

D. Conclusions

In this study, a novel method to disinfect and remove MS-2 from water was explored and evaluated by using magnetic nanoparticles coated with metal ions. The negatively charged Mag-PCMA can be positively charged by adsorbing different metal ions, and the zeta potential has a linear relationship with the concentration of adsorbed positive charge, which is determined by both the number of positive charges in each metal ion, and the adsorbed concentration of metal ions. The minimum adsorbed concentration of metal ion needed to convert the zeta potential from negative to positive for Mag-PCMA-MI can be calculated with a linear relationship. The Mag-PCMA-MI were then used to explore the removal process of MS-2 in the water. All three Mag-PCMA-MI achieved very good viral removal efficiency with proper concentration and within a short contact time (a log10 reduction above 2.8 with 2 h contact time). The differences in removal ability between Mag-PCMA-Ag, Mag-PCMA-Cu and Mag-PCMA-Fe were mainly due to the removal mechanisms, which is a combination of electrostatic attraction by the positively charged Mag-PCMA-MI and the destruction of viral structure caused by adsorbed metal ions on Mag-PCMA. Although Mag-PCMA-Ag can achieve better removal efficiency than Mag-PCMA-Cu and Mag-PCMA-Fe with similar zeta potential, the difference of removal efficiency between these three Mag-PCMA-MI is not significant (e.g. the difference of removal efficiency between 2.5 g/L Mag-

PCMA-Ag and Mag-PCMA-Fe after 3 h is merely 0.02%). Thus, Mag-PCMA-Fe is a competitive option for the removal process when considering the cost of each metal ion.

Various environmental conditions, including pH, water hardness, presence of Cl^- and NOM were evaluated to explore the possible influence on the removal process with three Mag-PCMA-MI. No obvious influence was observed with a change in water hardness and NOM concentration, as the presence of $CaCO_3$ and humic acid will not change the speciation of adsorbed metal ions thus will not influence the removal ability. pH does have a significant influence on the removal process. With increasing pH, the removal efficiency decreased noticeably for all three Mag-PCMA-MI, as the change of pH will influence the interaction between the protein of MS-2 and the metal ions. The presence of Cl^- will not influence the removal with Mag-PCMA-Cu or Mag-PCMA-Fe, but will influence the disinfection process with Mag-PCMA-Ag, as Cl^- can combine with the adsorbed Ag^+ and form AgCl, thus reducing the disinfection ability of Ag^+. Although some change of the environmental conditions will lead to a decrease of removal efficiency, the removal efficiency of MS-2 with three Mag-PCMA-MI still remain at a high level, indicating that this method is quite stable.

Reusability of Mag-PCMA-MI was evaluated in this study to explore the sustainability of this method, by regenerating and reusing the three Mag-PCMA-MI for 5 continuous removal cycles. Although the removal efficiency decreased slightly during the 5 cycles due to incomplete recovery of Mag-PCMA-MI, the removal efficiency still remained above 2.75 of log10 reduction, indicating the reuse of Mag-PCMA is very promising. Compared to conventional disinfection methods for viruses, this method with metal ion coated Mag-PCMA has several advantages. First, the free metal ions are fixed onto the surface of Mag-PCMA and can be removed by external magnet simultaneously, thus reducing the potential

risk caused by free metal ions left in the treated water after disinfection. Besides, no extra removal process is needed to deal with the residual metal ions after disinfection as they can be maintained within a safe level, which will simplify the disinfection process. Second, several metal ions can provide very good disinfection, which can be used alternatively to avoid the resistance of target microorganisms after long term application. Third, the Mag-PCMA-MI can be reused for several cycles, which makes this method quite sustainable. Thus, this method is very promising for practical use in the future.

E. Acknowledgements

This work was supported by the National Science Foundation (NSF) and the U.S. Environmental Protection Agency (EPA) under cooperative agreement number [NSF-EF0830117 and NSF 1901515]. Arturo A. Keller also appreciates Agilent Technologies for their Agilent Thought Leader Award. Any opinions, findings, conclusions, or recommendations expressed in this material are those of the authors and do not necessarily reflect the views of the funding agencies.

F. Appendix

1. Calculation of maximum sorption capacity of Ag^{+}, Cu^{2+} and Fe^{3+} by Mag-PCMA

The maximum sorption capacity (mg/g) can be calculated by Langmuir adsorption isotherm (equation S1):

$$C_e/q_e=1/(K_L*q_m)+C_e/q_m \quad \text{(S1)}$$

Here C_e is the concentration of metal ions (mg/L) at equilibrium and q_e is the amount of metal ions adsorbed (mg/g), q_m is the maximum sorption capacity (mg/g), K_L(L/mg) is the Langmuir Sorption equilibrium constants. The q_m and R^2 for each system are listed in Table S1.

Table S1. Maximum sorption capacity (q_m) of Ag^+, $Cu^{2+}$and Fe^{3+} by Mag-PCMA and the R^2 of each system.

Metal ions	q_m(mg/g)	R^2
Ag^+	43.48	0.9954
Cu^{2+}	19.90	0.9685
Fe^{3+}	11.09	0.9526

V. Summary

To sum up, this dissertation proposed a novel disinfection system with metal ions as the disinfectants and magnetic nanoparticles to achieve recyclable use, which addresses some of the concerns with the traditional disinfection technologies. Compared to other chemical disinfectants, the use of metal ions avoids the generation of disinfection byproducts and requires no extra generator, making this system easy to operate with low environmental effect. The use of magnetic nanoparticles in this disinfection system is the major novelty of this study, as the magnetic nanoparticles will not only reduce the concentration of metal ions after disinfection, but also help to achieve the sustainable use of the key materials (i.e., the metal ions) under simple recovery conditions. Chapter II-IV in this dissertation address various target microorganisms including bacteria, algae and viruses and optimize the method correspondingly, considering various water characteristics such as pH, water harness, temperature, the presence of Cl^- and natural organic matter. In Chapter II, the feasibility of this novel disinfection system was demonstrated with a case study on bacteria. This study addressed the issues related to the residual metal ions after disinfection by removing them via the efficient adsorption with magnetic nanoparticles, and achieved the use of metal ions with high recovery efficiency. In Chapter III, in addition to disinfection of cyanobacteria, the issues related to the production of cyanotoxins by the target cyanobacteria were addressed. To improve the disinfection efficiency of this system, a combination of metal ions was used to reduce the concentration of disinfectants and shorten the contact time. The released cyanotoxins and residual metal ions after disinfection were removed simultaneously with the magnetic nanoparticle, which can be easily recovered with external magnetic fields for regeneration. In Chapter IV, this disinfection method was further improved by first

combining the free metal ions and magnetic nanoparticles via sorption, and then the magnetic nanoparticles coated with metal ions were used as the disinfectants. The adsorbed metal ions on the magnetic nanoparticles largely enhanced the disinfection ability of these novel nanoparticles and made them more suitable for practical application compared to the methods in Chapter II and III, given the high disinfection efficiency they can reach with a short contact time.

The novel disinfection system described in this dissertation is proposed to be applied in drinking water treatment plants in the future, and this dissertation has demonstrated its effectiveness at a proof-of-concept level. To achieve commercial application, several factors need to be evaluated beforehand. Firstly, this disinfection system needs to be evaluated with water samples from drinking water treatment plants to determine its performance, since the evaluations in this study were at the lab scale, which is less complicated than the samples from drinking water treatment plants. Secondly, research to adapt the current batch system to a continuous flow system is needed. Based on the volume of treated water, the cost for key materials and the tank designed for the system, as well as other inputs such as electricity, need to be calculated and compared with conventional methods. Thirdly, the residual effects of this method need to be explored. According to the results from Chapter IV, a small fraction of metal ions will be released from the magnetic nanoparticles during disinfection. Thus, whether the released metal ions can serve as the residual disinfectants during the distribution of treated water while maintaining the concentration below safe levels according to EPA standards is another important topic to study. Last but not the least, the resistance of target microorganisms to the magnetic nanoparticles after long term application need to be considered, as this situation is common for other chemical disinfectants. To maintain a high

disinfection efficiency, the magnetic nanoparticles with various metal ions can be applied alternatively in this system. Thus, the length of time that the magnetic nanoparticles can be used need to be determined to maintain the expected disinfection effectiveness.

VI. References

1. Ashbolt, N. J. Microbial contamination of drinking water and human health from community water systems. *Curr. Environ. Health Rep.* **2,** 95-106 (2015).

2. Burdick, S. M., Hewitt, D. A., Martin, B. A., Schenk, L. and Rounds, S. A. Effects of harmful algal blooms and associated water-quality on endangered Lost River and shortnose suckers. *Harmful Algae* **97,** 101847 (2020).

3. Esschert, K. L. V., Mattioli, M. C., Hilborn, E. D., Roberts, V. A., Yu, A. T., Lamba, K., Arzaga, G., Zahn, M., Marsh, Z., Combes, S. M. and Smith, E. S. Outbreaks associated with untreated recreational water—California, Maine, and Minnesota, 2018–2019. *Morb. Mortal. Wkly. Rep.* **69,** 781 (2020).

4. Byrne, L., Jenkins, C., Launders, N., Elson, R. and Adak, G. K. The epidemiology, microbiology and clinical impact of Shiga toxin-producing Escherichia coli in England, 2009–2012. *Epidemiol. Infect.* **143**, 3475-3487 (2015).

5. Kabue, J. P., Meader, E., Hunter, P. R. and Potgieter, N. Norovirus prevalence and estimated viral load in symptomatic and asymptomatic children from rural communities of Vhembe district, South Africa. *J. Clin. Virol.* **84,** 12-18 (2016).

6. Mu, D., Ruan, R., Addy, M., Mack, S., Chen, P. and Zhou, Y. Life cycle assessment and nutrient analysis of various processing pathways in algal biofuel production. *Bioresour. Technol.* **230,** 33-42 (2017).

7. Sun, R., Sun, P., Zhang, J., Esquivel-Elizondo, S. and Wu, Y. Microorganisms-based methods for harmful algal blooms control: a review. *Bioresour. Technol.* **248,** 12-20 (2018).

8. Wood, R. Acute animal and human poisonings from cyanotoxin exposure—A review of the literature. *Environ. Int.* **91,** 276-282 (2016).

9. Garoma, T. and Yazdi, R.E., 2019. Investigation of the disruption of algal biomass with chlorine. BMC plant biology, 19(1), p.18.

10. Cho, M., Kim, J., Kim, J.Y., Yoon, J. and Kim, J.H., 2010. Mechanisms of Escherichia coli inactivation by several disinfectants. Water Research, 44(11), pp.3410-3418.

11. Collivignarelli, M., Abbà, A., Benigna, I., Sorlini, S. and Torretta, V. Overview of the main disinfection processes for wastewater and drinking water treatment plants. *Sustainability* **10,** 86 (2017).

12. Kimura, S. Y. and Ortega-Hernandez, A. Formation mechanisms of disinfection byproducts: Recent developments. *Curr. Opin. Environ. Sci. Health.* **7,** 61-68 (2019).

13. Genisoglu, M., Ergi-Kaytmaz, C. and Sofuoglu, S. C. Multi-route–Multi-pathway exposure to trihalomethanes and associated cumulative health risks with response and dose addition. *J. Environ. Manage.* **233,** 823-831 (2019).

14. Costa, C., Assunção, R., Sequeira, D., Esteves, F., Valdiglesias, V., Laffon, B., Teixeira, J. P. and Madureira, J. From trihalomethanes chronic daily intake through multiple exposure routes to cancer and non-cancer health risk assessment: Evidence from public Portuguese indoor swimming pools facilities using a probabilistic approach. *Sci. Total Environ.* 151790 (2021).

15. IARC (International Agency for Research on Cancer). Agents Classified by the IARC Monographs. **1–127** (1999).

16. Drogui, P. and Daghrir, R. Chlorine for Water Disinfection: Properties, Applications and Health Effects. In CO_2 Sequestration, Biofuels and Depollution. *Springer, Cham.* **5,** 1-32 (2015).

17. Hassenberg, K., Geyer, M., Mauerer, M., Praeger, U. and Herppich, W. B. Influence of temperature and organic matter load on chlorine dioxide efficacy on *Escherichia coli* inactivation. *LWT - Food Sci. Technol.* **79,** 349-354 (2017).

18. United States Environmental Protection Agency. Wastewater Technology Fact Sheet Ozone Disinfection. EPA 832-F99-063 (1999).

19. Adeleye, A. S., Conway, J. R., Garner, K., Huang, Y., Su, Y. and Keller, A. A. Engineered nanomaterials for water treatment and remediation: costs, benefits, and applicability. *Chem. Eng. J.* **286,** 640-662 (2016).

20. Agbaba, J., Molnar, J., Tubić, A., Watson, M., Maletić, S. and Dalmacija, B. Effects of water matrix and ozonation on natural organic matter fractionation and corresponding disinfection by-products formation. *Water Sci. Technol. Water Supply.* **15,** 75-83 (2015).

21. Metcalf and Eddy. Wastewater engineering treatment and reuse. McGraw-Hill Professional Publishing (2003).

22. Gopal, K., Tripathy, S. S., Bersillon, J. L. and Dubey, S. P. Chlorination byproducts, their toxicodynamics and removal from drinking water. *J. Hazard. Mater.* **140**, 1-6 (2007).

23. Hijnen, W. A. M., Beerendonk, E. F. and Medema, G. J. Inactivation credit of UV radiation for viruses, bacteria and protozoan (oo) cysts in water: a review. *Water Res.* **40**, 3-22 (2006).

24. Municipal Wastewater Disinfection Design Manual; U.S. Environmental Protection Agency: Cincinnati, OH, USA (1986).

25. Metcalf & Eddy. Ingegneria Della Acque Reflue, Trattamento e Riuso; McGraw-Hill: New York, NY, USA (2006).

26. Fang, J., Liu, H., Shang, C., Zeng, M., Ni, M. and Liu, W. *E. coli* and bacteriophage MS2 disinfection by UV, ozone and the combined UV and ozone processes. *Front. Environ. Sci. Eng.* **8,** 547-552 (2014).

27. Caretti, C. and Lubello, C. Wastewater disinfection with PAA and UV combined treatment: a pilot plant study. *Water Res.* **37,** 2365-2371 (2003).

28. Wu, Y. H., Chen, Z., Li, X., Wang, Y. H., Liu, B., Chen, G. Q., Luo, L. W., Wang, H. B., Tong, X., Bai, Y. and Xu, Y. Q. Effect of ultraviolet disinfection on the fouling of reverse osmosis membranes for municipal wastewater reclamation. *Water Res.* **195,** 116995 (2021).

29. Huang, Z., Maness, P. C., Blake, D. M., Wolfrum, E. J., Smolinski, S. L. and Jacoby, W. A. Bactericidal mode of titanium dioxide photocatalysis. *J. Photochem. Photobiol. A: Chem.* **130,** 163-170 (2000).

30. Hossain, F., Perales-Perez, O. J., Hwang, S. and Roman, F. Antimicrobial nanomaterials as water disinfectant: applications, limitations and future perspectives. *Sci. Total Environ.* **466,** 1047-1059 (2014).

31. Sreeja, S. and Shetty, V. Microbial disinfection of water with endotoxin degradation by photocatalysis using Ag@ TiO_2 core shell nanoparticles. *Environ. Sci. Pollut. Res.* **23,** 18154-18164 (2016).

32. Tallósy, S. P., Janovák, L., Ménesi, J., Nagy, E., Juhász, Á., Balázs, L., Deme, I., Buzás, N. and Dékány, I. Investigation of the antibacterial effects of silver-modified TiO_2 and ZnO plasmonic photocatalysts embedded in polymer thin films. *Environ. Sci. Pollut. Res.* **21,** 11155-11167 (2014).

33. Gupta, K., Singh, R. P., Pandey, A. and Pandey, A. Photocatalytic antibacterial performance of TiO_2 and Ag-doped TiO_2 against *S. aureus*, *P. aeruginosa* and *E. coli*. *Beilstein J. Nanotechnol.* **4,** 345-351 (2013).

34. Long, M., Wang, J., Zhuang, H., Zhang, Y., Wu, H. and Zhang, J. Performance and mechanism of standard nano-TiO_2 (P-25) in photocatalytic disinfection of foodborne microorganisms–Salmonella typhimurium and Listeria monocytogenes. *Food Control* **39,** 68-74 (2014).

35. Marambio-Jones, C. and Hoek, E. M. A review of the antibacterial effects of silver nanomaterials and potential implications for human health and the environment. *J. Nanopart. Res.* **12,** 1531-1551 (2010).

36. Le Ouay, B. and Stellacci, F. Antibacterial activity of silver nanoparticles: a surface science insight. *Nano Today* **10,** 339-354 (2015).

37. Maurer, L. L. and Meyer, J. N. A systematic review of evidence for silver nanoparticle-induced mitochondrial toxicity. *Environ. Sci. Nano* **3,** 311-322 (2016).

38. Wang, J., Wu, Y., Yang, Z., Guo, H., Cao, B. and Tang, C. Y. A novel gravity-driven nanofibrous membrane for point-of-use water disinfection: polydopamine-induced in situ silver incorporation. *Sci. Rep.* **7,** 1-8 (2017) .

39. Heidarpour, F., Ghani, W. A., Ahmadun, F. R., Sobri, S., Zargar, M. and Mozafari, M.R. Nano silver-coated polypropylene water filter: I. manufacture by electron beam gun using a modified balzers 760 machine. *Dig. J. Nanomater. Biostruct.* **5** (2010).

40. Heidarpour, F., Ghani, W. W. A. K., Fakhru'l-Razi, A., Sobri, S., Heydarpour, V., Zargar, M. and Mozafari, M. R. Complete removal of pathogenic bacteria from drinking water using nano silver-coated cylindrical polypropylene filters. *Clean Technol. Environ. Policy* **13,** 499-507 (2011).

41. Tan, X., Chen, C., Hu, Y., Wen, J., Qin, Y., Cheng, J. and Chen, Y. Novel AgNWs-PAN/TPU membrane for point-of-use drinking water electrochemical disinfection. *Sci. Total Environ.* **637,** 408-417 (2018).

42. Zeng, X., McCarthy, D. T., Deletic, A. and Zhang, X. Silver/reduced graphene oxide hydrogel as novel bactericidal filter for point-of-use water disinfection. *Adv. Funct. Mater.* **25,** 4344-4351 (2015).

43. Liu, Y., Tourbin, M., Lachaize, S. and Guiraud, P. Silica nanoparticles separation from water: aggregation by cetyltrimethylammonium bromide (CTAB). *Chemosphere* **92**, 681-687 (2013).

44. Sicairos-Ruelas, E. E., Gerba, C. P. and Bright, K. R. Efficacy of copper and silver as residual disinfectants in drinking water. *J. Environ. Sci. Health A* **54,** 146-155 (2019).

45. Tenaillon, O., Skurnik, D., Picard, B. and Denamur, E. The population genetics of commensal Escherichia coli. *Nat. Rev. Microbiol.* **8,** 207-217 (2010).

46. Li, Y., Yang, M., Zhang, X., Jiang, J., Liu, J., Yau, C. F., Graham, N. J. and Li, X. Two-step chlorination: a new approach to disinfection of a primary sewage effluent. *Water Res.* **108,** 339-347 (2017).

47. Ragazzo, P., Chiucchini, N., Piccolo, V., Spadolini, M., Carrer, S., Zanon, F. and Gehr, R. Wastewater Disinfection: Long-Term Laboratory and Full-Scale Studies on Performic Acid in Comparison with Peracetic Acid and Chlorine. *Water Res.* **184,** 116169 (2020).

48. Jones, I. G. and Roworth, M. An outbreak of *Escherichia coli* 0157 and campylobacteriosis associated with contamination of a drinking water supply. *Public Health* **110,** 277-282 (1996).

49. Hrudey, S. E., Payment, P., Huck, P. M., Gillham, R. W. and Hrudey, E. J. A fatal waterborne disease epidemic in Walkerton, Ontario: comparison with other waterborne outbreaks in the developed world. *Water Sci. Technol.* **47,** 7-14 (2003).

50. Lienemann, T., Pitkänen, T., Antikainen, J., Mölsä, E., Miettinen, I., Haukka, K., Vaara, M. and Siitonen, A. Shiga toxin-producing *Escherichia coli* O100: H–: stx 2e in drinking water contaminated by wastewater in Finland. *Curr. Microbiol.* **62,** 1239-1244 (2011).

51. Park, J., Kim, J. S., Kim, S., Shin, E., Oh, K. H., Kim, Y., Kim, C. H., Hwang, M. A., Jin, C. M., Na, K. and Lee, J. A waterborne outbreak of multiple diarrheagenic Escherichia coli infections associated with drinking water at a school camp. *Int. J. Infect. Dis.* **66,** 45-50 (2018).

52. Watahiki, M., Isobe, J., Kimata, K., Shima, T., Kanatani, J. I., Shimizu, M., Nagata, A., Kawakami, K., Yamada, M., Izumiya, H. and Iyoda, S. Characterization of enterohemorrhagic *Escherichia coli* O111 and O157 strains isolated from outbreak patients in Japan. *J. Clin. Microbiol.* **52,** 2757-2763 (2014).

53. Jiang, J., Han, J. and Zhang, X. Nonhalogenated aromatic DBPs in drinking water chlorination: a gap between NOM and halogenated aromatic DBPs. *Environ. Sci. Technol.* **54,** 1646-1656 (2020).

54. Mousel, D., Palmowski, L. and Pinnekamp, J. Energy demand for elimination of organic micropollutants in municipal wastewater treatment plants. *Sci. Total Environ.* **575,** 1139-1149 (2017).

55. Metcalf & Eddy, Tchobanoglous, G., Burton, F. L., Stensel, H. D., Eramo, B., Sirini, P., Chiavola, A., Polettini, A. and Pomi, R. Ingegneria delle acque reflue: trattamento e riuso; McGraw-Hill (2006).

56. Hajipour, M. J., Fromm, K. M., Ashkarran, A. A., de Aberasturi, D. J., de Larramendi, I. R., Rojo, T., Serpooshan, V., Parak, W. J. and Mahmoudi, M. Antibacterial properties of nanoparticles. *Trends Biotechnol.* **30,** 499-511 (2012).

57. Huang, Y. and Keller, A. A. EDTA functionalized magnetic nanoparticle sorbents for cadmium and lead contaminated water treatment. *Water Res.* **80,** 159-168 (2015).

58. Pina, A. S., Batalha, Í. L., Fernandes, C. S., Aoki, M. A. and Roque, A. C. Exploring the potential of magnetic antimicrobial agents for water disinfection. *Water Res.* **66,** 160-168 (2014).

59. Sutton, S. Measurement of microbial cells by optical density. *J. Valid. Technol.* **17,** 46-49 (2011).

60. Lemire, J. A., Harrison, J. J. and Turner, R. J. Antimicrobial activity of metals: mechanisms, molecular targets and applications. *Nat. Rev. Microbiol.* **11,** 371-384 (2013).

61. Recreational water quality criteria; U.S. Environmental Protection Agency Health and Ecological Criteria Division (2000).

62. Cliver, D. O., Foell, W. K.and Goepfert, J. M. Biocidal effects of silver. *Contract NAS* 9-9300 (1971).

63. Yu-sen, E. L., Vidic, R. D., Stout, J. E. and Victor, L. Y. Negative effect of high pH on biocidal efficacy of copper and silver ions in controlling *Legionella pneumophila*. *Appl. Environ. Microbiol.* **68,** 2711-2715 (2002).

64. Butkus, M. A., Edling, L. and Labare, M. P. The efficacy of silver as a bactericidal agent: advantages, limitations and considerations for future use. *J. Water Supply Res. T.* **52,** 407-416 (2003).

65. Johnson, F. H and Lewin, I. The growth rate of *E. coli* in relation to temperature, quinine and coenzyme. *J. Cell. Physiol.* **28,** 47-75 (1946).

66. Kadam, S. R., den Besten, H. M., van der Veen, S., Zwietering, M. H., Moezelaar, R. and Abee, T. Diversity assessment of Listeria monocytogenes biofilm formation: impact of growth condition, serotype and strain origin. *Int. J. Food Microbiol.* **165,** 259-264 (2013).

67. Harris, D. C. Quantitative chemical analysis; Macmillan (2010).

68. Secondary drinking water standards: Guidance for nuisance chemicals; U.S. Environmental Protection Agency Drinking Water Contaminants-Standards and Regulations (2020). https://www.epa.gov/sdwa/secondary-drinking-water-standards-guidance-nuisance-chemicals

69. Campbell, P. G. and Tessier, A. Metal speciation in natural waters: Influence of environmental acidification; ACS Publications (1987).

70. Zhu, Y., Liu, H., Yang, L. and Liu, J. Study on the synthesis of Ag/AgCl nanoparticles and their photocatalytic properties. *Mater. Res. Bull.* **47,** 3452-3458 (2012) .

71. Averill, B. and Eldredge, P. Chemistry: principles, patterns, and applications; Recording for the Blind & Dyslexic (2007).

72. Bi, X., Dai, W., Wang, X., Dong, S., Zhang, S., Zhang, D. and Wu, M. Microcystins distribution, bioaccumulation, and Microcystis genotype succession in a fish culture pond. *Sci. Total Environ.* **688,** 380-388 (2019) .
73. Zanchett, G. and Oliveira-Filho, E. C. Cyanobacteria and cyanotoxins: from impacts on aquatic ecosystems and human health to anticarcinogenic effects. *Toxins* 5, 1896-1917 (2013).

74. United States Environmental Protection Agency. Cyanobacteria and Cyanotoxins: Information for Drinking Water Systems. EPA-810F11001 (2014).

75. Shen, X., Zhang, H., He, X., Shi, H., Stephan, C., Jiang, H., Wan, C. and Eichholz, T. Evaluating the treatment effectiveness of copper-based algaecides on toxic algae *Microcystis aeruginosa* using single cell-inductively coupled plasma-mass spectrometry. *Anal. Bioanal. Chem.* **411,** 5531-5543 (2019).

76. Bishop, W. M., Lynch, C. L., Willis, B. E. and Cope, W. G. Copper-based aquatic algaecide adsorption and accumulation kinetics: influence of exposure concentration and duration for controlling the cyanobacterium *Lyngbya wollei*. *Bull. Environ. Contam. Toxicol.* **99,** 365-371 (2017).

77. Dong, F., Liu, J., Li, C., Lin, Q., Zhang, T., Zhang, K. and Sharma, V. K. Ferrate (VI) pre-treatment and subsequent chlorination of blue-green algae: quantification of disinfection byproducts. *Environ. Int.* **133,** 105195 (2019).

78. Chen, Y., Arnold, W. A., Griffin, C. G., Olmanson, L. G., Brezonik, P. L. and Hozalski, R. M. Assessment of the chlorine demand and disinfection byproduct formation potential of surface waters via satellite remote sensing. *Water Res.* **165,** 115001 (2019).

79. Kousar, S. and Javed, M. Evaluation of acute toxicity of copper to four freshwater fish species. *Int. J. Agric. Biol.* **14** (2012).

80. Martins, I., Godinho, A., Goulart, J. and Carreiro-Silva, M. Assessment of Cu sub-lethal toxicity (LC50) in the cold-water gorgonian *Dentomuricea meteor* under a deep-sea mining activity scenario. *Environ. Pollut.* **240,** 903-907 (2018).

81. Amé, M. V. and Wunderlin, D. A. Effects of iron, ammonium and temperature on microcystin content by a natural concentrated *Microcystis aeruginosa* population. *Water Air Soil Pollut.*, **168,** 235-248 (2005).

82. Huang, Y., Fulton, A. N. and Keller, A. A. Simultaneous removal of PAHs and metal contaminants from water using magnetic nanoparticle adsorbents. *Sci. Total Environ.* **571,** 1029-1036 (2016).

83. Wang, P., Shi, Q., Shi, Y., Clark, K. K., Stucky, G. D. and Keller, A. A. Magnetic permanently confined micelle arrays for treating hydrophobic organic compound contamination. *J. Am. Chem. Soc.* **131,** 182-188 (2009).

84. Wang, H., Keller, A. A. and Clark, K. K. Natural organic matter removal by adsorption onto magnetic permanently confined micelle arrays. *J. Hazard. Mater.* **194**, 156-161 (2011).

85. Clark, K. K. and Keller, A. A. Adsorption of perchlorate and other oxyanions onto magnetic permanently confined micelle arrays (Mag-PCMAs). *Water Res.* **46,** 635-644 (2012).

86. Clark, K. K. and Keller, A. A. Investigation of two magnetic permanently confined micelle array sorbents using nonionic and cationic surfactants for the removal of PAHs and pesticides from aqueous media. *Water Air Soil Pollut.* **223,** 3647-3655 (2012).

87. Huang, Y. and Keller, A. A. Magnetic nanoparticle adsorbents for emerging organic contaminants. *ACS Sustain. Chem. Eng.* **1,** 731-736 (2013).

88. Huang, Y., Fulton, A. N. and Keller, A. A. Optimization of porous structure of superparamagnetic nanoparticle adsorbents for higher and faster removal of emerging organic contaminants and PAHs. *Environ. Sci. Water Res. Technol.* **2,** 521-528 (2016).

89. Lin, Y. S. E., Vidic, R. D., Stout, J. E. and Victor, L. Y. Individual and combined effects of copper and silver ions on inactivation of Legionella pneumophila. *Water Res.* **30,** 1905-1913 (1996).

90. Gao, Q. and Keller, A. A. Redesigning water disinfection using recyclable nanomaterials and metal ions: evaluation with *Escherichia coli*. *ACS ES&T Water* **1,** 185-194 (2021).

91. Hermansson, A.C.L. Chemical speciation models: simplifying the complexity of the ocean. *The International Symposium on Macrocyclic and Supramolecular Chemistry* 143 (2019).

92. Singh, R., Edokpayi, J. N., Odiyo, J. O. and Smith, J. A. *E. coli* inactivation by metals and effects of changes in water chemistry. *J. Environ. Eng.* **145,** 04018136 (2019).

93. Markich, S. J., King, A. R. and Wilson, S. P. Noneffect of water hardness on the accumulation and toxicity of copper in a freshwater macrophyte (*Ceratophyllum demersum*): how useful are hardness-modified copper guidelines for protecting freshwater biota? *Chemosphere* **65,** 1791-1800 (2006).

94. Zhang, W., Ning, B., Sun, C., Song, K., Xu, X., Fang, T. and Yao, L. Dynamic nano-Ag colloids cytotoxicity to and accumulation by *Escherichia coli*: Effects of Fe^{3+}, ionic strength and humic acid. *J. Environ. Sci.* **89,** 180-193 (2020).

95. Thit, A., Huggins, K., Selck, H. and Baun, A. Acute toxicity of copper oxide nanoparticles to *Daphnia magna* under different test conditions. *Toxicol. Environ. Chem.* **99,** 665-679 (2017).

96. Kim, J. Y., Lee, C., Cho, M. and Yoon, J. Enhanced inactivation of *E. coli* and MS-2 phage by silver ions combined with UV-A and visible light irradiation. *Water Res.* **42,** 356-362 (2008).

97. Dyble, J., Tester, P. A. and Litaker, R. W. Effects of light intensity on cylindrospermopsin production in the cyanobacterial HAB species *Cylindrospermopsis raciborskii*. *Afr. J. Mar.* **28,** 309-312 (2006).

98. Preußel, K., Wessel, G., Fastner, J. and Chorus, I. Response of cylindrospermopsin production and release in *Aphanizomenon flos-aquae* (Cyanobacteria) to varying light and temperature conditions. *Harmful Algae* **8,** 645-650 (2009).

99. Shin, D. H., Ko, Y. G., Choi, U. S. and Kim, W. N. Synthesis and characteristics of novel chelate fiber containing amine and amidine groups. *Polym. Adv. Technol.* **15,** 459-466 (2004).

100. Westrick, J. A., Szlag, D. C., Southwell, B. J. and Sinclair, J. A review of cyanobacteria and cyanotoxins removal/inactivation in drinking water treatment. *Anal. Bioanal. Chem.* **397,** 1705-1714 (2010).

101. Klitzke, S., Beusch, C. and Fastner, J. Sorption of the cyanobacterial toxins cylindrospermopsin and anatoxin-a to sediments. *Water Res.* **45,** 1338-1346 (2011).

102. Wei, Z., Qiu, F., Wang, X., Long, S. and Yang, J. Improvements on electrical conductivity of the electrospun microfibers using the silver nanoparticles. *J. Appl. Polym. Sci.* **137,** 48788 (2020).

103. Wang, J., Zhu, L., Ji, L. and Chen, Z. Preparation of nanostructured $Cu(OH)_2$ and CuO electrocatalysts for water oxidation by electrophoresis deposition. *J. Mater. Res.* 33, 581-589 (2018).

104. Ma, M. G., Fu, L. H., Li, S. M., Zhang, X. M., Sun, R. C. and Dai, Y. D. Hydrothermal synthesis and characterization of wood powder/$CaCO_3$ composites. *Carbohydr. Polym.* **88,** 1470-1475 (2012).

105. Yang, K., Lin, D. and Xing, B. Interactions of humic acid with nanosized inorganic oxides. *Langmuir* **25,** 3571-3576 (2009).

106. Guidelines for drinking-water quality. *World Health Organization* **216,** 303-304 (2011).

107. Rashid, M., Khan, M.N. and Jalbani, N. Detection of human adenovirus, rotavirus, and enterovirus in tap water and their association with the overall quality of water in Karachi, Pakistan. *Food Environ. Virol.* **13,** 44-52 (2021).

108. Kittigul, L. and Pombubpa, K. Rotavirus Surveillance in Tap Water, Recycled Water, and Sewage Sludge in Thailand: A Longitudinal Study, 2007–2018. *Food Environ. Virol.* **13,** 53-63 (2021).

109. Verheyen, J., Timmen-Wego, M., Laudien, R., Boussaad, I., Sen, S., Koc, A., Uesbeck, A., Mazou, F. and Pfister, H. Detection of adenoviruses and rotaviruses in drinking water sources used in rural areas of Benin, West Africa. *Appl. Environ. Microbiol.* **75,** 2798-2801 (2009).

110. Baki, A. A., Haque, W., Giti, S., Khan, A. A., Rahman, M. M., Jubaida, N. and Rahman, M. Hepatitis E virus genotype 1f outbreak in Bangladesh, 2018. *J. Med.Virol.* **93,** 5177-5181 (2021).

111. Tzani, M., Mellou, K., Kyritsi, M., Kolokythopoulou, F., Vontas, A., Sideroglou, T., Chrysostomou, A., Mandilara, G. D., Tryfinopoulou, K., Georgakopoulou, T. and Hadjichristodoulou, C. Evidence for waterborne origin of an extended mixed gastroenteritis outbreak in a town in Northern Greece, 2019. *Epidemiol. Infect.* **149** (2020).

112. Kosel, J., Gutiérrez-Aguirre, I., Rački, N., Dreo, T., Ravnikar, M. and Dular, M. Efficient inactivation of MS-2 virus in water by hydrodynamic cavitation. *Water Res.* **124,** 465-471 (2017).

113. Hai, F. I., Riley, T., Shawkat, S., Magram, S. F. and Yamamoto, K. Removal of pathogens by membrane bioreactors: a review of the mechanisms, influencing factors and reduction in chemical disinfectant dosing. *Water* **6,** 3603-3630 (2014).

114. You, Y., Han, J., Chiu, P. C. and Jin, Y. Removal and inactivation of waterborne viruses using zerovalent iron. *Environ. Sci. Technol.* **39,** 9263-9269 (2005).

115. Yue, E., Bai, H., Lian, L., Li, J. and Blatchley III, E. R. Effect of chloride on the formation of volatile disinfection byproducts in chlorinated swimming pools. *Water Res.* **105,** 413-420 (2016).

116. Bond, T., Templeton, M. R., Kamal, N. H. M., Graham, N. and Kanda, R. Nitrogenous disinfection byproducts in English drinking water supply systems: occurrence, bromine substitution and correlation analysis. *Water Res.* **85,** 85-94 (2015).

117. Matsubara, T., Maki, S. and Toshimori, Y. The effectiveness of a nonalcoholic disinfectant containing metal ions, with broad antimicrobial activity. *Sci. Rep.* **11,** 1-7 (2021).

118. Thurman, R. B., Gerba, C. P. and Bitton, G. The molecular mechanisms of copper and silver ion disinfection of bacteria and viruses. *Crit. Rev. Environ. Sci. Technol.* **18,** 295-315 (1989).

119. Soliman, M. Y., Medema, G., Bonilla, B. E., Brouns, S. J. and van Halem, D. Inactivation of RNA and DNA viruses in water by copper and silver ions and their synergistic effect. *Water Res. X* **9,** 100077 (2020).

120. Xu, Y., Chu, X., Hu, J. and Ong, S. L. Disinfection performance of nanosilver and impacts of environmental conditions on viral inactivation by nanosilver. *Water Sci. Technol. Water Supply* **14,** 150-157 (2014).

121. Zheng, X., Shen, Z. P., Cheng, C., Shi, L., Cheng, R. and Yuan, D. H. Photocatalytic disinfection performance in virus and virus/bacteria system by Cu-TiO_2 nanofibers under visible light. *Environ. Pollut.* **237,** 452-459 (2018).

122. Mac Mahon, J., Pillai, S. C., Kelly, J. M. and Gill, L. W. Solar photocatalytic disinfection of *E. coli* and bacteriophages MS2, ΦX174 and PR772 using TiO_2, ZnO and ruthenium-based complexes in a continuous flow system. *J. Photochem. Photobiol. B, Biol.* **170,** 79-90 (2017).

123. Armstrong, A. M., Sobsey, M. D. and Casanova, L. M. Disinfection of bacteriophage MS2 by copper in water. *Appl. Microbiol. Biotechnol.* **101,** 6891-6897 (2017).

124. Jackson, K. N., Kahler, D. M., Kucharska, I., Rekosh, D., Hammarskjold, M. L. and Smith, J. A. Inactivation of MS2 bacteriophage and adenovirus with silver and copper in solution and embedded in ceramic water filters. *J. Environ. Eng.* **146,** 04019130 (2020).

125. Cormier, J. and Janes, M. A double layer plaque assay using spread plate technique for enumeration of bacteriophage MS2. *J. Virol. Methods* **196,** 86-92 (2014).

126. Berg, J. M., Romoser, A., Banerjee, N., Zebda, R. and Sayes, C. M. The relationship between pH and zeta potential of~ 30 nm metal oxide nanoparticle suspensions relevant to in vitro toxicological evaluations. *Nanotoxicology* **3,** 276-283 (2009).

127. Ehdaie, B., Su, Y. H., Swami, N. S. and Smith, J. A. Protozoa and virus disinfection by silver-and copper-embedded ceramic tablets for water purification. *J. Environ. Eng.* **146,** 04020015 (2020) .

128. Monette, A. and Mouland, A. J. Zinc and copper ions differentially regulate prion-like phase separation dynamics of pan-virus nucleocapsid biomolecular condensates. *Viruses* **12,** 1179 (2020).

129. Zhu, K., Hopwood, M. J., Groenenberg, J. E., Engel, A., Achterberg, E. P. and Gledhill, M. Influence of pH and Dissolved Organic Matter on Iron Speciation and Apparent Iron Solubility in the Peruvian Shelf and Slope Region. *Environ. Sci. Technol.* **55,** 9372–9383 (2021).

130. Nieto-Juarez, J. I., Pierzchła, K., Sienkiewicz, A. and Kohn, T. Inactivation of MS2 coliphage in Fenton and Fenton-like systems: role of transition metals, hydrogen peroxide and sunlight. *Environ. Sci. Technol.* **44,** 3351-3356 (2010).

131. Zanin, L., Tomasi, N., Cesco, S., Varanini, Z. and Pinton, R. Humic substances contribute to plant iron nutrition acting as chelators and biostimulants. *Front. Plant Sci.* **10,** 675 (2019).